How to detect fluctuating stripes in the high-temperature superconductors

S. A. Kivelson and I. P. Bindloss

Department of Physics, University of California at Los Angeles, Los Angeles, California 90095, USA

E. Fradkin

Department of Physics, University of Illinois, Urbana, Illinois 61801-3080, USA

V. Oganesyan

Department of Physics, Princeton University, Princeton, New Jersey 08544, USA

J. M. Tranquada

Physics Department, Brookhaven National Laboratory, Upton, New York 11973-5000, USA

A. Kapitulnik and C. Howald

Department of Physics, Stanford University, Stanford, California 94305-4045, USA

(Published 8 October 2003)

This article discusses fluctuating order in a quantum disordered phase proximate to a quantum critical point, with particular emphasis on fluctuating stripe order. Optimal strategies are derived for extracting information concerning such local order from experiments, with emphasis on neutron scattering and scanning tunneling microscopy. These ideas are tested by application to two model systems—an exactly solvable one-dimensional (1D) electron gas with an impurity, and a weakly interacting 2D electron gas. Experiments on the cuprate high-temperature superconductors which can be analyzed using these strategies are extensively reviewed. The authors adduce evidence that stripe correlations are widespread in the cuprates. They compare and contrast the advantages of two limiting perspectives on the high-temperature superconductor: weak coupling, in which correlation effects are treated as a perturbation on an underlying metallic (although renormalized) Fermi-liquid state, and strong coupling, in which the magnetism is associated with well-defined localized spins, and stripes are viewed as a form of micro phase separation. The authors present quantitative indicators that the latter view better accounts for the observed stripe phenomena in the cuprates.

CONTENTS

I. INTRODUCTION

Ordered states of matter are characterized by broken symmetry. Depending on various real-world details, this may be relatively easier or harder to detect experimentally, but once detected it is unambiguous. The notion that order-parameter fluctuations are important in the disordered phase proximate to an ordered state is a

 ©2003 The American Physical Society

rather obvious extension of the idea of broken symmetry; however, this notion is more difficult to define precisely. To develop this important concept, we shall discuss strategies for detecting quantum fluctuating order in the particular context of high-temperature superconductors. We shall focus on the detection of stripe order in the putative stripe liquid phase of these systems.[1] More generally, we are interested in electronic liquid-crystalline states and their associated fluctuations (Kivelson *et al.*, 1998), but the results are also easily generalized to other forms of order.[2]

Since the whole notion of fluctuating order is based on proximity of an ordered state, it is essential first to establish the existence of the "nearby" ordered state by directly detecting the relevant broken symmetry. The ordered phase may be induced by making small changes to the chemical composition of the material, applying pressure or magnetic fields, etc. Unless an actual ordered state can be reached, it is dangerous to speculate about the effects of related fluctuating order.

Typically, the best way to detect both the broken-symmetry state and the relevant fluctuations is by measuring the appropriate dynamical structure factor $S(\mathbf{q},\omega)$. Indeed, x-ray and neutron scattering studies have provided the best evidence[3] of ordered and fluctuating stripe phases, as we shall discuss. However, in many interesting materials, appropriate crystals are not available and so such experiments are not possible. Here, probes of local order, such as nuclear magnetic resonance (NMR), nuclear quadrupole resonance (NQR), muon spin rotation (μSR), and scanning tunneling microscopy (STM) techniques, may be the best available. All of these are quasistatic (i.e., nearly zero-frequency) probes. In a pure quantum system, in its disordered phase, the order-parameter fluctuations are not static, but rather fluctuate with a characteristic frequency that grows with the distance ℓ to the quantum critical point. Thus, unless something is done to "pin" these fluctuations, they are invisible to local probes. Such pinning is induced by boundaries, vortices, crystal-field effects, weak quenched disorder, etc.

In this article, we first discuss results obtained for solvable model systems, which we analyze in various ways to illustrate the optimal strategies for extracting information about local order. In particular, much of this discussion addresses the character of the local order in a quantum disordered phase close to a quantum critical point; we believe that the intuitions gleaned from this study are more generally valid, but without the proximity to the critical point as a small parameter, it is difficult to treat the problem in a controlled fashion. We also review in some depth, although by no means exhaustively, the experimental evidence of various forms of stripe order in the cuprate superconductors. There are several related topics that we do not cover in this article; instead, we direct the interested reader to recent reviews. Specifically, the mechanism of stripe formation[4] is given short shrift, and the possible relevance[5] of local stripe order to the mechanism of high-temperature superconductivity and to the various remarkable normal-state properties observed in the cuprates is only touched on briefly. More broadly, the context for this review is the role of "competing orders" in high-temperature superconductors.[6]

In Sec. II we discuss basic scaling considerations that govern the relevant length, frequency, and energy scales of fluctuating order in the neighborhood of a quantum critical point, and the consequences of the pinning induced by disorder and other perturbations. We show that it is the low-frequency part of the dynamical structure factor, rather than its integral over all frequencies, that contains the clearest information concerning local order. We also define a new response function which determines the local density-of-states modulations induced by a weak-impurity potential. Finally, we sketch various possible versions of the phase diagram of a system with competing stripe and superconducting phases.

In Sec. III (and Appendix A), we consider a theoretically well-understood system, the one-dimensional electron gas (1DEG) in the presence of an impurity. We compute the local density of states, as would be measured in STM, and the dynamical structure factor, and show by this explicit example how the general considerations articulated in the present paper are manifest in this solvable model. (The 1DEG can also be viewed as a quantum critical state associated with charge-density-wave order.) In addition to its pedagogical value, this section contains explicit results that should be useful for analyzing STM experiments on quasi-1D systems with dilute impurities, such as the chain layers of YBCO

[1]For brief reviews of the current evidence on various types of stripe order in the cuprates, see Emery *et al.*, 1999; Orenstein and Millis, 2000; Zaanen, 2000; Sachdev, 2002; Carlson *et al.*, 2003; Castro Neto and Morais Smith, 2003.

[2]Fluctuations associated with off-diagonal (i.e., superconducting) order are best studied using different strategies; see, for example, Jankó *et al.*, 1999; Carlson *et al.*, 2000; Xu *et al.*, 2000; Iguchi *et al.*, 2001; Wang *et al.*, 2001; Ussishkin *et al.*, 2002.

[3]For reviews of neutron and x-ray evidence of stripes, see Tranquada, 1998a, 1998b; Emery *et al.*, 1999.

[4]Recent reviews of the mechanisms of stripe formation in the cuprates and, more generally in doped antiferromagnets, often with rather different perspectives on the issue, are those of Zaanen and Littlewood, 1994; Zaanen, 1998; Emery *et al.*, 1999; Ichioka and Machida, 1999; Vojta and Sachdev, 1999; White and Scalapino, 2000; Hasselmann *et al.*, 2002; White *et al.*, 2002; Carlson *et al.*, 2003.

[5]Various perspectives concerning the relevance of local stripe order to other properties of the high-temperature superconductor are reviewed by Castro Neto, 2001; Lorenzana *et al.*, 2001a, 2001b; Zaanen *et al.*, 2001; Carlson *et al.*, 2003.

[6]Recent discussions of the role of competing orders in determining the phase diagram of the high-temperature superconductors are contained in Varma, 1997; Emery *et al.*, 1999; Orenstein and Millis, 2000; Sachdev, 2000; Zaanen, 2000; Chakravarty, Laughlin, *et al.*, 2001; Kivelson *et al.*, 2001.

(Derro *et al.*, 2002), or on carbon nanotubes (Hornbaker *et al.*, 2002; Odom *et al.*, 2002).

In Sec. IV we calculate the local density of states in the context of a simple model system with quasiparticles and incipient order—the weakly interacting electron gas in two dimensions.

In Sec. V we discuss applications of these ideas to experiments in the cuprates. Section V.A treats diffraction studies, and Sec. V.B scanning tunneling microscope studies. This latter section contains new insights concerning the optimal way to analyze STM data to extract information about fluctuating order. Applying these ideas to the recent experimental results of Hoffman *et al.* (Hoffman, Hudson, *et al.*, 2002; Hoffman, McElroy, *et al.*, 2002) and Howald *et al.* (2003a, 2003b) reveals the existence of a nearby stripe-ordered phase in optimally doped BSCCO.[7] Section V.C contains a discussion of experiments to detect local nematic order, and a discussion of recent STM evidence of such order on the same BSCCO surfaces. In Sec. V.D, we discuss indirect evidence of stripe order that comes from the "1/8 anomaly." In Sec. V.E we briefly discuss other probes of stripe order, including NMR, NQR, and μSR.

In Sec. VI, we address an important issue of perspective: In the weak-coupling limit, the electronic properties of a solid are essentially determined by the quasiparticle band structure, while collective modes and various forms of order reflect slight rearrangements of the states near the Fermi surface. Often these effects can be plausibly treated in the context of a Hartree-Fock or random-phase approximation (RPA) treatment of the residual interactions. Conversely, in the strong-coupling limit, the physics is more simply understood in terms of interacting collective modes, such as spin waves, superconducting phase fluctuations, and the "phonons" of a charge-ordered state. Here, we discuss the interrelation between these opposite perspectives. In particular we present evidence that the stripe order observed in the cuprates and related compounds is best thought of as arising from the strong-coupling antiferromagnetism of the undoped Mott insulating parent compounds than from the more conventionally metallic physics of the strongly overdoped materials.

Our most important conclusions are embodied in five numbered "lessons," which are stated in Secs. II, III, and IV, and summarized in Sec. VII.

II. GENERAL CONSIDERATIONS

Since the discovery (Bednorz and Müller, 1986) of high-temperature superconductivity in the cuprate superconductors, there has been intense interest in the question of how a Mott insulating antiferromagnet is converted, upon doping, into a high-temperature superconductor. Generally, in electronic systems, there is a competition between the kinetic energy (Fermi pressure), which favors a uniform Fermi-liquid phase with sharply defined, itinerant quasiparticles, and the Coulomb repulsion between electrons, which favors various forms of insulating magnetic and/or charge-ordered states. Thus it should not be at all surprising to find various forms of charge-ordered states appearing in doped antiferromagnets. In particular, "stripe" states have consistently turned up in theoretical studies of doped antiferromagnets, including early Hartree-Fock solutions of the Hubbard model,[8] studies of Coulomb frustrated phase separation,[9] slave-boson mean-field theories of the t-J model,[10] and various Monte Carlo and density-matrix renormalization-group studies of t-J and Hubbard models.[11] The discovery[12] of stripe order in $La_{2-x}Sr_xNiO_{4+\delta}$ and soon after in $La_{1.6-x}Nd_{0.4}Sr_xCuO_4$ (Tranquada, Sternlieb, *et al.*, 1995) added considerable credibility to the suggestion that stripe states form an important bridge between the Mott insulator, and the more metallic state at heavy doping.

"Stripes" is a term that is used to describe unidirectional density-wave states, which can involve unidirectional charge modulations ("charge stripes") or coexisting charge and spin-density order ("spin stripes").[13] Charge-density wave states can occur in the weak-coupling limit if there are sufficiently well nested portions of the Fermi surface. From the strong-coupling perspective, stripes are a real-space pattern of micro phase separation (hence the name), driven largely by a lowering of the doped-hole kinetic energy,[14] in which the doped holes are itinerant in metallic rivers, and the antiferromagnetic correlations of the parent insulator are preserved in between. Although the characteristic dynamics of the stripes may be quite different in these two limits, as are the possible implications for other physical properties, from a broken-symmetry viewpoint there is no difference between a unidirectional charge-density-wave-ordered and a stripe-ordered state.

---

[7]This conclusion is in agreement with the inferences drawn from the data by Howald *et al.* (2002, 2003), but in disagreement with those drawn by Hoffman, McElroy, *et al.* (2002); we shall discuss the origins of the differing conclusions.

[8]See Machida, 1989; Schulz, 1989; Zaanen and Gunnarsson, 1989.

[9]See Emery and Kivelson, 1993; Low *et al.*, 1994; Castellani *et al.*, 1995; Seul and Andelman, 1995; Hasselmann *et al.*, 1999.

[10]See Seibold *et al.*, 1998; Han *et al.*, 2001; Lorenzana and Seibold, 2002.

[11]For varying perspectives, see Hellberg and Manousakis, 1997, 2000; White and Scalapino, 1998, 2000.

[12]See Hayden *et al.*, 1992; Chen *et al.*, 1993; Tranquada *et al.*, 1994.

[13]One can also imagine "orbital stripes" which involve a unidirectional modulation of a staggered flux or d-density wave order (Schollwoeck *et al.*, 2003); in large part, the analysis of the present paper would apply equally well to this form of order.

[14]As discussed, for instance, by Poilblanc and Rice, 1989; Schulz 1989; White and Scalapino, 1998; Emery *et al.*, 1999; Chernyshev *et al.*, 2000; Zachar, 2000; Castro Neto and Morais Smith, 2003.

Since the principal purpose of the present paper is to address questions concerning the existence of local stripe order, we shall for the most part consider unidirectional charge-density-wave order and stripe order as two limits of the same physics. Indeed, it is important to stress that the microscopic mechanism of stripe formation in particular materials is still not clear. Questions such as whether or not the long-range Coulomb interactions are important have been widely debated, but remain unresolved. There is always a linear coupling between any form of charge order and equal-period lattice distortions, so it is obvious that lattice distortions play a significant role in enhancing all the observed stripe phenomena, whether or not they are fundamental to the mechanism. This observation is further corroborated by the observed stabilization of stripes by particular orientational orders of the apical oxygens in some of the cuprates (Axe and Crawford, 1994; Büchner *et al.*, 1994), and by a series of thermal-transport (Baberski *et al.*, 1998; Sun *et al.*, 2003) and isotope-effect (Crawford *et al.*, 1990) anomalies associated with the onset of stripe order (Tranquada, Sternlieb, *et al.*, 1995).

A. Stripe-ordered phases

In two dimensions, an ordered stripe phase with the stripes running in the y direction gives rise to new Bragg peaks in the electronic charge scattering (and corresponding peaks in the nuclear scattering) at $\mathbf{k}=\pm\mathbf{Q}_{\rm ch}=(2\pi/a)(\pm\delta_{\rm ch},0)$ and its harmonics, where $\delta_{\rm ch}=1/\lambda_{\rm ch}$ and $\lambda_{\rm ch}a$ is the charge-stripe period. Where spin order coexists with charge order, new magnetic Bragg peaks occur at harmonics of $\mathbf{k}=\mathbf{Q}_{\rm s}=\mathbf{Q}_{\rm AF}\pm\frac{1}{2}\mathbf{Q}_{\rm ch}$ where $\mathbf{Q}_{\rm AF}=(2\pi/a)(\frac{1}{2},\frac{1}{2})$ is the Néel ordering vector.[15]

Charge stripes break rotational symmetry and translation symmetry perpendicular to the stripes. In a crystal, these are to be interpreted as a breaking of the crystal symmetry group, rather than of the continuous symmetries of free space. The relevant order parameter, $\langle\rho_{\mathbf{Q}_{\rm ch}}\rangle$, is the Fourier component of the electron charge density at the ordering wave vector. If the state is, in addition, a conducting or superconducting electron fluid, it is a charge-stripe smectic. Spin stripes also break spin-rotational and time-reversal invariance (although a particular combination of time reversal and translation is preserved). Wherever there is spin-stripe order, there is necessarily charge-stripe order (Zachar *et al.*, 1998). The new order parameter that distinguishes the spin-stripe phase $\langle\mathbf{s}_{\mathbf{Q}_{\rm s}}\rangle$ is the Fourier component of the spin density.

There is more than one possible stripe liquid phase. In particular, there is the possibility of a "stripe nematic phase," in which thermal or quantum fluctuations have caused the stripe-ordered state to melt (i.e., translational symmetry is restored) but orientational symmetry remains broken (i.e., a snapshot of the system is more likely to see stripe segments oriented in the y than in the x direction). The nematic shares with the charge-ordered state a precise definition in terms of broken symmetry. The order parameter can be taken to be any physical quantity transforming like a traceless symmetric tensor. For instance, the traceless part of the dielectric tensor is a measure of the nematic order of the charged fluid. In two dimensions, a useful nematic order parameter is (Chaikin and Lubensky, 1995)

$$\mathcal{Q}_{\mathbf{k}}\equiv\frac{S(\mathbf{k})-S(\mathcal{R}[\mathbf{k}])}{S(\mathbf{k})+S(\mathcal{R}[\mathbf{k}])},\tag{2.1}$$

where $\mathcal{R}$ is a rotation by $\pi/2$, and

$$S(\mathbf{k})=\int_{-\infty}^{\infty}\frac{d\omega}{2\pi}S(\mathbf{k},\omega)\tag{2.2}$$

is the thermodynamic (equal-time) structure factor. More exotic states can also occur, such as a "nematic spin nematic," which breaks rotational, spin-rotational, and time-reversal symmetry, but not the product of $\mathcal{R}$ and time reversal.[16]

B. Fluctuating order near a quantum critical point

We consider a system in a quantum disordered phase near a quantum critical point beyond which the ground state would be ordered.[17] To be concrete, we shall discuss charge-stripe order. By a quantum disordered phase, we mean one in which there is no long-range stripe order as $T\to 0$, but in which there may be other forms of order, for instance superconducting order.

The charge-density dynamical structure factor, $S_{\rm ch}(\mathbf{k},\omega)$, for $\mathbf{k}$ in the neighborhood of $\mathbf{Q}_{\rm ch}$, measures the collective fluctuations that are most sensitive to the proximity of the quantum critical point. The scaling theory of quantum critical phenomena tells us that, on the quantum-disordered side of the quantum critical point, there are diverging length and time scales, $\xi\sim\ell^{-\nu}$ and $\tau\sim\ell^{-\nu z}$, where ν is a critical exponent, z is the dynamical critical exponent, and ℓ is the dimensionless distance to the quantum critical point.[18]

In the quantum disordered phase, and in the absence of quenched disorder, the fluctuation spectrum has a characteristic frequency scale $E_{\rm G}/\hbar$. In the absence of

[15]Note that, in a crystal, wave-vector equalities are always to be interpreted as meaning equal up to a reciprocal lattice vector.

[16]A nematic spin nematic is most easily pictured as a state in which the spin-up and spin-down electrons each form a nematic state, with their principle axes at 90° to each other.

[17]For extremely clear reviews, see Sachdev, 1999a and Sachdev, 2000, as well as Sondhi *et al.*, 1997.

[18]The values of the critical exponents are universal in the sense that they are a small discrete set of numbers depending on some general features of the critical point. Under many circumstances, z is either 1 or 2. ν depends on the effective dimension $D+z$ and, to a lesser extent, on the symmetry of the order parameter; typically, for $D\geq 2$, ν is in the range $2/3\geq\nu\geq 1/2$.

dissipation,[19] which is the case we shall treat for concreteness, E_G typically is a gap in the collective-mode spectrum. E_G is related to the correlation time by the scaling law $E_G \sim \hbar/\tau \sim \ell^{\nu z}$. For $\hbar\omega$ slightly larger than E_G, $S(\mathbf{k},\omega)$ has a pole corresponding to a sharply defined elementary excitation; this "soft mode" is the quantity that condenses across the quantum critical point, so its quantum numbers and characteristic wave vector directly encode the nature of the nearby ordered state. At somewhat higher energy (typically, for $\hbar\omega > 3E_G$) $S(\mathbf{k},\omega)$ exhibits a multiparticle continuum. Deep in the continuum the system effectively exhibits scale invariance, and it behaves in much the same way as if it were precisely at the quantum critical point. Both in this high-frequency regime and at the quantum critical point the notion of a quasiparticle is, truly speaking, ill defined, although for systems with small anomalous dimension η (the typical case for $D \geq 2$) the continuum will often exhibit features (branch points, not poles) whose dispersion resembles that of the Goldstone modes of the ordered phase.[20]

A classical critical point is described by thermodynamics alone, so none of these dynamical considerations affect the critical phenomena. In particular, it follows from the classical limit of the fluctuation-dissipation theorem that $S(\mathbf{k}) = T\chi(\mathbf{k},\omega=0) \equiv T\chi(\mathbf{k})$, so S has the same critical behavior as the (static) susceptibility χ, even though S involves an integral over the dynamical structure factor at all frequencies. Consequently, a growing peak in $S(\mathbf{k})$ at the ordering vector, $\mathbf{k}=\mathbf{Q}_{ch}$ with width $|\mathbf{k}-\mathbf{Q}_{ch}| \sim 1/\xi$ and amplitude $S(\mathbf{Q}_{ch}) \sim |T-T_c|^{-\gamma}$, reflects the presence of fluctuating stripe order near a thermal transition. Here $\gamma = \nu(2-\eta)$ is typically about 1 or greater, so the amplitude is strongly divergent.

The situation is quite different at a quantum critical point, where the dynamics and the thermodynamics are inextricably linked. Here, the fact that the largest contribution to $S(\mathbf{k})$ comes from the high-frequency multiparticle continuum, which does not directly probe the fluctuating order, means that the relevant structure in $S(\mathbf{k})$ is relatively small and can be difficult to detect in practice. To see this, we compare the expressions in terms of the dissipative response function $\chi''(\mathbf{k},\omega)$ for the susceptibility (obtained from the Kramers-Krönig relation) and $S(\mathbf{k})$ (obtained from the fluctuation-dissipation theorem):

$$\chi(\mathbf{k},\omega=0) = \int \frac{d\omega}{2\pi} \chi''(\mathbf{k},\omega)/\omega,$$

$$S(\mathbf{k}) = \int \frac{d\omega}{2\pi} \coth\left(\frac{\beta\hbar\omega}{2}\right) \chi''(\mathbf{k},\omega). \tag{2.3}$$

In the limit $T \to 0$, $\coth(\beta\hbar\omega) \to 1$; then, clearly, the factor $1/\omega$ weights the important low-frequency part of the integral expression for χ much more heavily than in the expression for S. Consequently, it follows under fairly general circumstances (Chakravarty *et al.*, 1989; Chubukov *et al.*, 1994) from the scaling form of χ'' that $S(\mathbf{Q}_{ch}) \sim \tau^{-1}\chi(\mathbf{Q}_{ch})$ or, in other words, that $\chi(\mathbf{Q}_{ch}) \sim \ell^{-\gamma}$ is strongly divergent in the neighborhood of the quantum critical point, while $S(\mathbf{Q}_{ch}) \sim \ell^{\nu z-\gamma} = \ell^{-\nu(2-z-\eta)}$ is much more weakly divergent, or, if perchance $z \geq 2-\eta$, not divergent at all. At criticality ($\ell = 0$), similar considerations imply that $S(\mathbf{k},\omega)$ is a less singular function at small momentum/frequency than the corresponding susceptibility.

These considerations apply even on the ordered side of the quantum critical point, where the Bragg peak makes an exceedingly small (although sharp) contribution to the total structure factor, which vanishes in proportion to $\ell^{2\beta}$. By contrast, the Bragg peak constitutes the entire contribution to $S(\mathbf{k},\omega=0)$ and is the dominant piece of the structure factor integrated over any small frequency window that includes $\omega = 0$.

Lesson 1: There is an important lesson to be gleaned from this general discussion concerning the best way to analyze experiments. It is the low-frequency part of $S(\mathbf{k},\omega)$ that is most directly sensitive to the stripe order. Rather than analyze $S(\mathbf{k})$, one can best obtain information concerning local stripe order by studying $\chi(\mathbf{k},\omega=0)$ or by analyzing the partially frequency-integrated spectral function,

$$\tilde{S}(\mathbf{k},\Omega) \equiv (2\Omega)^{-1} \int_{-\Omega}^{\Omega} \frac{d\omega}{2\pi} S_{ch}(\mathbf{k},\omega), \tag{2.4}$$

where on the ordered side of the critical point, the smaller Ω the better, while on the quantum-disordered side, Ω must be taken larger than $E_G/\hbar$, but not more than a few times $E_G/\hbar$. This quantity is less severely contaminated by a "background" arising from incoherent high-energy excitations. As we shall discuss in Sec. V.A, this is precisely the way local stripe order is best detected in clean, high-temperature superconductors.

C. How weak disorder can make life simpler

In the absence of quenched disorder, there is no useful information available from the structure factor at frequencies less than E_G, which means in particular that static experiments ($\omega = 0$) are blind to fluctuating order. However, a small amount of quenched disorder, with characteristic energy scale $V_{dis} \sim E_G$ but much smaller than the "bandwidth" of the continuum of the spectral

[19] In the presence of zero-temperature dissipation, such as one expects in a normal metal, the collective-mode spectrum may be gapless, in which case the interpretation of τ is more subtle. Most of the scaling arguments we make in the present paper are readily generalized to this case, as well. For a recent perspective on the effect of dissipation on quantum critical phenomena, see Kapitulnik *et al.* (2001). See also Millis (1993) and Sachdev (1999b) on quantum critical points in metals.

[20] The naive argument, which is often made, that at frequencies larger than E_G the quantum disordered phase looks like the ordered phase is thus not completely correct. There is, however, a more nearly correct version of this statement: at high frequencies, on both the ordered and disordered sides of the quantum critical point, the system looks quantum critical, and so looks the same whichever state is being probed.

function, has important effects on the low-energy states. It is intuitively clear that the induced low-frequency structure of $S(\mathbf{k},\omega)$ will be largest for values of $\mathbf{k}$ where, in the absence of disorder, S has spectral weight at the lowest frequencies, i.e., for $\mathbf{k}\sim\mathbf{Q}_{\rm ch}$. Although the effects of quenched randomness on the pure critical theory can be subtle (McCoy and Wu, 1968; Griffiths, 1969; Fisher, 1992) and are rarely well understood (unless disorder happens to be irrelevant), low-energy states are frequently produced.

Lesson 2: The upshot is that the effect of weak quenched randomness in a quantum disordered phase is to produce a low-frequency "quasielastic" part of the spectral function $S(\mathbf{k},\omega)$. In other words, disorder will eliminate the spectral gap, but will only weakly affect the partially integrated spectral function, Eq. (2.4), with the integration scale set by $V_{\rm dis}$. In particular, in the presence of weak disorder, the static structure factor $S(\mathbf{k},\omega=0)$ should exhibit similar $\mathbf{k}$ dependence to that of $\tilde{S}(\mathbf{k},\Omega)$ of the pure system, and so can be used to reveal the nature of the nearby ordered phase.

To formalize some of these notions, we consider the somewhat simpler problem of the response of the system to a weak, applied external field which couples to the order parameter. In a quantum disordered phase the existence of an order parameter can only be made apparent directly by coupling the system to a suitable symmetry-breaking field. For a charge-stripe smectic, a nonuniform potential couples to the order parameter and thus serves as a suitable symmetry-breaking field. Thus the Fourier component $V_{\mathbf{k}}$ of a weak potential induces a nonvanishing expectation value of the order parameter which, in linear response, is

$$\langle\rho_{\mathbf{k}}\rangle=\chi_{\rm ch}(\mathbf{k})V_{\mathbf{k}}+\cdots. \tag{2.5}$$

The linear response law of Eq. (2.5) is valid provided $V_{\mathbf{k}}$ is sufficiently small. However, if the typical magnitude of V with Fourier components in the range $|\mathbf{k}-\mathbf{Q}_{\rm ch}|\xi\lesssim 1$ is not small, $\overline{V}_{\mathbf{k}_{\rm ch}}\gg E_{\rm G}$, then the critical region is accessed and Eq. (2.5) is replaced by the law

$$\langle\rho_{\mathbf{Q}_{\rm ch}}\rangle\sim[\overline{V}_{\mathbf{Q}_{\rm ch}}]^{1/\delta}, \tag{2.6}$$

where $\delta=2/(D-2+\eta)$ is another critical exponent.

Many local probes, including STM and NMR, are more sensitive to the local density of electronic states $\mathcal{N}(\mathbf{r},E)$. Again, in the quantum disordered state, translation invariance implies that, in the absence of an external perturbation, $\mathcal{N}(\mathbf{r},E)=\mathcal{N}_0(E)$ is independent of $\mathbf{r}$. In the presence of a weak potential, it is possible to define a relation for the local density of states as

$$N(\mathbf{k},E)=\chi_{\rm DOS}(\mathbf{k},E)V_{\mathbf{k}}+\cdots, \tag{2.7}$$

where $N(\mathbf{k},E)$ is the Fourier transform of $\mathcal{N}(\mathbf{r},E)$. From linear-response theory it follows that

$$\chi_{\rm DOS}(\mathbf{k},E)=(2\pi)^{-1}\int d\mathbf{r}\,dt\,d\tau\,e^{iEt-i\mathbf{k}\cdot\mathbf{r}}\theta(\tau) \times\langle[\{\Psi^{\dagger}_{\sigma}(\mathbf{r},t+\tau),\Psi_{\sigma}(\mathbf{r},\tau)\},\hat{n}(\mathbf{0})]\rangle, \tag{2.8}$$

where θ is the Heaviside function, $\Psi^{\dagger}_{\sigma}$ is the electron creation operator, and $\hat{n}=\Sigma_{\sigma}\Psi^{\dagger}_{\sigma}\Psi_{\sigma}$ is the electron density operator. Note that, despite appearances, E is not a frequency variable, but is rather the energy at which the time-independent density of states is measured. A simple sum rule relates $\chi_{\rm ch}$ to $\chi_{\rm DOS}$:

$$\chi_{\rm ch}(\mathbf{k})=\int dE\,f(E)\chi_{\rm DOS}(\mathbf{k},E), \tag{2.9}$$

where $f(E)$ is the Fermi function.

It is also interesting to consider stripe orientational (nematic) order. Since $\chi_{\rm ch}(\mathbf{k})$ is a property of the uniform fluid phase, it respects all the symmetries of the underlying crystal; in particular, if rotation by $\pi/2$ is a symmetry of the crystal, then $\chi_{\rm ch}(\mathbf{k})=\chi_{\rm ch}(\mathcal{R}[\mathbf{k}])$, so no information about incipient nematic order can be obtained to linear order in the applied field. However, the leading nonlinear response yields a susceptibility for the nematic order parameter, defined in Eq. (2.1), as

$$\mathcal{Q}_{\mathbf{k}}=\int d\mathbf{p}\,\chi_{\rm nem}(\mathbf{k};\mathbf{p})[V_{\mathbf{p}}-V_{\mathcal{R}[\mathbf{p}]}][V_{-\mathbf{p}}+V_{-\mathcal{R}[\mathbf{p}]}]. \tag{2.10}$$

This nonlinear susceptibility ($\chi_{\rm nem}$ contains a four-density correlator) diverges at the nematic-to-isotropic quantum critical point, and we would generally expect it to be largest for $\mathbf{k}\approx\mathbf{Q}_{\rm ch}$. It is important to note that the density modulations, reflecting the proximity of stripe order, are a first-order effect, while the nematic response, which differentiates $\mathbf{Q}_{\rm ch}$ from $\mathcal{R}[\mathbf{Q}_{\rm ch}]$, is second order and so will tend to be weaker, even if the nematic quantum critical point is somewhat nearer at hand than that involving the stripe-ordered state.

D. Phase diagrams

When there is more than one competing ordered phase, the phase diagram can be very complicated and moreover can be quite different, depending on various microscopic details. Nonetheless, it is often useful to have a concrete realization of the phase diagram in mind, especially when thinking about issues related to order and order-parameter fluctuations. In this subsection, we sketch schematic phase diagrams which characterize some of the ordered phases and fluctuation effects discussed above; the reader is cautioned, however, that the shape, topology, and even the number of ordered phases may vary for material-specific reasons.

Figure 1(a) represents the essential features we have in mind, in the absence of any quenched disorder. Here, there is a stripe-ordered phase which occurs at low doping and low temperature, with a phase boundary that ends at a quantum critical point deep in the superconducting phase. In the region marked "fluctuating stripes," there is significant local stripe order, whose character is governed by proximity to the quantum critical point. Notice that this fluctuation region extends into the stripe-ordered phase itself; although there is true long-range stripe order in this region of the phase diagram, close to the quantum critical point the degree of

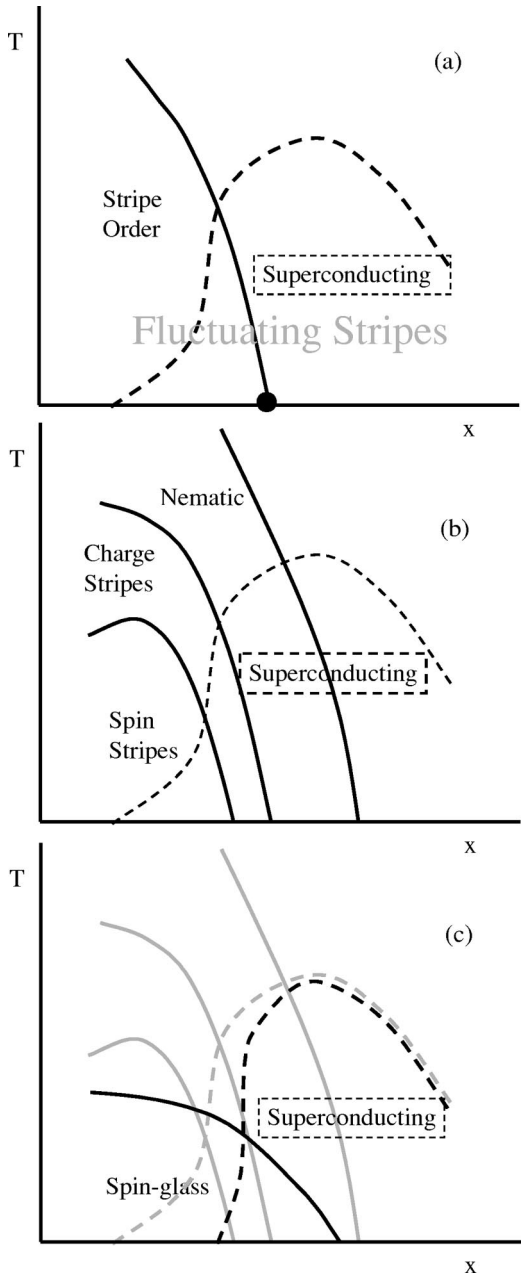

FIG. 1. Schematic phase diagrams showing various forms of stripe order, and their interactions with high-temperature superconductivity; see text for discussion.

striping at the local level is much greater than the small ordered component. There is no universal statement possible concerning how far the fluctuating stripe region extends beyond the ordered phase. Clearly, if the region in which there is *local* stripe order does not at least include the entire region of the phase diagram in which high-temperature superconductivity occurs, it cannot be essential for the mechanism of superconductivity.

Under many circumstances, the stripe-ordered phase will not end at a quantum critical point, but rather will terminate at a first-order line (Kivelson *et al.*, 2001). If the transition is only weakly first order, this will not affect the general considerations presented here. If it is strongly first order, fluctuation effects are much weaker, and the effects of even very weak quenched disorder are much more severe than in the case of a continuous transition. This limit warrants further study (Cardy, 1999), both for application to the cuprates and more generally; it is likely relevant for the organic superconductors.[21]

Figure 1(b) is a more ornate version[22] of the phase diagram, in which all the different broken-symmetry phases discussed in the present paper are exhibited. Here, we illustrate the case in which the nematic, charge, and spin ordering occur at distinct transitions, under which circumstances the nematic ordering must precede the charge ordering, which must in turn precede the spin ordering (Zachar *et al.*, 1998). In general, there are also distinctions between commensurate and incommensurate, diagonal and vertical, bond-centered and site-centered stripe order, so the same general considerations could lead to significantly more complicated phase diagrams.

Since the superconducting order is suppressed in the vortex state, and eliminated above the critical field H_{c2}, studies of the magnetic-field-induced changes in the local stripe order have recently emerged as one of the best ways of determining the nature of the interplay between stripe and superconducting order. There has been a flurry of recent papers, both experimental[23] and theoretical[24] on this subject. Since the subject is fairly involved and is well reviewed in the literature, we shall not elaborate here on the phase diagram in a field, although we will briefly mention some of the salient findings in Sec. V.

Finally, Fig. 1(c) shows the effect of weak disorder on the phase diagram illustrated in Fig. 1(b). Phase transitions involving breaking of spatial symmetries are generally rounded by quenched disorder. The resulting crossovers should have a glassy character, i.e., the apparent transition temperature should be frequency dependent. Thus the only true phase transitions in the presence of disorder are the superconducting and spin-glass

[21]A first-order transition of this sort has been reported in the BEDT system (Lefebvre *et al.*, 2000) and in $(TMTSF)_2PF_6$ (Brown *et al.*, 2003).

[22]In sketching the global shape of the phase diagram, we have included the prejudice that static stripe order, especially static spin-stripe order, competes strongly with superconductivity, but that a degree of local stripe order is necessary for high-temperature pairing—the latter prejudice is reflected in the vanishing of the superconducting T_c as the local stripe order is suppressed upon overdoping. However, these prejudices affect only the interplay between stripe order and superconducting order in the phase diagram, and not the central features on which we focus in the present article, concerning the character of fluctuating stripe order.

[23]Recent experimental studies of induced stripe order in the vortex state of high-temperature superconductors have been carried out, including Katano *et al.*, 2000; Lake *et al.*, 2001, 2002; Hoffman, Hudson, *et al.*, 2002; Khaykovich *et al.*, 2002.

[24]Theoretical studies of the effect of magnetic fields on the competition between stripe and superconducting order have been extensive; see, for instance, Demler *et al.*, 2001; Kivelson *et al.*, 2002; Zhang *et al.*, 2002, and references therein. For an earlier related discussion, see Arovas *et al.*, 1997; Zhang, 1997.

transitions, although the spin glass should have a local stripe character—it is (Emery and Kivelson, 1993) a "cluster spin glass." Note that quenched disorder generally introduces some frustration (Zachar, 2000), so that whereas in the absence of quenched disorder the spin-freezing temperature is large, quenched disorder tends to suppress it. Conversely, where quantum fluctuations have destroyed the ordered state, the additional pinning effect of quenched disorder can lead to a spin-glass phase extending beyond the border that the magnetic phase would have in the zero-disorder limit.

III. ONE-DIMENSIONAL LUTTINGER LIQUID

In this section, we show how the general features described above play out in the case of the 1DEG. For simplicity, we present results for a spin-rotation-invariant Tomonaga-Luttinger liquid; in a forthcoming publication (Bindloss *et al.*, 2003) we shall provide details of the derivations, and will also discuss the Luther-Emery liquid, i.e., the spin-gap case. In this section we will describe the most salient aspects of the ways fluctuating order manifests itself in these critical systems. In Appendix A we give more details of this theory. (We use units in which $\hbar = k_B = 1$.)

Both the Tomonaga-Luttinger and the Luther-Emery liquids can be regarded as quantum critical systems[25] with dynamic critical exponent $z=1$. So long as the charge Luttinger parameter is in the range $0<K_c<1$ (which is typically the case for repulsive interactions), the charge susceptibility of the Tomonaga-Luttinger liquid diverges as $k \to 2k_F$ as

$$\chi(2k_F+q) \sim |q|^{-g}, \tag{3.1}$$

where k_F is the Fermi wave vector and $g=1-K_c$. This system can rightly be viewed as a quantum critical charge-density wave state. (The charge-density wave fluctuations are still stronger in the case of a Luther-Emery liquid, where the susceptibility exponent is replaced by K_c-2.) Thus it is the perfect laboratory for testing the validity of the general scaling considerations of Sec. II.

The charge-density structure factor of the Tomonaga-Luttinger liquid is the Fourier transform of the more readily evaluated space-time structure factor

$$S(k,\omega) = \int_{-\infty}^{\infty} dt \int_{-\infty}^{\infty} dx\, \mathcal{S}(x,t) e^{ikx - i\omega t}, \tag{3.2}$$

where the charge correlation function $\mathcal{S}(r,t)$ is given by

$$\mathcal{S}(r,t) = \mathcal{S}_0(r,t) + [e^{i2k_F r}\mathcal{S}_{2k_F}(r,t) + \text{c.c.}] + [e^{i4k_F r}\mathcal{S}_{4k_F}(r,t) + \text{c.c.}] + \cdots. \tag{3.3}$$

Explicit expressions for $\mathcal{S}_0$, $\mathcal{S}_{2k_F}$, etc. are given in the literature (see footnote 25). These expressions can be Fourier transformed (although in general, this must be done numerically) to yield expressions for the dynamical structure factor. Since the Luttinger liquid is quantum critical, this (and other) correlation functions have a scaling form; for example, near $2k_F$ (i.e., for small q)

$$S(2k_F+q,\omega) = \frac{1}{v_c}\left(\frac{D}{v_c q}\right)^g \Phi_{2k_F}\left(\frac{\omega}{v_c q}, \frac{\omega}{T}\right), \tag{3.4}$$

where D is an ultraviolet cutoff, i.e., the bandwidth of the Tomonaga-Luttinger liquid. The scaling function Φ_{2k_F} of Eq. (3.4) depends implicitly on the dimensionless parameters K_c and v_c/v_s with v_c and v_s, respectively, the charge and spin velocities. (Spin rotation invariance constrains the spin Luttinger exponent K_s to be equal to 1.) To exhibit the general features we are interested in, while making the Fourier transform as simple as possible, we can consider the limit $T=0$ and set $v_s = v_c = v$. Then, for q small,

$$S(2k_F+q,\omega) \sim \frac{1}{v}\left(\frac{D}{vq}\right)^g \theta\left(\frac{\omega^2}{v^2q^2}-1\right)\left[\frac{\omega^2}{v^2q^2}-1\right]^{-g/2}, \tag{3.5}$$

where $\theta(x)$ is the step function.

For fixed ω, as a function of q, the dynamic structure factor exhibits a multiparticle continuum for $-\omega/v \leqslant q \leqslant \omega/v$, but it does have singular structure, which can be thought of as an image of the Goldstone (phason) modes one would find were there true charge-density-wave order:

$$S(2k_F+q,\omega) \sim [\omega - v|q|]^{-g/2} \quad \text{as } |q| \to \omega/v. \tag{3.6}$$

The equal-time structure factor can also be readily computed by integrating the dynamical structure factor; as $q \to 0$,

$$S(2k_F+q) \sim A - A'(|q|\alpha/2)^{K_c}, \tag{3.7}$$

where A and A' are numbers of order 1 and α is a short-distance cutoff which we take to be $\alpha \sim v_F/D$. As promised, this singularity is much weaker than that exhibited by χ, and indeed the $2k_F$ component of the structure factor remains finite (but not differentiable) as $q \to 0$ (see Fig. 2).

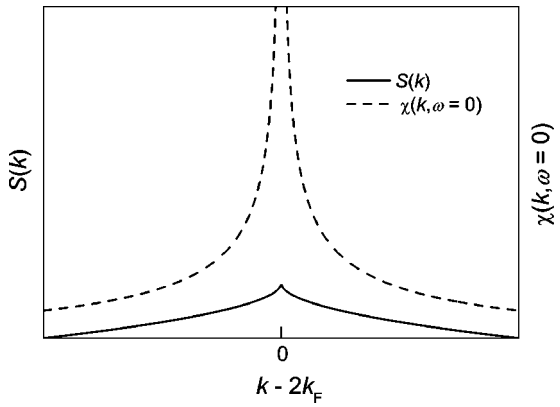

FIG. 2. The $T=0$ charge structure factor $S(k)$ (solid line) and the static susceptibility $\chi(k,\omega=0)$ (dashed line), of the Tomonaga-Luttinger liquid with $v_s=v_c$ and $K_c=0.5$.

[25] For reviews of the theory of the 1DEG, see Emery, 1979; Fradkin, 1991; Stone, 1994; Gogolin *et al.*, 1998.

We now turn to the spatial structure in the 1DEG induced by a single impurity at the origin. For K_c in this range, the $2k_F$ component of an impurity potential, whose amplitude we will denote by Γ, is a relevant perturbation (Kane and Fisher, 1992, 1994) with (boundary) scaling dimension $d=\frac{1}{2}(K_c+1)$. Thus there is a *crossover energy scale* $T_K \propto \Gamma^{2/(1-K_c)}$ such that excitations with energy large compared to T_K see a weak backscattering potential and are thus only weakly perturbed by the impurity. Conversely, for energies low compared to T_K, the system is controlled (Kane and Fisher, 1992, 1994) by the fixed point at $\Gamma \to \infty$. However, at this fixed point, the high-energy cutoff is replaced by a renormalized cutoff, $D \to T_K$.

We begin therefore by considering the limit $\Gamma=\infty$, i.e., a semi-infinite system with $x \geqslant 0$ and the boundary condition that no current can flow past $x=0$. For finite Γ, this solution is applicable for all energies $|E| \ll T_K$. The Fourier transform of the impurity-induced local density of states,

$$N(k,E)=N^{>}(k,E)+N^{<}(k,E), \tag{3.8}$$

$$N^{<}(k,E)=\frac{1}{2\pi}\int_{-\infty}^{\infty} dt \int_0^{\infty} dx\, g^{<}(x,x;t)e^{i(Et-kx)},$$

can be computed using exact expressions for the appropriate single-hole Green's function (Eggert *et al.*, 1996; Mattsson *et al.*, 1997; Eggert, 2000):

$$\begin{aligned} g^{<}(x,x;t) &= \sum_{\sigma} \langle \Psi_{\sigma}^{\dagger}(x,t)\Psi_{\sigma}(x,0)\rangle \\ &\equiv g_0(x,t)+[e^{i2k_F x}g_{2k_F}(x,t) \\ &\quad + e^{-i2k_F x}g_{-2k_F}(x,t)]+\cdots, \end{aligned} \tag{3.9}$$

where $g_0(x,t)$ is the long-wavelength part and $g_{2k_F}(x,t)$ is the $2k_F$ part; the single-electron piece can be computed similarly from $g^{>}$, or more simply from the relation between their respective spectral densities, $N^{<}(k,E)=e^{-E/T}N^{>}(k,E)$. We shall be interested in the $2k_F$ component, which clearly contains information about charge-density-wave correlations in this semi-infinite 1DEG, and for which a general expression in space and time has been given by Eggert and others (Eggert *et al.*, 1996; Mattsson *et al.*, 1997; Eggert, 2000). As with the structure factor, the $2k_F$ part of $N(k,E)$ can also be expressed in terms of a scaling function Φ as (see Appendix A)

$$N(q+2k_F,E)=\frac{B}{2E}\left(\frac{\alpha E}{v_c}\right)^{2b}\Phi\left(\frac{2E}{v_c q},\frac{E}{T}\right), \tag{3.10}$$

where $b=(1-K_c)^2/8K_c$ and B is a dimensionless constant; we have left implicit the dependence on the dimensionless parameters K_c and v_c/v_s.

The scaling form of $N(k,E)$, given in Eq. (3.10), expresses the fact that the Luttinger liquid is a quantum critical system. The spectrum of the Luttinger liquid and the existence of a charge-ordered state induced by the impurity dictate entirely the structure of the scaling function $\Phi(x,y)$: it has a multisoliton continuum for both right- and left-moving excitations, each with leading thresholds associated with one-soliton states carrying separate spin and charge quantum numbers and moving at their respective velocities, as well as a nonpropagating feature associated with the pinning of the charge-density-wave order by the impurity. Thus the STM spectrum exhibits all the striking features of the Luttinger liquid: spin-charge separation and quantum criticality, i.e., fluctuating order. The beauty of the 1DEG is that much of this can be worked out explicitly.

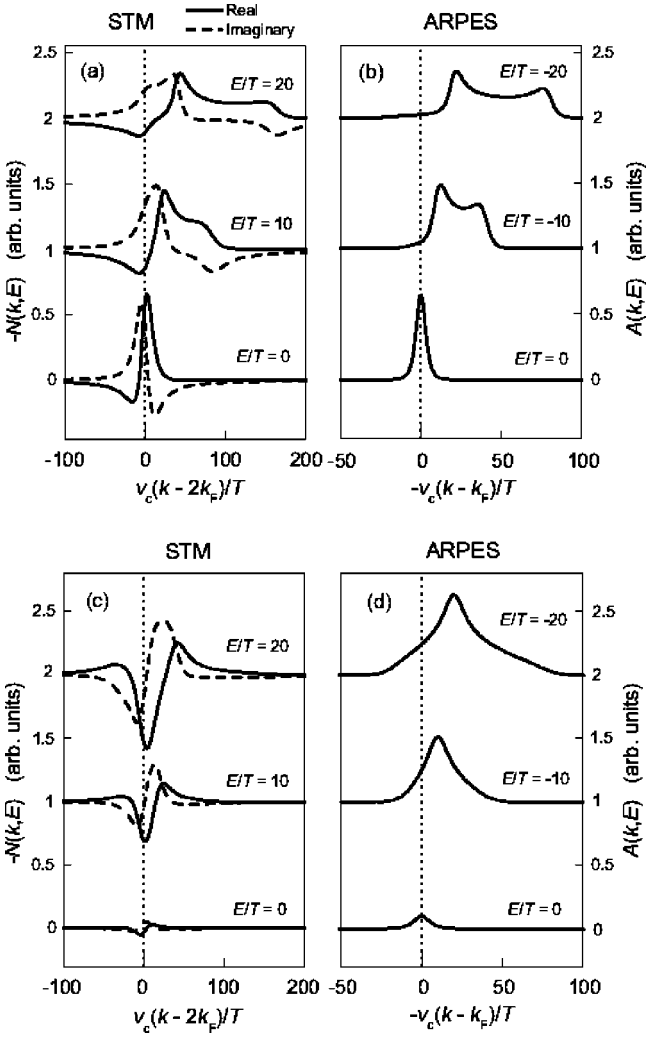

FIG. 3. Thermally scaled scanning-tunneling-microscope (STM) spectra $N(k,E)$ in the neighborhood of $k=2k_F$ [(a) and (c)] and angle-resolved photoemission spectroscopy (ARPES) spectra near $k=k_F$ [(b) and (d)]. In all cases, $v_c/v_s=4$ and $K_s=1$; for (a) and (b) $K_c=0.5$ ($b=1/16$), while for (c) and (d) $K_c=0.17$ ($b=1/2$). In (a) and (c), the density-of-states oscillations are induced by an impurity scatterer at the origin with $T_K \gg E$. In the STM spectra, the real and imaginary parts are represented by the solid and dashed lines, respectively. The curves for $E/T=10$ and $E/T=20$ are offset by 1 and 2, respectively, in arbitrary units.

In Figs. 3(a) and 3(c) we show the scaling function computed numerically for various representative values of the parameters. The plots show the real and imaginary parts of $N(2k_F+q,E)$ at fixed E/T as a function of

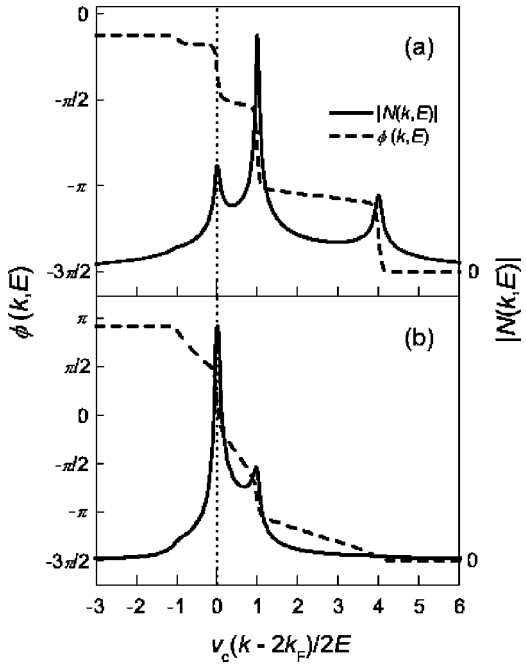

FIG. 4. Low-temperature ($E/T=100$) form of the STM spectra with k near $2k_F$, for the same parameters as in Fig. 3; (a) $K_c=0.5$; and (b) $K_c=0.17$. Here, we have expressed $N(k,E)=|N(k,E)|\exp[i\phi(k,E)]$ where the amplitude is shown as a solid line and the phase as a dashed line.

the scaled momentum $v_c q/T$, for $|q|\ll k_F$. For comparison, we also show (Orgad *et al.*, 2001) in Figs. 3(b) and 3(d), the single hole spectral function $A(k_F+q,\omega)$ that would be measured in an angle resolved photoemission spectroscopy (ARPES) experiment on the same system in the absence of an impurity.

There are several things to note about these plots.[26]

(1) Because of the quantum critical scaling form, high energy and low temperature are equivalent. Note, however, that in interpreting the large E/T spectra as representative of the low-temperature behavior of the system, it is important to remember that the thermal scaling of the k axis of the figure hides the fact that all features of the spectrum are becoming sharper as $T\to 0$; this is made apparent in Fig. 4.

(2) It is clear that there are right-dispersing features of the scaling functions characterized by the spin and charge velocities. The interference between dispersing features of the ARPES spectrum near k_F and $-k_F$ can be loosely thought of as giving rise to the dispersing features in the STM spectrum; indeed, as $K_c\to 1$ (the noninteracting limit), $\mathrm{Re}\{N(2k_F+q,E)\}\propto A(k_F-q/2,-E)$ at fixed $E>0$. However, it is also clear from the figure that the stronger the interactions, the less direct is the resemblance between $N(2k_F+q,E)$ and $A(k_F-q/2,-E)$.

(3) There is also a very weak feature in the spectrum, visible only at quite large E/T (compare Figs. 3 and 4), which disperses in the opposite direction (left) to the main features of the spectra with velocity $-v_c$. Because these spectra are shown only for k's in the neighborhood of $+2k_F$ [or $+k_F$ for $A(k,E)$], there is no symmetry between right- and left-moving excitations. If we showed the spectra on a larger scale, there would of course be the mirror symmetric spectra near $-2k_F$ (or $-k_F$) as required by Kramer's theorem.

(4) In the STM spectrum, but not in the ARPES spectrum, there is a feature near $q=0$ which does not disperse with increasing energy; this is directly related to the pinned charge-density-wave order. Note that for $K_c=0.5$, this feature is weak in Fig. 3, and only becomes prominent at very large E/T, as shown in Fig. 4; but this is the most important feature of the data if one is interested in evidence of pinned charge-density-wave order.

Lesson 3: From this explicit example we learn that dispersing features in an STM measurement that resemble the interference effects that arise from noninteracting quasiparticles do not necessarily imply the existence of well-defined quasiparticles!

It is interesting to compare $N(k,E)$ with the local density of states averaged over some energy scale,

$$\tilde{N}(2k_F+q,E)\equiv E^{-1}\int_{-E}^{0} d\epsilon\, N(2k_F+q,\epsilon). \qquad (3.11)$$

Note that at $T=0$, $E\tilde{N}(k,E)\to\langle\rho_k\rangle$ as $E\to\infty$. However, the expression we have used for $N(k,E)$ was derived for an infinite strength scattering potential, and so is only valid up to energies of the order of $T_K\ll D$. This integrated quantity is shown in Fig. 5 for representative parameters[27] at $T=0$. In the limit as $q\to 0$, $\tilde{N}(2k_F+q,T_K)$ has the asymptotic behavior

$$\tilde{N}(2k_F+q,T_K)\propto\left(\frac{1}{T_K}\right)\left(\frac{\alpha T_K}{v_c}\right)^{2b}\left(\frac{T_K}{v_c q}\right)^{g/2}. \qquad (3.12)$$

Both the integrated induced tunneling density of states and the induced tunneling density of states at fixed voltage E have a singular behavior of the form $q^{-g/2}$ (see Appendix A). However, the big difference is that $N(k,E)$ has dispersing singularities in addition to the nondispersing singularity at $k\to 2k_F$, while the singularity at $k\to 2k_F$ is the only singular feature of $\tilde{N}(k,T_K)$. Thus $\tilde{N}(k,T_K)$ is more easily analyzed for evidence of an almost ordered charge-density-wave state.

At energies $E>T_K$, the response of the system to the presence of the impurity is weak (i.e., proportional to Γ), and can be computed in perturbation theory. For in-

[26]Details of the asymptotic analytic behaviors of the singularities exhibited in these plots can be found in Appendix A.

[27]For technical reasons, what is actually plotted in Fig. 5 is $\tilde{N}(k)\equiv\lim_{T_K\to\infty}\int_{-\infty}^{\infty}dE[1-f(E)]N(k,E)$, where f is the Fermi function, but the distinction between this and $\tilde{N}(k,T_K)$ is not important here.

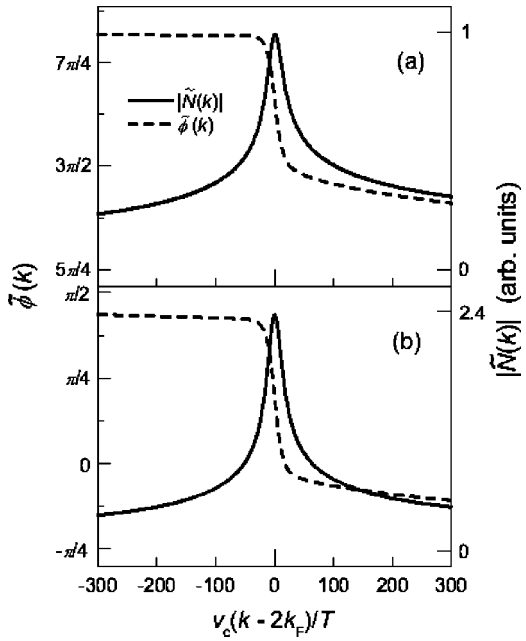

FIG. 5. Thermally scaled integrated STM spectra $\tilde{N}(k) \equiv |\tilde{N}(k)|e^{i\tilde{\phi}(k)} \sim \tilde{N}(k,T_K)$ in the neighborhood of $k=2k_F$ for $v_c/v_s=4$ and $K_s=1$: (a) $K_c=0.5$; and (b) $K_c=0.17$. The solid line is the amplitude and the dashed line is the phase. (See Appendix A for details.)

stance, in the weak-impurity limit $T_K \to 0$ the integrated response of the system over all energies is dominated by the high-energy, perturbative regime where at $T=0$ we find, in agreement with the sum rule of Eq. (2.9) (see also Appendix A),

$$\tilde{N}(2k_F+q,D) = \chi_{\rm ch}(2k_F+q)\Gamma + O(\Gamma^2). \tag{3.13}$$

By comparing the weak Γ behavior of $\tilde{N}(2k_F+q,D)$ [Eq. (3.13)] with its behavior in the opposite $\Gamma \to \infty$ limit, Eq. (3.12), we see that since $\chi_{\rm ch} \sim |q|^{K_c-1}$ (as $q \to 0$), the integrated local density of states for small Γ is much more singular as $q \to 0$ than for large Γ. This is a necessary consequence of the fact that the backscattering impurity potential is a relevant perturbation.

It is also worth noting that the impurity-induced local density of states at a fixed finite distance x from the impurity,

$$\delta\mathcal{N}(x,E) \sim E^{(1-K_c)/2K_c}, \tag{3.14}$$

is always large at low energies $|E| \ll v/x$ compared to the background density of states of the clean Tomonaga-Luttinger liquid,

$$\mathcal{N}(E) \sim E^{(1-K_c)^2/4K_c}. \tag{3.15}$$

This is yet another illustration of the way impurities enhance the low-energy effects of fluctuating order.

IV. TWO-DIMENSIONAL FERMI LIQUID

In this section, we consider the application of these ideas to the case of weakly interacting electrons in two dimensions. To obtain explicit results, we shall consider electrons with a quadratic dispersion $\epsilon_{\mathbf{k}} = \hbar^2\mathbf{k}^2/2m$.

Although, as seen in Eq. (2.8), $\chi_{\rm DOS}$ is a two-particle correlator, for noninteracting quasiparticles, it can be expressed as a convolution (Byers *et al.*, 1993; Polkovnikov *et al.*, 2003) of two single-particle Green's functions:

$$\chi_{\rm DOS}(\mathbf{k},E) = -\frac{1}{\pi}\mathrm{Im}\left\{ \int \frac{d\mathbf{q}}{(2\pi)^d} G(\mathbf{k}+\mathbf{q},E)G(\mathbf{q},E) \right\}. \tag{4.1}$$

Therefore, in weakly interacting systems, $\chi_{\rm DOS}$ can be analyzed to obtain information about the single-particle spectrum. Explicitly, it is easy to see that for free electrons in 2D $\chi_{\rm DOS}(\mathbf{k},E)$ is given by

$$\chi_0(\mathbf{k},E) = \frac{m}{\pi\hbar^2} \frac{\theta(\epsilon_{\mathbf{k}} - 4E)}{\sqrt{\epsilon_{\mathbf{k}}(\epsilon_{\mathbf{k}} - 4E)}}. \tag{4.2}$$

Here, the subscript 0 is introduced for later convenience to signify χ in the noninteracting limit, and once again $\theta(x)$ is the Heaviside (step) function. For fixed E as a function of $\mathbf{k}$, this quantity diverges along curves in $\mathbf{k}$ space, where $\epsilon_{\mathbf{k}} = 4E$ ($|\mathbf{k}| = 2k_F$). Note that the fact that χ_0 vanishes for $\epsilon_{\mathbf{k}} < 4E$ is a peculiarity of the 2D case with infinite quasiparticle lifetime. In three dimensions,

$$\chi_0(\mathbf{k},E) = \frac{1}{8\pi^2}\left(\frac{2m}{\hbar^2}\right)^{3/2} \frac{1}{\sqrt{\epsilon_{\mathbf{k}}}} \ln\left| \frac{2\sqrt{E} + \sqrt{\epsilon_{\mathbf{k}}}}{2\sqrt{E} - \sqrt{\epsilon_{\mathbf{k}}}} \right|, \tag{4.3}$$

which also has a singularity as $\epsilon_{\mathbf{k}} \to 4E$, but is nonzero (and positive) for all $E > 0$. In contrast, as shown in Sec. III, in a 1D Luttinger liquid the induced density of states has a phase jump as k crosses any of the propagating or nonpropagating singularities. It is straightforward to see that in both two and three dimensions a finite quasiparticle lifetime leads to a rounding of the singularities and that in two dimensions it also leads to a positive induced density of states for all $E > 0$. It is also simple to verify that to nonlinear order in the external potential, the induced density of states in two dimensions may or may not have a phase jump across the singularity, depending on the details of the perturbing potential. For instance, the induced local density of states produced by a single impurity can be computed (from the impurity t matrix); it exhibits sign reversal (π phase shift) across the singularity at $\epsilon_{\mathbf{k}} = 4E$ for a repulsive potential, but not for an attractive one. In contrast, as we shall show below, any $\mathbf{k}$-space structure that arises from proximity to a quantum critical point is derived from the susceptibility $\chi(\mathbf{k})$, which is real and positive, so it always produces a signal whose phase is constant.

Lesson 4: The density-of-states modulations induced by weak disorder in a noninteracting metal are quite different in character from those expected to arise from proximity to a charge-density-wave quantum critical point, both in that they disperse strongly as a function of energy, and that the peak intensities lie along curves (surfaces in three dimensions) in $\mathbf{k}$ space, as opposed to

the structure associated with isolated points in **k** space expected from near-critical fluctuations.[28]

The charge susceptibility itself, $\chi_0(\mathbf{k})$, is well known from many studies of the 2DEG. It has an extremely weak nonanalyticity, whenever $|\mathbf{q}|=2k_F$,

$$\chi_0(\mathbf{q})=\frac{m}{2\pi\hbar^2}\left(1-\theta(q-2k_F)\frac{\sqrt{q^2-4k_F^2}}{q}\right). \tag{4.4}$$

The inverse Fourier transform of this meager nonanalyticity is what gives rise to the famous Friedel oscillations in the neighborhood of an isolated impurity,

$$\langle\rho(r)\rangle\sim\frac{1}{r^2}\cos(2k_Fr). \tag{4.5}$$

What this means is that, for all intents and purposes, the Friedel oscillations are all but invisible in the Fourier transform of any conceivable STM experiment on a simple metal in $D>1$. Some nontrivial method of data analysis is necessary instead (Sprunger *et al.*, 1997; Briner *et al.*, 1998).

It is worthwhile considering the effects of interactions on this picture. For weak enough interactions, the effects can be treated in a Hartree-Fock approximation. Thus, if we absorb any interaction-induced changes in the band parameters into a renormalized band structure, the only change in the above analysis is that the external perturbation $V_{\mathbf{k}}$ in Eqs. (2.5) and (2.7) must be replaced by an effective potential, $V_{\mathbf{k}}\rightarrow V_{\mathbf{k}}+U_{\mathbf{k}}\rho_{\mathbf{k}}$, where U (which can be weakly **k** dependent) is the strength of the electron-electron repulsion. This leads to the usual RPA expression for the susceptibilities of the interacting system, and to

$$\chi_{\rm ch}(\mathbf{k})=[1-U_{\mathbf{k}}\chi_0(\mathbf{k})]^{-1}\chi_0(\mathbf{k}),$$
$$\chi_{\rm DOS}(\mathbf{k},E)=[1-U_{\mathbf{k}}\chi_0(\mathbf{k})]^{-1}\chi_0(\mathbf{k},E). \tag{4.6}$$

[It is the fact that E is a probe energy, not a frequency, that is responsible for the appearance simply of $\chi_0(\mathbf{k})$, rather than a frequency-dependent factor, in the expression for $\chi_{\rm DOS}(\mathbf{k},E)$.] Not surprisingly, since $\chi_0(\mathbf{k})$ is finite for all **k**, for small U there is little qualitative difference between $\chi_0(\mathbf{k})$ and $\chi(\mathbf{k})$. However, if we imagine, as is often done (although we are not aware of any reason it is justified) that this RPA expression applies qualitatively for larger magnitudes of U, then as a function of increasing magnitude of U we would eventually satisfy a Stoner criterion for a charge-density-wave, $U_{\mathbf{k}}\chi_0(\mathbf{k})=1$. Here, due to the relatively weak **k** dependence of $\chi_0(\mathbf{k})$, the charge-density-wave ordering vector $\mathbf{Q}_{\rm ch}$ is determined as much by the **k** dependence of $U_{\mathbf{k}}$ as by effects intrinsic to the 2DEG.

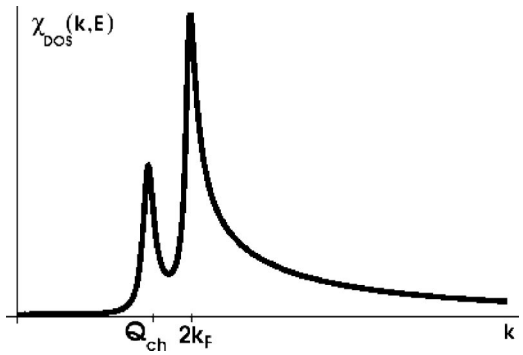

FIG. 6. The RPA expression for $\chi_{\rm DOS}(\mathbf{k},E)$ plotted as a function of momentum at a fixed, low-energy $E-\mu=0.2\mu$. A small decay rate, $\Gamma=0.025\mu$, is included to round the singularity and produce a finite $\chi_0(k,E)$ at all k. We have taken the phenomenological form for $\chi_{\rm ch}(\mathbf{k})$ discussed in the text. The figure was plotted with $\xi=5k_F^{-1}$ and $Q_{\rm ch}=1.8k_F$.

Following this line of analysis, let us consider the behavior of $\chi_{\rm DOS}(\mathbf{k},E)$ in the quantum disordered phase close to such a putative Stoner instability, where $\chi_{\rm ch}(\mathbf{k})$ is highly peaked at $\mathbf{k}=\mathbf{Q}_{\rm ch}$. For **k** far from the ordering vector, both the **k** and E dependence of $\chi_{\rm DOS}$ are determined largely by $\chi_0(\mathbf{k},E)$. However, at fixed voltage, $\chi_{\rm DOS}(\mathbf{k},E)$ will also exhibit a peak at a $\mathbf{k}\approx\mathbf{Q}_{\rm ch}$, with a voltage-dependent intensity proportional to $\chi_0(\mathbf{Q}_{\rm ch},E)$. Note, particularly, that as long as there is a finite correlation length associated with the incipient order, i.e., so long as the peak in $\chi_{\rm ch}(\mathbf{k})$ has a finite width, the corresponding peak in $\chi_{\rm DOS}(\mathbf{k},E)$ will not generally occur precisely at $\mathbf{Q}_{\rm ch}$. To illustrate this point, here and in Fig. 6 we adopt as a simple phenomenological model, $\chi_{\rm ch}(\mathbf{k})=A(\xi k_F)^2\exp[-(\xi^2/2)(|\mathbf{k}|-Q_{\rm ch})^2]$, where ξ is the stripe correlation length. From Eq. (4.6), it follows that in addition to the singularity inherited from $\chi_0(\mathbf{k},E)$, $\chi_{\rm DOS}(\mathbf{K},E)$ has a peak at a momentum **k** which satisfies

$$\mathbf{k}=\mathbf{Q}_{\rm ch}-\xi^{-2}\left[\frac{\epsilon_{\mathbf{k}}-2E}{\epsilon_{\mathbf{k}}-4E}\right]\nabla_{\mathbf{k}}\ln[\epsilon_{\mathbf{k}}]. \tag{4.7}$$

In short, the peak associated with incipient order is weakly dispersing (especially at energies far from any quasiparticle resonance condition) but so long as ξ is finite, the peak is never "nondispersing." (In contrast, the 1D example discussed above is quantum critical, so ξ is infinite, and the feature associated with fluctuating order is strictly nondispersive.)

Although the calculations are somewhat more involved (and therefore must be implemented numerically), the same sort of weak-coupling analysis can be carried out in the superconducting state. Oscillations induced by a mean field with period 4, representing stripes

[28]In practice, the distinction between an $N(\mathbf{k},\mathbf{E})$, which is peaked along curves, indicative of quasiparticle interference effects, and an $N(\mathbf{k},\mathbf{E})$ peaked at isolated "ordering" vectors $\mathbf{k}=\mathbf{Q}$ may not always be straightforward to establish in experiment. Consider the case in which there is an anisotropy of strength α in the effective mass of the 2DEG, i.e., $\epsilon_{\mathbf{k}}=\hbar^2(k_x^2+\alpha k_y^2)/2m$. In the limit of large anisotropy, $\alpha\gg1$, when the effects of the finite **k** resolution of actual experiments are taken into account, apparent peaklike structures can emerge. If we represent the effect of finite resolution by integrating the expression in Eq. (4.2) over a range of momenta around different points along the ellipse $\epsilon_{\mathbf{k}}=4E$, the integrated expression is peaked near $\mathbf{k}=\pm2\sqrt{2mE}\,\hat{e}_x$, where it is a factor of $\sqrt{\alpha}$ larger than at its minimum near $\sqrt{\alpha}\,\mathbf{k}=\pm2\sqrt{2mE}\,\hat{e}_y$.

with various internal structures in a *d*-wave superconductor, were carried out by Podolsky *et al.* (2002). As expected, the stripes induced oscillations in the local density of states with the period 4, but with energy dependences that reflected both the quasiparticle dispersion and the specific stripe structure assumed. Impurity-induced oscillations in the local density of states in a *d*-wave superconductor were computed by Byers *et al.* (1993) and Wang and Lee (2003), and the effects of proximity to a stripe-ordered state, at RPA level, were investigated by Polkovnikov *et al.* (2002). In all cases, interference and stripe-related effects interacted in fairly complex ways that required detailed analysis to disentangle.

Lesson 5: Depending on what regions of **k** space are probed, the STM spectrum can either be dominated largely by band-structure effects, or by the incipient charge-density-wave order. The most singular enhancement of the STM signal is expected to occur at energies such that a dispersing feature reflecting the underlying band structure passes through the ordering wave vector.

V. REGARDING EXPERIMENTS IN THE CUPRATES

Even where broken symmetry associated with stripe order has ultimately been proven to exist, establishing this fact has often turned out to be difficult for a number of practical reasons. In addition, since quenched disorder is always a relevant perturbation (in the renormalization-group sense), macroscopic manifestations of broken spatial symmetries are sharply defined only in the zero-disorder limit. Nevertheless, the existence of some form of order which coexists with superconductivity has implications for the phase diagram which can, in principle and sometimes in practice, be tested by macroscopic measurements. A particularly revealing set of phenomena occur when the strength of the superconducting order is modulated by the application of an external magnetic field.[29] Moreover, as discussed in Sec. V.C, from measurements of macroscopic transport anisotropies, electronic nematic order (e.g., point-group symmetry breaking) has been identified beyond all reasonable doubt in quantum Hall systems (Du *et al.*, 1999; Lilly *et al.*, 1999a), and very compelling evidence for its existence has been reported in the last year in underdoped $La_{2-x}Sr_xCuO_4$ and $YBa_2Cu_3O_{6+y}$ (Ando, 2002; Ando, Segawa, *et al.*, 2002).

However, most searches for stripe order rely on more microscopic measurements, especially elastic neutron scattering. One aspect of this that has caused considerable confusion is that, unless an external perturbation (such as weak crystalline orthorhombicity) aligns the stripes in one direction, one generally finds equal numbers of y-directed and x-directed domains, leading to quartets of apparently equivalent Bragg peaks, rather than the expected pairs. Fortunately, where sufficiently long-ranged order exists, it is possible, by carefully analyzing the scattering data, to distinguish this situation from one in which the peaks arise from a more symmetric "checkerboard" pattern of translation-symmetry breaking. From elastic neutron scattering [i.e., measurements of both the magnetic and the nuclear $S(\mathbf{k},\omega=0)$], and to a lesser extent from x-ray scattering, it has been possible to establish the existence of stripe-ordered phases in a wide range of members of the lanthanum cuprate family of high-temperature superconductors: $La_{1.6-x}Nd_{0.4}Sr_xCuO_4$ over the whole range of doped hole concentrations[30] from $0.05<x\leqslant 0.2$, $La_{2-x}Ba_xCuO_4$ (Fujita *et al.*, 2002), $La_{2-x}Sr_xCuO_4$ for[31] $0.02<x<0.13$, and $La_2CuO_{4+\delta}$ (Lee *et al.*, 1999) (including optimally doped material with a doped hole concentration ≈ 0.15 and a superconducting T_c of 42 K). Exciting preliminary evidence of charge-stripe order has been recently reported, as well, from elastic neutron scattering studies on underdoped $YBa_2Cu_3O_{6+y}$ [with $y=0.35$ and $T_c=39$ K (Mook *et al.*, 2002)] and optimally doped $YBa_2Cu_3O_{6+y}$ [with $y=0.93$ and $T_c=93$ K (Mook, 2002)]. And, it is worth mentioning, stripe order has also been similarly detected in a number of nonsuperconducting doped antiferromagnets,[32] including $La_{2-x}Sr_xNiO_{4+\delta}$ and the colossal magnetoresistance manganites.[33]

Conversely, it is important to note that so far no evidence of stripe order, or incipient stripe order, has been found in any of the electron-doped cuprate superconductors. Indeed, all the low-energy magnetism that has been reported to date (Yamada *et al.*, 2003) is peaked at the commensurate ordering wave vector $\mathbf{Q}_{AF}$, rather than at an incommensurate wave vector. This is rather strong evidence that at least spin-stripe order is absent in these materials. This does not rule out a possible role for charge inhomogeneity; perhaps the electron-doped materials are more prone to form bubble phases, i.e., crystalline phases with more than one doped electron per unit cell (Seul and Andelman, 1995; Fogler *et al.*, 1996).

We now turn to the core problem: Given a system that in the absence of quenched disorder or explicit

[29]For experimental studies, see Ando *et al.*, 1997; Tyler *et al.*, 1998; Katano *et al.*, 2000; Ono *et al.*, 2000; Lake *et al.*, 2001, 2002; Ando, 2002; Hoffman, Hudson, *et al.*, 2002; Khaykovich *et al.*, 2002; Hawthorn *et al.*, 2003; Liu *et al.*, 2003; for theoretical analysis, see Arovas *et al.*, 1997; Zhang, 1997; Ivanov *et al.*, 2000; Chakravarty, Laughlin, *et al.*, 2001; Demler *et al.*, 2001; Kivelson *et al.*, 2002; Polkovnikov *et al.*, 2002; Zhang *et al.*, 2002.

[30]See Tranquada *et al.* (1997); Ichikawa *et al.* (2000); Wakimoto *et al.* (2001).

[31]See Niedermayer *et al.* (1998); Suzuki *et al.* (1998); Kimura *et al.* (1999); Wakimoto *et al.* (1999, 2001); Matsuda *et al.* (2000).

[32]See Lee and Cheong (1997); Tranquada (1998a); Yoshizawa *et al.* (2000); Kajimoto *et al.* (2003).

[33]See Mori *et al.* (1998a, 1998b); Radaelli *et al.* (1999); Wang *et al.* (2000).

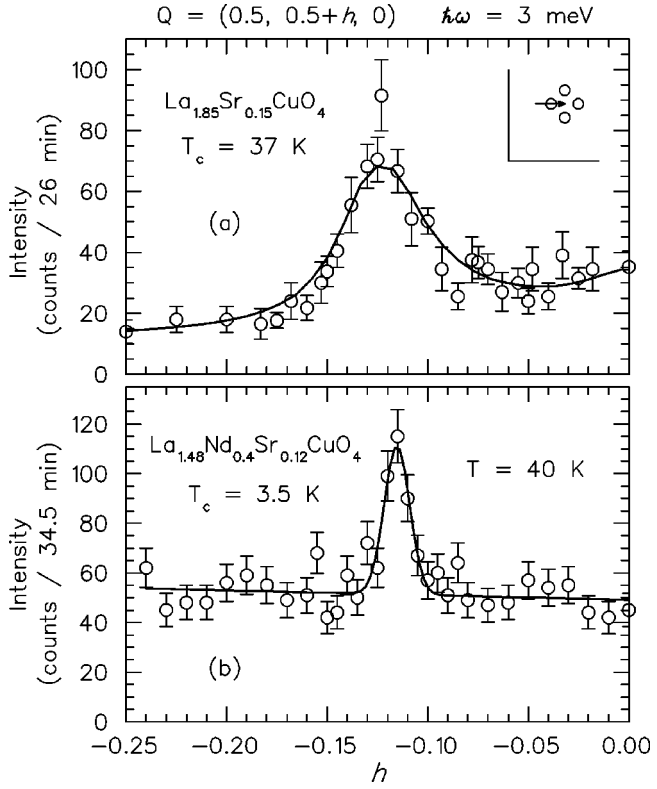

FIG. 7. Comparison of constant-energy scans at $\hbar\omega=3$ meV through an incommensurate magnetic peak (along path shown in inset) for (a) $La_{1.85}Sr_{0.15}CuO_4$ and (b) $La_{1.48}Nd_{0.4}Sr_{0.12}CuO_4$. Both scans are at $T=40$ K$>T_c$. Measurement conditions are described by Tranquada *et al.* (1999b).

symmetry-breaking terms is in an isotropic fluid state, how is the existence of substantial local stripe order identified?

A. Diffraction from stripes

Peaks in $S(\mathbf{k},\omega)$ at the characteristic stripe-ordering vectors indicate a degree of local stripe order. The k width of these peaks can be interpreted as an indication of the spatial extent of local stripe order, and the low-frequency cutoff as an indication of the typical stripe fluctuation frequency. So long as there is no spontaneous symmetry breaking, $S(\mathbf{k},\omega)$ necessarily respects all the point-group symmetries of the crystal, and thus will necessarily always show peaks at quartets of $\mathbf{k}$ values, never the pairs of $\mathbf{k}$ values of a single-domain stripe-ordered state.

Low-frequency spin fluctuations with relatively sharp peaks at incommensurate wave vectors were detected many years ago in inelastic neutron-scattering studies (Thurston *et al.*, 1989, 1992; Cheong *et al.*, 1991) of optimally doped ($x\approx0.15$, $T_c\sim38$ K) $La_{2-x}Sr_xCuO_4$. However, not until the discovery (Tranquada, Sternlieb, *et al.*, 1995) of "honest" stripe-ordered phases in the closely related compound $La_{1.6-x}Nd_{0.4}Sr_xCuO_4$ was the interpretation of these peaks as being due to stripe fluctuations made unambiguously clear. For instance, as shown in Fig. 7, the magnetic structure factor at low temperature and small but finite frequency, $\hbar\omega=3$ meV, looks very similar (in absolute magnitude and width) in both $La_{1.6-x}Nd_{0.4}Sr_xCuO_4$ with $x=0.12$, where elastic scattering indicating statistically ordered stripes has been detected (Tranquada, Sternlieb, *et al.*, 1995), and in $La_{2-x}Sr_xCuO_4$ with $x=0.15$, where no such static order is discernible (Yamada *et al.*, 1995). As discussed in the previous section, this is precisely the expected behavior near a quantum critical point, where presumably the partial substitution of La by Nd has moved the system from slightly on the quantum-disordered side to slightly on the ordered side of a stripe-ordering quantum critical point.[34] We can now confidently characterize $La_{2-x}Sr_xCuO_4$ over an extremely broad range of doping as being either in a stripe-ordered or a nearly ordered stripe liquid phase.

An important test of this idea comes from studies of the changes in $S(\mathbf{k},\omega)$ produced by weak disorder. Specifically, in Fig. 8, we compare the low-frequency (Matsuda *et al.*, 1993) and elastic (Hirota *et al.*, 1998) pieces of the magnetic structure factor of $La_{2-x}Sr_xCuO_4$ in the presence and absence of a small concentration (1.2%) of Zn impurities. (Zn substitutes for Cu.) As one might have expected, the Zn slightly broadens the $\mathbf{k}$-space structure, although not enormously (Kimura *et al.*, 1999; Tranquada *et al.*, 1999a). Most dramatically, the Zn "pins" the stripe fluctuations, in the sense that what appear only as finite-frequency fluctuation effects in the Zn-free material are pushed to lower frequencies and even to $\omega=0$ by the quenched disorder.[35]

The issue still remains actively debated whether or not various fluctuation effects seen in neutron-scattering studies of the other widely studied families of high-temperature superconductors, especially $YBa_2Cu_3O_{6+y}$ and $Bi_2Sr_2CaCu_2O_{8+\delta}$, can be associated with stripe fluctuations. We will not review this debate here, but will touch on it again in Secs. V.B and V.C, below.

One question arises (Chen *et al.*, 2002) concerning how we can distinguish a fluctuating stripe phase from a fluctuating checkerboard phase (which breaks translation symmetry but preserves the symmetry under exchange of x and y). Of course, the strongest indication that stripes, rather than checkerboards, are responsible for the observed fluctuations comes from the presence of nearby stripe-ordered phases, and the absence of any clear evidence of actual ordered checkerboard phases in

[34]This interpretation is further supported by the finding that the magnetic $S(\mathbf{k},\omega)$ in near-optimally doped $La_{2-x}Sr_xCuO_4$ has scaling properties consistent with its being dominated by a nearby stripe-ordering quantum critical point; see Aeppli *et al.*, 1997.

[35]It is certain that one effect of the Zn impurities is to pin the charge-stripe fluctuations. It may also be that the missing Cu spin plays an important role in slowing the spin fluctuations in the neighborhood of the Zn; the potential importance of this form of coupling, based on the behavior of a Kondo impurity in a system close to a magnetic quantum critical point, has been stressed by Sachdev *et al.*, 1999.

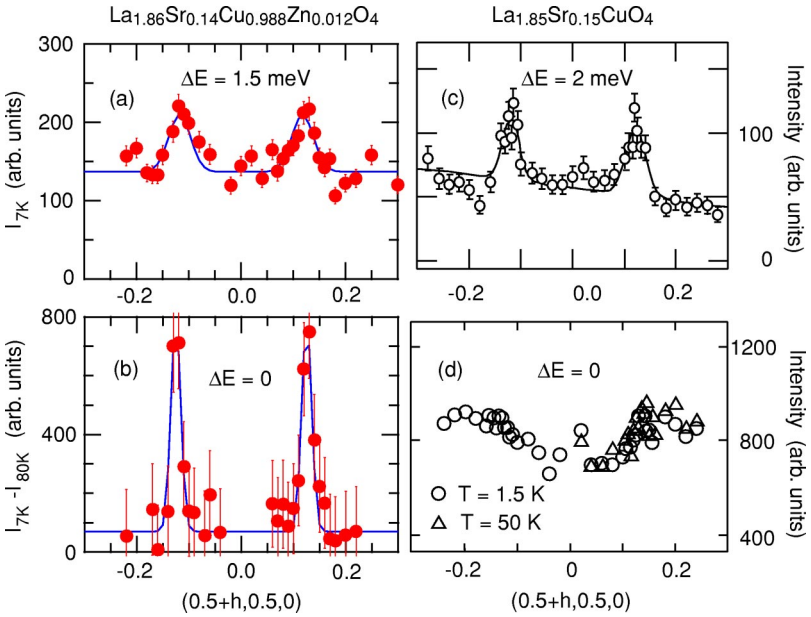

FIG. 8. (Color in online edition) Comparison of magnetic scattering measurements in $La_{2-x}Sr_xCuO_4$ with and without Zn; all scans are along $Q=(\frac{1}{2}+h,\frac{1}{2},0)$, measured in reciprocal lattice units. (a) Scan at $E=1.5$ meV and $T=7$ K; (b) difference between elastic scans measured at 7 and 80 K, both for $La_{1.86}Sr_{0.14}Cu_{0.988}Zn_{0.012}O_4$ ($T_c=19$ K) (Hirota, 2001); (c) scan at $E=2$ meV and $T=38$ K (Yamada *et al.*, 1998); (d) elastic scans at $T=1.5$ K (○) and 50 K (△) (Kimura *et al.*, 1999), for $La_{1.85}Sr_{0.15}CuO_4$ ($T_c=38$ K). Measurement conditions were different for each panel; see references for details.

any doped antiferromagnet, to date. However, in theoretical studies (Löw *et al.*, 1994; Fogler *et al.*, 1996; Moessner and Chalker, 1996; Chen *et al.*, 2002) both types of order appear to be close to each other in energy, so this argument should not be given undue weight.

Where both spin and charge peaks are observed, it turns out that there is a straightforward way to distinguish between the two. From Landau theory it follows (Zachar *et al.*, 1998) that there is a preferred relation between the spin- and charge-ordering wave vectors, $\mathbf{Q}_s+\mathbf{Q}'_s=\mathbf{Q}_{ch}$. For stripe order, this means that the spin and charge wave vectors are parallel to each other, and related (up to a reciprocal lattice vector) by the relation $2\mathbf{Q}_s=\mathbf{Q}_{ch}$. However, in the case of checkerboard order, the dominant spin-ordering wave vector is *not* parallel to the charge-ordering wave vectors; if $\mathbf{Q}_{ch}=(2\pi/a)(\pm\delta_{ch},0)$ and $\mathbf{Q}'_{ch}=(2\pi/a)(0,\pm\delta_{ch})$, the corresponding spin-ordering vectors, $\mathbf{Q}_s=\mathbf{Q}_{AF}\pm(2\pi/a)\times(\frac{1}{2}\delta_{ch},\frac{1}{2}\delta_{ch})$ and $\mathbf{Q}'_s=\mathbf{Q}_{AF}\pm(2\pi/a)(\frac{1}{2}\delta_{ch},-\frac{1}{2}\delta_{ch})$ satisfy the requisite identities. Thus the relative orientation of the spin and charge peaks can be used to distinguish fluctuating stripe order from fluctuating checkerboard order (Tranquada *et al.*, 1999a).

B. Scanning tunneling microscope measurements and stripes

1. General features

Scanning tunneling microscopy is a static probe and thus cannot detect any structure associated with fluctuating order unless something pins it.[36] Density or "Friedel oscillations" (Friedel, 1958) in simple metals produced by the presence of a defect are directly related to Fermi-surface-derived nonanalyticities in the susceptibility $\chi(\mathbf{k})$. However, "generalized Friedel oscillations" can occur in more diverse systems in which the relevant structure in $\chi(\mathbf{k})$ is not directly related to any feature of a Fermi surface. For instance, a bosonic superfluid on a lattice close to a second-order transition to an insulating, bosonic crystalline phase would exhibit generalized Friedel oscillations with the characteristic wavelength of the roton minimum—these oscillations, in a very direct sense, would image the fluctuating crystalline order present in the fluid state.

There are a few important features of generalized Friedel oscillations which follow from general principles. If the liquid state is proximate to a highly anisotropic state, such as a stripe state, the values of $\mathbf{k}=\mathbf{Q}$ at which χ has maxima will reflect the pattern of spatial symmetry breaking of the ordered state, but $\chi(\mathbf{k})$ will respect the full point-group symmetry of the crystal unless the liquid state spontaneously breaks this symmetry, e.g., is a nematic. So, the generalized Friedel oscillations around a point impurity in a stripe liquid phase will inevitably form a checkerboard pattern, unless some form of external symmetry-breaking field is applied (Polkovnikov *et al.*, 2002).

There is another form of spatial modulation of the density of states, one with a period that disperses as a function of the probe energy, which is sometimes (incorrectly, we believe) referred to in the STM literature as Friedel oscillations. This latter effect, which was first demonstrated by Crommie *et al.* (1993), is produced by the elastic scattering of quasiparticles of a given energy off an impurity. The resulting interference between scattered waves leads to variations of the local density of states at wave vectors $\mathbf{Q}=\mathbf{k}-\mathbf{k}'$, where $\mathbf{k}$ and $\mathbf{k}'$ are the wave vectors of states with energy $E=\epsilon(\mathbf{k})=\epsilon(\mathbf{k}')$, as determined by the band structure, $\epsilon(\mathbf{k})$. Generalized ver-

[36]See Sprunger *et al.*, 1997; Renner *et al.*, 1998; Hudson *et al.*, 1999; Yazdani *et al.*, 1999; Lang *et al.*, 2000; Pan *et al.*, 2000a, 2000b, 2001; Hoffman, Hudson, *et al.*, 2002; Howald *et al.*, 2003a, 2003b.

sions of these oscillations can occur even when there are no well-defined quasiparticles, so long as there are some elementary excitations of the system with well-defined dispersion relations, as is shown in Sec. III.

Thus in STM studies of cuprates we would expect stripe correlations to make an appearance as generalized Friedel oscillations, while quasiparticlelike interference is a distinct phenomenon that could also be present. The observation of a checkerboard pattern with a $4a$ period about vortex cores in $Bi_2Sr_2CaCu_2O_{8+\delta}$ by Hoffman, Hudson, *et al.* (2002) is provocative evidence for pinned charge stripes. These results motivated Howald *et al.* (2003a, 2003b), to search for similar evidence of stripes in $Bi_2Sr_2CaCu_2O_{8+\delta}$ with no applied field. The discussion below is focused on approaches for distinguishing and enhancing modulations due to generalized Friedel oscillations associated with such incipient order. Before continuing, though, we should note that compelling evidence for a quasiparticle interference response has been reported by Hoffman, McElroy, *et al.* (2002) and by McElroy *et al.* (2003). Those experimental results are not in direct conflict with those of Howald *et al.* (2003a, 2003b); however, there has been some controversy over interpretation, regarding whether the observed spatial modulations in the tunneling conductance are explained entirely by the interference mechanism, or whether interference modulations coexist with generalized Friedel oscillations. We shall return to that controversy in a subsection below.

Modulations that reflect the spectrum of elementary excitations are distinguishable (Polkovnikov *et al.*, 2003) from those related to incipient order in a variety of ways: whereas incipient order produces effects peaked near isolated ordering vectors $\mathbf{Q}$, the single-particle effects are peaked along extremal curves in $\mathbf{k}$ space which disperse as a function of E. Peaks in the Fourier-transformed local density of states $N(\mathbf{k},E)$ produced by incipient order tend to be phase coherent, while other features either have a random phase or a phase that is strongly energy dependent. Indeed, the phase information may be the best way to distinguish the consequences of incipient order from interference effects. Naturally, in the presence of true long-range charge order, $N(\mathbf{k},E)$ should exhibit sharp (resolution-limited) peaks which reflect the charge-density modulation in real space. This effect has been seen in STM measurements of the quasi-two-dimensional incommensurate charge-density-wave system $1T$-TaS_2, lightly doped with Nb, by Dai *et al.* (1991).

To demonstrate the effect of the phase, assume we have measured $N_L(\mathbf{r},\mathbf{E})$, the local density of states at a particular bias voltage, $V=E/e$ on a sample of size $L\times L$. Its Fourier transform, $N_L(\mathbf{k},E)$, has an arbitrary $\mathbf{k}$-dependent but E-independent phase, $e^{-i\mathbf{k}\cdot\mathbf{r}_0}$, which depends on the choice of origin of coordinates, $\mathbf{r}_0$. As discussed above, $N_L(\mathbf{k},E)$ can be expected to have contributions from incipient order (with wave vector $\mathbf{Q}$), and dispersing quasiparticles. Integrating the signal over a finite energy window yields the quantity $\tilde{N}(\mathbf{k},E)$, in which the contributions from incipient order over the entire range of integration add constructively, while other features tend to interfere destructively.[37] This mode of analysis is particularly useful if an energy window can be found in which none of the dispersing features expected on the basis of band-structure considerations have wave vectors equal to the expected ordering wave vector $\mathbf{Q}$.

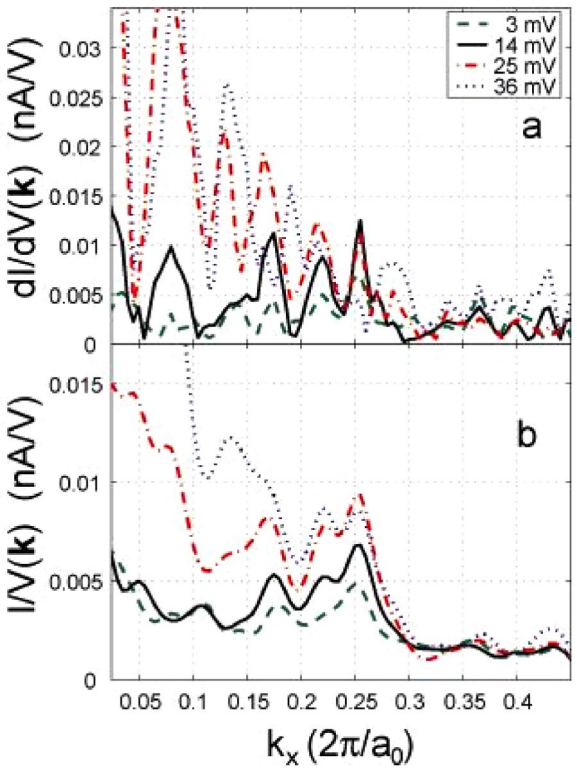

FIG. 9. (Color in online edition) The real part of the Fourier transform of the local density of states from an STM study of a near-optimally doped crystal of $Bi_2Sr_2CaCu_2O_{8+\delta}$. $\mathbf{k}$ is taken along the (1,0) direction, in a tetragonal convention: (a) $dI/dV\propto N(\mathbf{k},E)$ measured at fixed voltage, $V=E/e$; (b) $I/V\propto\tilde{N}(\mathbf{k},E)$, which is the integral of the quantity shown in (a) from $V=0$ to $V=E/e$.

Indeed, Howald *et al.* (2003b) have already demonstrated the first half of this point in STM studies of a very slightly overdoped sample of $Bi_2Sr_2CaCu_2O_{8+\delta}$ ($T_c=86$). They identified a peak which in $N(\mathbf{k},E)$ at approximately $\mathbf{k}=\pm\mathbf{Q}_{ch}\approx\pm(2\pi/a)(0.25,0)$ and $\mathbf{k}=\pm\mathcal{R}[\mathbf{Q}_{ch}]=\pm(2\pi/a)(0,0.25)$ (see Fig. 9), and showed that at these wave numbers the phase of $N(\mathbf{k},E)$ is energy independent for E between 0 and 40 meV, at which point the amplitude crosses through zero, i.e., the sign of the signal changes. The constancy of the phase implies that the location in real space of the density-of-states

[37]It is important to emphasize that both the phase and the amplitude information encoded in $N_L(\mathbf{k},E)$ are physically significant. The commonly used power spectrum $|N_L(\mathbf{k},E)|^2$ will not lead to destructive interference of propagating features when integrated over energies.

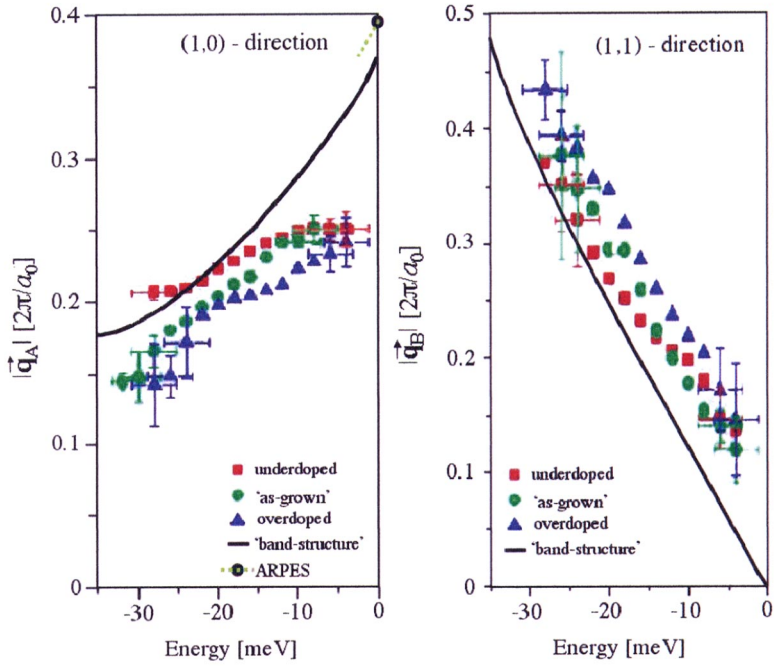

FIG. 10. (Color in online edition) Dispersion of the peaks in $N(\mathbf{k},E)$ (from STM measurements on near-optimally doped $Bi_2Sr_2CaCu_2O_{8+\delta}$) at wave vectors $\mathbf{k}_1$ [along the (1,0) direction] (left panel) and $\mathbf{k}_2$ along the (1,1) direction from Fig. 4 of Hoffman, McElroy, *et al.* (2002) (right panel). The solid lines are from a global fit to the ARPES spectrum, as described in the text.

modulation is fixed at all energies, which strongly indicates that it reflects pinned incipient order.

However, as explained above, the existence of incipient order can be magnified if we integrate the local density of states as a function of energy. In Fig. 9(a) we show data from Howald *et al.* (2003a, 2003b), in which the values of dI/dV were obtained by a Fourier transform of a real-space image at various voltages, $V=E/e$, on a patch of surface of size $L=160$ Å. The origin of coordinates was chosen such that $N_L(\mathbf{k},E)$ is real and positive for $\mathbf{k}=\mathbf{Q}_{\rm ch}$. In the figure, $\mathbf{k}$ is taken to lie along the (1,0) direction and what is shown is the real part of $N_L(\mathbf{k},E)$ (the imaginary part is generally small and noisy.) In Fig. 9(b), we show the same data averaged over energy from 0 to E, $I/V\propto\tilde{N}_L(\mathbf{k},E)$. It is apparent that integration enhances the strength of the peak at $\mathbf{Q}_{\rm ch}$ and depresses the remaining signal, especially when E is smaller than the maximum superconducting gap value, $\Delta_0\approx 35$ meV. Indeed, precisely this same integration technique was used previously by Hoffman, Hudson, *et al.* (2002) to enhance the magnetic-field-induced checkerboard pattern in vortex cores.

2. Differing interpretations of the STM spectra

As mentioned in the Introduction, there is controversy in the literature concerning the interpretation of the STM spectra, although there seem to be only relatively minor disagreements concerning the data themselves. Specifically, Hoffman, McElroy, *et al.* (2002) and still more recently McElroy *et al.* (2003) have suggested that the peaks seen in $N(\mathbf{k},E)$ can be accounted for entirely in terms of the interference pattern of sharply defined quasiparticles in a *d*-wave superconductor, with no need to invoke incipient stripe order—or any non-Fermi-liquid character of the elementary excitations, for that matter. Let us briefly review the line of reasoning that leads to this conclusion.

As we have seen (lesson 4), interference between quasiparticles in two dimensions naturally produces ridges in $N(\mathbf{k},E)$ along closed curves in $\mathbf{k}$ space, rather than the peaks observed in experiment. However, as was first recognized by Wang and Lee (2003), this result is modified by the extreme eccentricity of the contours of constant quasiparticle energy in a *d*-wave superconductor, where the dispersion in one direction is v_F and in the other is proportional to Δ_0. Consequently, with finite experimental resolution, at energies less than Δ_0, one obtains peaks in the interference patterns at points in $\mathbf{k}$ space which connect the tips of the contours that surround each of the four distinct nodal points on the Fermi surface.

Specifically, if we assume that there are well-defined quasiparticles with energy obtained by solving the Bogoliubov–de Gennes equations for a *d*-wave superconductor, then for each energy E there are eight values $\mathbf{q}_j$ (two in the neighborhood of each nodal point) which simultaneously satisfy the equations $\epsilon(\mathbf{q}_j)=0$ (i.e., they lie on the normal-state Fermi surface) and $\Delta_{\mathbf{q}_j}=E(\mathbf{q}_j)=E$ (i.e., the quasiparticle creation energy is E). Peaks in $N(\mathbf{k},E)$ will then occur at the various distinct values of $\mathbf{k}_{ij}=\mathbf{q}_i-\mathbf{q}_j$, of which there are seven (up to symmetry). For instance, the two wave vectors with smallest magnitudes are $\mathbf{k}_{12}=2q_x(1,0)$ and $\mathbf{k}_{13}=\sqrt{2}(q_x-q_y)(1/\sqrt{2},1/\sqrt{2})$, which come from the interference between the state $\mathbf{q}_1=(q_x,q_y)$ and, respectively, the states at $\mathbf{q}_2=(-q_x,q_y)$ and $\mathbf{q}_3=(q_y,q_x)$. The positions of the peaks in $N(\mathbf{k},E)$ thought to correspond to $\mathbf{k}_{12}$ and $\mathbf{k}_{13}$ from the work of Hoffman, McElroy, *et al.* (2002) are reproduced in Fig. 10. Given the quasiparticle interpretation of the STM spectrum, then from the observed

location of any two distinct peak positions $\mathbf{k}_{ij}$ at a given energy, it is possible to reconstruct the positions of all eight locations in the Brillouin zone $\mathbf{q}_j$ which give rise to all the expected peaks at this energy. Thus, where seven distinct peaks are observed [as are reported by McElroy *et al.* (2003) in some ranges of energy], the quasiparticle spectrum is highly overconstrained, and this provides a very stringent self-consistency check on the quasiparticle interpretation. According to McElroy *et al.* (2003), the peaks they observe generally pass this consistency check. The experimental case for dispersive features in $N(\mathbf{k},E)$ that are consistent with the quasiparticle interference mechanism is quite persuasive.

The controversy over interpretation revolves around the degree to which quasiparticle interference is sufficient to explain all of the structure in $N(\mathbf{k},E)$. Examining Fig. 10 (left panel) one can see that, for energies below $\sim$20 meV, $\mathbf{k}_{12}$ lies close to the expected stripe-ordering vector $\mathbf{Q}_{\rm ch}$. This is consistent with the experimental measurements and analysis by Howald *et al.* (2003b), who had interpreted this behavior as evidence for stripe order; in contrast, Hoffman, McElroy, *et al.* (2002) argued that the continuity with the dispersive signal favors a single mechanism based on band-structure effects.

In weighing these alternatives, it is useful to consider a second consistency check that the quasiparticle picture should satisfy. While, as shown in Eq. (4.1), $N(\mathbf{k},E)$ is actually a measure of a two-particle response function, to the extent that it is dominated by single-particle effects it should be expressible in terms of a convolution of single-particle Green's functions, as in Eq. (4.1). Thus it should be consistent with the behavior of the spectral function measured in ARPES. In evaluating this connection, significant challenges arise with respect to the sufficiency of the quasiparticle interpretation.

In the first place, ARPES consistently reveals strong deviations from a noninteracting line shape.[38] Well below T_c, the measured energy distribution curve at fixed $\mathbf{q}$ on the Fermi surface consists of a dispersing quasiparticlelike peak with a small weight, $Z \ll 1$, and a broad, and largely featureless multiparticle continuum which contains most of the spectral weight. Moreover, the quasiparticle peak is always anomalously broad with a distinctly non-Fermi-liquid temperature and energy dependence (Gweon *et al.*, 2001; Orgad *et al.*, 2001). If this measured spectral function were used to predict the structure of $N(\mathbf{k},E)$, then the quasiparticle interference features would be weak (Capriotti *et al.*, 2003) (in proportion to Z^2), which is something of a surprise given the apparent robustness of the experimental features. One might also expect the interference features to be broadened significantly by the short quasiparticle lifetimes at the probed energies. Perhaps the most important consequence is that the intensities of the structures should have a dramatic temperature dependence, going to zero as Z goes to zero at T_c. This provides a crucial test to which we shall return shortly.

In the second place, $\Delta_{\mathbf{q}}$ determined from the dispersion of the quasiparticlelike peak in ARPES differs significantly, especially at low energies, from that obtained by Hoffman, McElroy, *et al.* (2002) and McElroy *et al.* (2003) in STM. This is illustrated in Fig. 10, as well. The solid lines in the figure were computed [using the method of Wang and Lee (2003)] from a global fit to the measured ARPES spectrum, as follows: (1) The location of the Fermi surface, $\epsilon(\mathbf{q})=0$, was computed from the phenomenological band structure that had been obtained (Norman *et al.*, 1994; Damascelli *et al.*, 2003) from a fit to ARPES experiments. (2) The gap function along the Fermi surface was assumed to be of the simple d-wave form, $\Delta_{\mathbf{q}}=(\Delta_0/2)[\cos(q_x a)-\cos(q_y a)]$, a form that has been widely found to fit the measured ARPES spectrum in optimally doped and overdoped $Bi_2Sr_2CaCu_2O_{8+\delta}$, although significant deviations from this form are often seen in underdoped samples (Mesot *et al.*, 1999). The gap observed in ARPES experiments corresponds to $\Delta_0 \sim 35-45$ meV (Ding *et al.*, 1995; Loeser *et al.*, 1997; Fedorov *et al.*, 1999), near-optimal doping. For purposes of the figure, we have adopted $\Delta_0=40$ meV. The solid black circle in the figure was obtained from the location of the nodal point (which determines the zero-energy limit of all dispersion curves) as determined from ARPES experiments; this is a feature of the ARPES spectrum that has been looked at in great detail by several groups (Ding *et al.*, 1997; Valla *et al.*, 1999). There is agreement[39] within 1% accuracy that the nodal point, where $E(\mathbf{q})=0$, is $\mathbf{q}=(2\pi/a)(0.195,0.195)$. (Note that the phenomenological band structure was determined from a fit to older, less precise ARPES data, which is why the line in Fig. 10 does not quite approach the correct zero-energy limit; manifestly, correcting this discrepancy would only exacerbate the disagreement between STM and ARPES.)

It is clear from Fig. 10, as originally emphasized by Howald *et al.* (2003b), that there are significant discrepancies between the ARPES and STM results, especially below 20 meV. In particular, in the region of $\mathbf{k}$ space near the expected stripe-ordering wave vector, $\mathbf{k}=\mathbf{Q}_{\rm ch} \sim (2\pi/a)(\frac{1}{4},0)$, the STM spectrum is considerably less dispersive than would be expected on the basis of the ARPES data; it appears that the peak in $N(\mathbf{k},E)$ largely stops dispersing when it reaches this magic wave vector

[38] At very low energies and at low temperatures there is good reason to believe, and compelling evidence (although not from ARPES or STM) to confirm, that the nodal quasiparticles in the superconducting state are well defined and long lived; see May *et al.* (2000). However, most of the dispersing features seen in STM are at higher energies, typically at energies on the order of $\Delta_0/2$, where even at low temperatures there is no evidence of well-defined quasiparticles.

[39] We thank P. Johnson for pointing this out to us.

[see, for instance, the discussion surrounding Eq. (4.7)].[40]

It is not clear *a priori* how much significance one should attach to the discrepancies between ARPES data and the quasiparticle interpretation of the STM. Both are highly surface sensitive probes, so there is always the issue of whether either is telling us anything about the bulk properties of the materials, but this worry does not affect the comparison between the two sets of measurements.

It seems significant to us that the most serious quantitative differences between the ARPES dispersion and those inferred from a quasiparticle interpretation of the STM data occur at low energies and are particularly pronounced for $\mathbf{k}$'s near $\mathbf{Q}_{\rm ch}$, where effects of incipient stripe order are largest. In this context, it is worth noting that in the STM studies of Howald *et al.* (2003a) shown in Fig. 9, a peak at $\mathbf{k}=\mathbf{Q}_{\rm ch}$ is seen in all the curves with $E\leqslant 15$ meV all the way to $E=0$. Hoffman, McElroy, *et al.* (2002) and McElroy *et al.* (2003) do not report spectra below about 6 meV. It is possible that, as suggested by Howald *et al.* (2003a), this difference is a consequence of the stripe signal's being washed out due to the existence of many domains in the larger field of view used in the experiment of Hoffman, McElroy, *et al.* (2002).

Moreover, in their STM study of the magnetic-field-induced structure in vortex-core halos, Hoffman, Hudson, *et al.* (2002) observed oscillations at precisely these same wave vectors, $\mathbf{k}=\mathbf{Q}_{\rm ch}$, in the energy-integrated local density of states (in a 12-meV window about 0 voltage). The amplitude of these latter oscillations is very large compared with that of the disorder-induced signal, and the dominant contribution comes from energies around 7 meV.

We believe that the issues of interpretation can be definitively resolved by studies of the temperature and impurity concentration dependence of the signal. Since the contribution to $N(\mathbf{k},E)$ from quasiparticle interference is proportional to Z^2, and since Z is observed in ARPES experiments to have a strong temperature dependence and vanish above T_c, it should be very easy to quench the interference signal by heating; what is left at temperatures approaching T_c cannot be due to quasiparticle interference. And, of course, above T_c in overdoped samples, and above a suitable pseudogap temperature in underdoped samples, the superconducting gap vanishes, so only the more usual rings can possibly arise from quasiparticle interference. Conversely, as discussed previously, light Zn doping is known to pin stripes in $La_{2-x}Sr_xCuO_4$, so it is reasonable to expect the same effect in $Bi_2Sr_2CaCu_2O_{8+\delta}$. Thus stripe-related signals should be strengthened and made less sensitive to thermal depinning by small concentrations of Zn impurities in the Cu-O planes.

STM studies at elevated temperatures are technically demanding, but recently Vershinin *et al.* (2003) have achieved atomic-scale resolution at temperatures well above T_c on a $Bi_2Sr_2CaCu_2O_{8+\delta}$ surface. They report that for $T\sim T_c/2$ many of the peaks in $N(\mathbf{k},E)$ have, indeed, been extinguished. However, the low-energy portion of the peak at $\mathbf{k}_{12}$ (in Fig. 10) survives and even remains unattenuated, well above T_c. This effect clearly cannot be explained by the quasiparticle interference mechanism. An explanation in terms of pinned stripes seems much more plausible (although the persistence of a stripe-induced signal at such an elevated temperature requires further investigation).

One further feature of all the data that have been reported to date is worth commenting on. This is the large (factors of 2 or 3) differences observed (Hoffman, McElroy, *et al.*, 2002) in the peak intensities at $\mathbf{Q}_{\rm ch}$ and $R[\mathbf{Q}_{\rm ch}]$. Systematic experiments have not yet been conducted to verify whether this effect is real or an experimental artifact. If it is not an artifact, then this observation is among the first microscopic pieces of evidence of a strong local tendency to stripe-orientational (i.e., nematic) order. In addition, such large anisotropies are something that cannot be accounted for in any simple way by quasiparticle interference (nor local checkerboard order). It is important to bear in mind, however, that even if the observed anisotropy reflects nematic order, it is expected to decrease in magnitude (Howald *et al.*, 2003b) in direct proportion to $A^{-1/2}$, where A is the area of the field of view, due to the unavoidable domain structure produced by quenched disorder.

C. Detecting nematic order

While stripe order necessarily implies nematic order, the converse is not true. Although nematic order involves the spontaneous breaking of a spatial (point-group) symmetry, when there is no accompanying breaking of translation symmetry, even the identification of the ordered state is somewhat subtle, and this holds doubly for fluctuation effects. Moreover, since quenched disorder is always relevant and results in domain structure, true macroscopic measurements of spontaneous nematic symmetry breaking are not possible. The difficulty of detecting the rotational symmetry breaking associated with ordered stripes is illustrated by the case of $La_{2-x}Sr_xNiO_{4+\delta}$, a nonsuperconducting structural analog of $La_{2-x}Sr_xCuO_4$. Even transmission electron microscopy, which is capable of measuring over a fairly small sample area, tends to yield superlattice diffraction peaks for stripe order that reflect the fourfold symmetry of the NiO_2 planes in the tetragonal crystal structure (Chen *et al.*, 1993). Only recently have electron diffraction patterns consistent with the twofold symmetry of an ordered stripe domain been reported (Li *et al.*, 2003).

[40]The same discrepancy between ARPES and STM at low energies can be seen directly from full microscopic calculations of $N(\mathbf{k},E)$ for noninteracting quasiparticles. For instance, $N(\mathbf{k},E)$ was recently computed by Polkovnikov *et al.* (2003) for noninteracting quasiparticles scattering from a point impurity; it is apparent from their Fig. 4 that, at energies of 20 meV and below, there is a local *minimum* in the neighborhood of $\mathbf{k}=\mathbf{Q}_{\rm ch}$, rather than a peak! The same is apparent in Figs. 2 and 3 of Wang and Lee (2003).

Thus almost all tests of nematic order in solids necessarily involve the observation of an unreasonably large, and strongly temperature-dependent, anisotropy in the electronic response to a small symmetry-breaking field which favors the x direction over the y direction.

1. Transport anisotropies

An example of a system in which the electronic response shows a large anisotropy is provided by the 2DEG in quantum Hall devices. While the fractional quantum Hall effect dominates the physics at very high magnetic fields, at intermediate magnetic fields (so that more than one Landau level is occupied), it has recently been discovered (Du *et al.*, 1999; Lilly *et al.*, 1999a) that there is a set of anisotropic states which have been identified (Fradkin and Kivelson, 1999; Fradkin *et al.*, 2000; Cooper *et al.*, 2002) as being quantum Hall nematics. These states can be thought of as melted versions of the long-predicted (Fukuyama *et al.*, 1979; Koulakov *et al.*, 1996; Moessner and Chalker, 1996) quantum Hall smectic (or stripe) phases. They are characterized by a large resistance anisotropy, $\rho_{xx} \gg \rho_{yy}$, which onsets very strongly below a characteristic temperature $T_n \sim 100$ mK. The precise origin of the symmetry-breaking field which aligns the nematic domains in these experiments has not been unambiguously determined (Cooper *et al.*, 2001; Zhu *et al.*, 2002). However, by applying (Lilly *et al.*, 1999b; Pan, Jangwirth, *et al.*, 2000; Cooper *et al.*, 2002) an in-plane magnetic field, one can vary the magnitude of the symmetry-breaking field, and the transition can be significantly rounded, giving evidence (Cooper *et al.*, 2002) that local stripe order persists up to temperatures well in excess of T_n. Even the orientation of the nematic order can be switched, resulting in a state with $\rho_{xx} \ll \rho_{yy}$.

Experiments that involve such fine control of an external symmetry-breaking field are considerably harder to carry out in the context of the cuprates. Some of the relevant materials, such as $Bi_2Sr_2CaCu_2O_{8+\delta}$ and $La_{2-x}Sr_xCuO_4$ with $x > 0.05$, have an orthorhombic axis at 45° to the expected stripe directions (i.e., a nematic phase can be defined in terms of spontaneous breaking of the mirror plane which lies along the orthorhombic a axis). In these materials, if one wishes to align the nematic domains, one must apply a suitable external symmetry-breaking field such as a uniaxial strain or in-plane magnetic field; however, such experiments tend to be challenging.

When the principle axes of an orthorhombic phase lie parallel to the expected stripe directions, the orthorhombicity (typically $<2\%$ in cuprates) plays the role of a small, external symmetry-breaking field. Examples where this occurs are superconducting $YBa_2Cu_3O_{6+y}$ with $0.35 \leqslant y \leqslant 1$ and nonsuperconducting $La_{2-x}Sr_xCuO_4$ with $0.02 \leqslant x < 0.05$. In both of these cases, resistivity anisotropies as large as a factor of 2 have been observed (Ando, Segawa, *et al.*, 2002) in detwinned single crystals. Moreover, as in the quantum Hall case, this anisotropy is strongly temperature dependent; in $La_{2-x}Sr_xCuO_4$, $|\rho_{aa}/\rho_{bb} - 1| < 10\%$ for temperatures in excess of $T_n \sim 150$ K. Polarization-dependent measurements of the infrared conductivity on a detwinned $x = 0.03$ crystal of $La_{2-x}Sr_xCuO_4$ reveal that the frequency dependence of the conductivity anisotropy has a scale comparable to kT_n (Basov, 2002). Large anisotropies in the frequency-dependent conductivity have also been observed (Basov *et al.*, 1995) in $YBa_2Cu_3O_{6+y}$ and in $YBa_2Cu_4O_8$, although in those cases, some part of the conductivity anisotropy must be due directly to the Cu-O chains. Taken together, these various observations are circumstantial evidence of a fair degree of local stripe order and of the presence of a nematic phase, the trouble being that, without a somewhat quantitative theory (which does not exist), it is hard to say how large an observed resistance anisotropy must be in order to be accepted as being an "unreasonably large" response to the orthorhombicity, that is, one that can only be understood in terms of the alignment of nematic domains.

More subtle investigations of orientational symmetry breaking can be undertaken by studying the transport in the presence of a magnetic field. A very clever approach along these lines was introduced by Noda *et al.* (1999). They applied a voltage along one axis of the CuO_2 planes and a magnetic field perpendicular to the planes in order to break the fourfold symmetry of the crystal structure and to obtain evidence of one-dimensional charge transport. In a stripe-ordered state, the geometry used should be sensitive primarily to those domains in which the stripes are aligned parallel to the direction of the applied voltage. For $x \leqslant \frac{1}{8}$, they found that, within the stripe-ordered phase, the transverse conductivity tends to zero at low temperature while the longitudinal conductivity remains finite. [This effect has been explained in terms of the electron-hole symmetry of a $\frac{1}{4}$-filled charge stripe (Emery *et al.*, 2000; Prelovšek *et al.*, 2001).]

Ando *et al.* (1999) have observed a remarkable anisotropy of the resistivity tensor induced by an in-plane magnetic field in nonsuperconducting $YBa_2Cu_3O_{6+y}$ with $y = 0.32$ and $y = 0.3$. (Presumably, these samples are antiferromagnetic.) The results were interpreted as evidence for nematic stripe order. Alternative explanations in terms of anisotropy associated with spin-orbit coupling in the antiferromagnetic phase have also been proposed (Jánossy *et al.*, 2000; Moskvin and Panov, 2002). This example illustrates the difficulty of making a unique association between a bulk anisotropy and microscopic stripe order.

Finally, we note that there is a very direct way to detect nematic order using light scattering. This approach is well known from studies of classical nematic liquid crystals (de Gennes, 1974). Recently Rübhausen and coworkers (Rübhausen *et al.*, 2000; Yoon *et al.*, 2000) have used light-scattering techniques to study the behavior of the low-frequency dielectric tensor of the manganite $Bi_{1-x}Ca_xMnO_3$ near and below the charge-ordering transition at $T_{co} \sim 160$ K. In these experiments, a pronounced anisotropy of the dielectric tensor was found with a sharp temperature dependence near T_{co}. Raman

scattering studies by the same group show that long-range positional stripe order sets in only at much lower temperatures. These experiments suggest that this manganite is in a nematic state below the transition at T_{co}, and long-range charge-stripe order occurs at much lower temperatures.

2. Anisotropic diffraction patterns

A more microscopic approach is to measure directly the nematic order parameter $\mathcal{Q}_{\mathbf{k}}$ of Eq. (2.1), by diffraction. This was done (more or less) by Mook *et al.* (2000), in neutron-scattering studies of the magnetic dynamic structure factor of a partially (2 to 1) detwinned sample of $YBa_2Cu_3O_{6+y}$ with $y=0.6$ and $T_c \approx 60$ K. No elastic scattering corresponding to actual stripe order was detected; however, well-developed structure was observed in the inelastic spectrum at the two-dimensional wave vectors $\mathbf{Q}_s \approx (0.5 \pm 0.1, 0.5)$ and $\mathbf{Q}_s' \approx (0.5, 0.5 \pm 0.1)$ in units of $2\pi/a$. Remarkably, the intensities of the peaks at $\mathbf{Q}_s$ were found to be about a factor of 2 larger than those of the $\mathbf{Q}_s'$ peaks, consistent with the supposition that, in a single twin domain, the incommensurate inelastic structure is entirely associated with ordering vectors perpendicular to the chain direction, i.e., $\mathcal{Q}_{\mathbf{Q}} \approx 1$.

More recently, inelastic neutron-scattering studies of Stock *et al.* (2003) on a nearly single-domain sample of the ortho-II phase of $YBa_2Cu_3O_{6.5}$ (Stock *et al.*, 2002) have revealed substantial structure down to the lowest energies in the magnetic structure factor. These spectra are highly anisotropic about the Néel ordering vector: For a scan perpendicular to the chain direction, there is a broad flat-topped peak [reminiscent of earlier results on underdoped YBCO (Sternlieb *et al.*, 1994)] which is strongly suggestive of two barely resolved incommensurate peaks at the expected stripe-ordering wave vector. However, a scan along the chain direction reveals a single, sharp peak at the commensurate wave vector π/a. Moreover, in the normal state, this structure is observed at all energies below the resonant peak energy, $\omega \approx 25$ meV, down to the lowest energies probed.

Although the presence of chains in this material certainly means that there is no symmetry operation that interchanges the a and b axes, the copper-oxide planes are nearly tetragonal. Thus it seems to us that the extreme anisotropy of the inelastic scattering is very strong evidence of a nematic liquid phase in this material. As pointed out by Mook *et al.* (2000), this conclusion also offers a potential explanation for the observed (Basov *et al.*, 1995) large but nearly temperature-independent superfluid anisotropy in the a-b plane.

Interesting anisotropies have also been observed in optical phonon branches of $YBa_2Cu_3O_{6+y}$ with $y=0.6$. The identification by Mook *et al.* (2000) of an anomalous broadening of a bond-bending mode at a wave vector expected for charge-stripe order is potentially the most direct evidence of nematic order. However, conflicting results have been reported by Pintschovius *et al.* (2002), who have instead observed a zone-boundary softening of the bond-stretching mode propagating along **b** but not for that along **a**. This latter anisotropy is unlikely to be directly associated with a stripe modulation wave vector, since the anomaly occurs along the direction parallel to the Cu-O chains. Of course, this does not necessarily rule out a connection with stripes, as the softening might be associated with anisotropic screening due to charge fluctuations along the stripes.

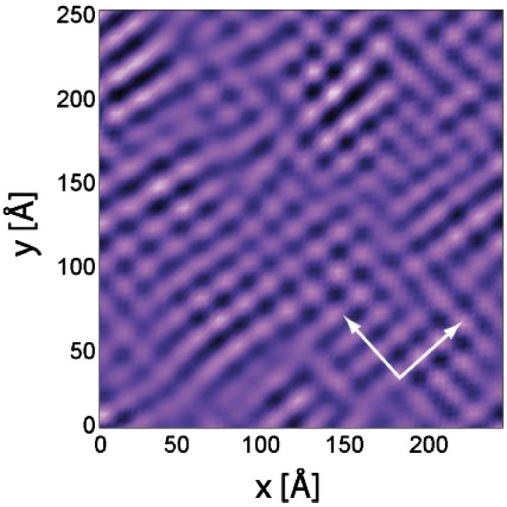

FIG. 11. (Color in online edition) A filtered version of the local-density-of-states map $N_f(\mathbf{r},E)$ on a surface patch of a $Bi_2Sr_2CaCu_2O_{8+\delta}$ crystal. Here, $E=15$ meV and the distances on the x and y axes are measured in angstroms. The filter is defined in Eq. (5.1) with $\Lambda=(2\pi/15a)$. The arrows point along the directions of the Cu-O bonds.

In an attempt to understand the effects of stripe order on phonons, a neutron-scattering study (Tranquada *et al.*, 2002) was recently performed on $La_{1.69}Sr_{0.31}NiO_4$. Although the charge-ordering wave vector did not play an obvious role, the high-energy bond-stretching mode propagating parallel (and perpendicular) to the stripe modulation exhibited an energy splitting toward the zone boundary, while along the Ni-O bond direction (at 45° to the stripes) a softening from zone center to zone boundary was observed with a magnitude similar to that in the cuprates. A better understanding of the nature of the relevant electron-phonon coupling processes is required to make progress here.

3. STM imaging of nematic order

Because it is a local but spatially resolved probe, STM is actually the optimal probe of nematic order. One way it can be used, which is illustrated in Fig. 11, has been explored by Howald *et al.* (2003a, 2003b). What is shown here is a filtered version of $N(\mathbf{r},E)$ measured on a patch of surface of a very slightly overdoped crystal of $Bi_2Sr_2CaCu_2O_{8+\delta}$ ($T_c=86$ K). Specifically, Howald *et al.* defined a filtered image

$$N_f(\mathbf{r},E)=\int d\mathbf{r}' f(\mathbf{r}-\mathbf{r}')N(\mathbf{r}',E), \tag{5.1}$$

where in the present case, the filter function f has been defined so as to accentuate the portions of the signal associated with stripe order,

$$f(\mathbf{r}) \propto \Lambda^2 e^{-r^2\Lambda^2/2}[\cos(\pi x/2a)+\cos(\pi y/2a)]. \tag{5.2}$$

Clearly, $f(\mathbf{r}) \to \delta(\mathbf{r})$ when $\Lambda \to \infty$, while $N_f = N(\mathbf{Q}_{\rm ch}, E) + N(\mathcal{R}[\mathbf{Q}_{\rm ch}], E) + \text{c.c.}$ in the limit $\Lambda \to 0$. For intermediate values of Λ, the filtered image shows only that portion of the signal we have associated with pinned stripes. The roughly periodic structure in the image has a period of $4a$. We know independently from the analysis in Sec. V.B that there is prominent structure in the raw data with this period, but even were there not, the filtering would build in such structure. However, what is clear from the image is that there is a characteristic domain structure, within which the stripes appear to lie predominantly in one direction or the other. The domain size is seen to be on the order of 100 Å$\sim 25a$, which is large compared to Λ^{-1} and, more importantly, roughly independent (Howald *et al.*, 2003a) of the precise value of Λ. This domain size is a characteristic correlation length of the pinned nematic order.

This particular method of analysis builds directly on the realization of the nematic as a melted stripe-ordered state. Indeed, looking at the figure, one can clearly identify dislocations and disclinations in what looks like a fairly well-developed locally ordered stripe array.

More generally, STM could be used to measure directly the two independent components of a suitably defined traceless symmetric tensorial density. The simplest such quantities are

$$\mathcal{Q}_{xx}(\mathbf{r},E) = [\partial_x^2 - \partial_y^2]N(\mathbf{r},E),$$
$$\mathcal{Q}_{\rm xy}(\mathbf{r},E) = 2\partial_x\partial_y N(\mathbf{r},E). \tag{5.3}$$

Of course, these quantities, like the local density of states itself, will typically have features that reflect the interference between elementary excitations, and other extraneous information. To obtain a better view of the long-wavelength nematic correlations, we should again integrate these densities over a suitable energy interval Ω, and filter out the short-wavelength components:

$$\tilde{\mathcal{Q}}_f(\mathbf{r}) = \int_0^\Omega \frac{dE}{\Omega} \int d\mathbf{r}' f(\mathbf{r}-\mathbf{r}')\mathcal{Q}(\mathbf{r}',E), \tag{5.4}$$

where f might be a Gaussian filter, as in Eq. (5.2), but without the cosine factors. A map of $\tilde{\mathcal{Q}}_f$ should produce a domain structure, similar to that shown in Fig. 11, but without all the short-wavelength detail. Where the domain size L_N is large compared to a, the resulting picture should look qualitatively the same independent of the range over which the signal is coarse grained, so long as $L_N \gg \Lambda^{-1} \gg a$. The above procedure should work well if there are no other long-wavelength features in the data. Unfortunately, for BSCCO, the inhomogeneities in the gap structure (Lang *et al.*, 2000; Howald *et al.*, 2003b) hamper such a procedure.

D. "1/8 anomaly"

Many members of the lanthanum cuprate family of high-temperature superconductors exhibit strong singularities in the doping dependence of various interesting low-temperature properties at $x = 1/8$; together, these phenomena are referred to as the "1/8 anomaly." For instance, in $La_{2-x}Ba_xCuO_4$ and $La_{1.6-x}Nd_{0.4}Sr_xCuO_4$, there is (Moodenbaugh *et al.*, 1988; Crawford *et al.*, 1991) a deep minimum in $T_c(x)$; in $La_{2-x}Ba_xCuO_4$ and $La_{2-x}Sr_xCuO_4$ there is a pronounced (Crawford *et al.*, 1990; Zhao *et al.*, 1997) maximum in $\alpha(x)$, the isotope exponent $\alpha \equiv d\ln(T_c)/d\ln(M)$; and in $La_{2-x}Sr_xCuO_4$ there is (Panagopoulos *et al.*, 2002) a pronounced minimum in the superfluid density $n_s(x)$. One of the central inferences drawn by Tranquada, Sternlieb, *et al.* (1995) following the discovery of stripe order in $La_{1.6-x}Nd_{0.4}Sr_xCuO_4$ is that this 1/8 anomaly is associated with a commensurate lock-in of the stripe structure. At $x = 1/8$ the preferred spacing between charge stripes is four lattice constants, so there is an additional commensuration energy which stabilizes stripe order at this particular hole density.

While it is possible to imagine other forms of charge-density-wave order which would similarly be stabilized at $x = 1/8$, there can be no doubt that in this family of materials the 1/8 effect is associated with stripe order. This has been confirmed, for example, in $La_{2-x}Sr_xCuO_4$ where quasielastic magnetic scattering from spin-stripe order has been detected (Suzuki *et al.*, 1998; Kimura *et al.*, 1999) for x in the neighborhood of 1/8; in low-energy inelastic measurements, Yamada *et al.* (1998) have shown that the magnetic peak width is narrowest at $x = 1/8$. Correspondingly, slow (probably glassy) spin fluctuations have been detected by μSR in the same material with a somewhat arbitrarily defined onset temperature, $T_g(x)$, which has (Panagopoulos *et al.*, 2002) a pronounced peak at $x = 1/8$. The fact that quasielastic magnetic order as detected by neutron scattering onsets at a considerably higher temperature than that detected by μSR is clearly a consequence of the inevitable glassiness of a density-wave transition in the presence of quenched disorder; it reflects the differences in the time scales of the two probes, not the presence of two distinct ordering phenomena. More recently, new experiments on $La_{2-x}Sr_xCuO_4$ as a function of x show pronounced singularities in the x dependence of the c axis Josephson plasma edge (Basov, 2002) and in the low-temperature thermal conductivity (Takeya *et al.*, 2002); these effects can be interpreted straightforwardly in terms of a peak in the stability of the charge-stripe order at $x = 1/8$. Furthermore, charge-stripe order has now been detected directly by neutron diffraction in $La_{1.875}Ba_{0.125-x}Sr_xCuO_4$ (Fujita *et al.*, 2002).

The large drop in T_c at $x = 1/8$ found in $La_{2-x}Ba_xCuO_4$ is not observed in $La_{2-x}Sr_xCuO_4$; however, such a dip in the doping dependence of T_c can be induced in $La_{2-x}Sr_xCuO_4$ (centered at $x = 0.115$) by substitution of 1% Zn for Cu, as shown some time ago by Koike *et al.* (1992). Zn substitution enhances local magnetic order at low temperature near the dip minimum, as detected by μSR (Panagopoulos *et al.*, 2002; Watanabe *et al.*, 2002). Given the clear association between the 1/8 anomaly and stripe order in

$La_{2-x}Sr_xCuO_4$, an indirect method of looking for the presence of local stripe order in other families of cuprate superconductors is to test whether a 1/8 anomaly can be induced by Zn substitution. In the case of $YBa_2Cu_3O_{6+y}$, there already exists in the literature strong evidence from the work of Tallon and collaborators (Tallon *et al.*, 1995) that the "60-K plateau" in the y dependence of T_c is not, primarily, a reflection of some form of oxygen ordering in the chain layers, as is commonly assumed, but rather is a barely resolved 1/8 anomaly; this conclusion is also supported by a Ca-substitution study (Akoshima and Koike, 1998) and by a recent study of transport properties (Ando and Segawa, 2002). To further test this idea, Koike and collaborators (Akoshima and Koike, 1998; Akoshima *et al.*, 2000; Watanabe *et al.*, 2000) studied the doping dependence of T_c, and of T_g measured by μSR, in lightly Zn-doped $YBa_2Cu_3O_{6+y}$ and $Bi_2Sr_2CaCu_2O_{8+\delta}$. They found that there is some tendency for light Zn doping to produce a dip in $T_c(x)$ and a more impressive peak in $T_g(x)$ at $x \approx 1/8$ in both $YBa_2Cu_3O_{6+y}$ and $Bi_2Sr_2CaCu_2O_{8+\delta}$. Related results have been reported (Yang *et al.*, 2000; Balakirev *et al.*, 2002) for the single-layer system $Bi_2Sr_{2-x}La_xCuO_{6+\delta}$. While it is clear that more work is needed to test the connection between the 1/8 anomaly and stripe pinning in these various systems, we consider this a promising approach to the problem, as it permits evidence of local order to be obtained using a variety of probes that can be applied in materials for which large crystals, and/or easily cleaved surfaces are not easily obtained.

E. Other probes

It is clear that the most direct evidence for stripes comes from techniques that can provide images of charge, spin, and/or lattice modulations in real space (STM) or in reciprocal space (diffraction techniques). We have already discussed neutron and x-ray diffraction, but explicit mention should also be made of transmission electron microscopy (TEM). The charge stripes in $La_{2-x}Sr_xNiO_{4+\delta}$ were first detected by TEM (Chen *et al.*, 1993), and a recent study has provided high-resolution TEM images of local stripe order in $La_{1.725}Sr_{0.275}NiO_4$ (Li *et al.*, 2003). So far, TEM studies have not provided positive evidence for stripes in any cuprates, but, though challenging, it should be possible to do so.

Less direct but extremely valuable information comes from techniques that are sensitive to local order. We have already mentioned evidence for local, static hyperfine fields and slowly fluctuating hyperfine fields obtained by μSR. Besides providing a practical measure of local magnetic order as a function of doping (Niedermayer *et al.*, 1998; Klauss *et al.*, 2000), μSR can detect the distribution of local hyperfine fields in a sample with relatively uniform order (Nachumi *et al.*, 1998), as well as being able to detect inhomogeneous magnetic or superconducting order (Savici *et al.*, 2002). Related information can be obtained by NMR and NQR techniques, where the latter also provides information on the distribution of local electric-field gradients. Some of the first evidence for spatial inhomogeneity of magnetism in lightly doped $La_{2-x}Sr_xCuO_4$, consistent with stripelike behavior, was obtained in a La NQR experiment by Cho *et al.* (1992). Later experiments (Tou *et al.*, 1993; Goto *et al.*, 1994, 1997; Ohsugi *et al.*, 1994) (including La and Cu NMR and NQR) provided evidence for local magnetic order near $x=1/8$ in $La_{2-x}Sr_xCuO_4$ and $La_{2-x}Ba_xCuO_4$.

The work by Imai's group (Hunt *et al.*, 1999) suggesting that local stripe order in variants of $La_{2-x}Sr_xCuO_4$ could be detected through the "wipeout effect" of Cu NQR has motivated a considerable number of further studies using Cu and La NMR and NQR (Julien *et al.*, 1999, 2001; Singer *et al.*, 1999; Suh *et al.*, 1999, 2000; Curro, Hammel, *et al.*, 2000; Teitel'baum *et al.*, 2000, 2001; Hunt *et al.*, 2001; Simovič *et al.*, 2003). Although there has been some controversy over details of interpretation (and in certain cases, there may be differences between samples), it is now generally agreed that NQR and NMR are sensitive to the onset of slow spin fluctuations whose appearance tends to correlate with the onset of local charge-stripe pinning as determined by diffraction. In particular, the glassy nature of the ordering has been investigated. In the case of Eu-doped $La_{2-x}Sr_xCuO_4$, related information has been obtained by electron-spin resonance detected from a very low density of Gd impurities (Kataev *et al.*, 1997, 1998). A recent Cu NQR and Y NMR study (Singer and Imai, 2002) has shown that similar signatures are observed in Ca-doped $YBa_2Cu_3O_6$, consistent with the μSR study of Niedermayer *et al.* (1998) and suggestive of the presence of pinned stripes in that system at low temperatures. Direct evidence for local spatial inhomogeneities in $La_{2-x}Sr_xCuO_4$ has been obtained from studies of NMR line broadening (Haase *et al.*, 2000) and frequency-dependent NQR relaxation rates (Singer *et al.*, 2002).

Very recently, a fascinating study (Haase and Slichter, 2003) of the NMR/NQR spectra in $YBa_2Cu_3O_{6+y}$ has found evidence of two distinct planar O environments in the unit cell, but only one Cu environment. This finding is not consistent with any form of translation-symmetry breaking. It is, however, suggestive of substantial nematic order, in which the O sites midway between two copper sites in one direction (for instance, the chain direction) have substantially larger hole density than the O's on the bonds in the perpendicular direction. Of course, because the crystal is orthorhombic, this does not truly imply any symmetry breaking, but it should be possible, in principle, to establish whether the magnitude of the effect is out of proportion with the small distortions produced by the orthorhombicity.

Several recent NMR studies (Curro, Milling, *et al.*, 2000; Kakuyanagi *et al.*, 2002; Mitrović *et al.*, 2001, 2003) have exploited the magnetic-field dependence of the technique to probe the spatial variation of nuclear spin-lattice relaxation rates in the vortex lattice state of cuprate superconductors. Vortex cores are regions of

suppressed superconductivity, so if there is a competing spin-stripe ordered phase, it will be enhanced and pinned (Demler *et al.*, 2001; Kivelson *et al.*, 2002; Zhang *et al.*, 2002) in the neighborhood of the vortex core. Indeed, ^{17}O NMR measurements on $YBa_2Cu_3O_{6+y}$ and $YBa_2Cu_4O_8$ indicate antiferromagneticlike spin fluctuations and a reduced density of states associated with the vortex cores (Kakuyanagi *et al.*, 2002; Mitrović *et al.*, 2003). [Similar results, along with evidence of static spin ordering in the vortex cores at low temperatures, have been reported (Kakuyanagi *et al.*, 2003) in $Tl_2Ba_2CuO_{6+\delta}$.] A μSR study of the details of the magnetic-field distribution in $YBa_2Cu_3O_{6.50}$ suggests the presence of a small local hyperfine field near vortex cores (Miller *et al.*, 2002). For completeness, we note that while one neutron scattering study has indicated very weak, field-induced, elastic antiferromagnetic scattering in superconducting $YBa_2Cu_3O_{6+y}$ (Vaknin *et al.*, 2000), two other studies, focusing on the effect of a magnetic field on inelastic scattering, found no low-frequency enhancement (Bourges, Casalta, *et al.*, 1997; Dai *et al.*, 2000).

It has been demonstrated that stripe order has an impact on phonon heat transport (Hess *et al.*, 1999). The thermal conductivity increases slightly on cooling through the charge-ordering transition, exhibiting a normal peak at ~ 25 K. The suppression of the latter peak in superconducting $La_{2-x}Sr_xCuO_4$ has been attributed to the scattering of phonons by fluctuating stripes (Baberski *et al.*, 1998). The doping dependence of the thermal conductivity measured in $YBa_2Cu_3O_{6+y}$ and in mercury cuprates has been interpreted as evidence for a 1/8 anomaly in those materials (Cohn *et al.*, 1999). An enhancement of the thermal conductivity in $La_{1.88}Ba_{0.12}CuO_4$ was originally noted by Sera *et al.* (1990).

Indirect evidence of some form of local charge order can also be gleaned from the response of a system to electromagnetic radiation.[41] For instance, Raman scattering (Blumberg *et al.*, 2002) was recently used to reveal charge ordering and, more importantly for present purposes, to detect the effect of collective charge-density-wave motion at higher temperatures in $Sr_{12}Cu_{24}O_{41}$, a ladder system with a local electronic structure very similar to that of the cuprate superconductors. Careful measurements of the optical response of optimally doped $YBa_2Cu_3O_{6+y}$ have revealed (Homes *et al.*, 2000; Bernhard *et al.*, 2001) infrared active phonons with oscillator strength comparable to those in the undoped insulating compound. This has been plausibly interpreted as giving evidence of "fluctuating charge inhomogeneities" in the copper oxide planes—the point being that for the phonons to be unscreened at that frequency, their local environment on some scale must be insulating.

ARPES experiments can also be interpreted as giving indirect evidence of local stripe order. At an empirical level, this can be done by looking (Zhou *et al.*, 1999, 2001) at the evolution of the ARPES spectra in a sequence of materials in the La_2CuO_4 family in which various types of stripe order have been detected; this provides a basis for identifying similar features in the ARPES spectra of materials in which stripe order has not been established. For instance, stripe long-range order produces a tendency for the Fermi surface in the antinodal region of the Brillouin zone to be flat (one dimensional) and to suppress spectral weight in the nodal region. Some of these same features, especially the differing impact on the nodal and antinodal regions, are induced by Zn doping of $Bi_2Sr_2CaCu_2O_{8+\delta}$, as well, plausibly reflecting (White *et al.*, 1999) the tendency of Zn to pin local stripe order. More broadly, many of the most striking features of the observed (Fedorov *et al.*, 1999; Ino *et al.*, 1999; Valla *et al.*, 1999; Damascelli *et al.*, 2002; Campuzano *et al.*, 2003) ARPES spectra can be naturally interpreted in terms of an underlying quasi-one-dimensional electronic structure (Carlson *et al.*, 2003). Examples of this are the disappearance of the coherent quasiparticle peak (Carlson *et al.*, 2001) upon heating above T_c, the dichotomy between the widths of the peaks as a function of momentum and energy in the normal-state spectrum (Gweon *et al.*, 2001; Orgad *et al.*, 2001) and the general structure of the spectra and the evolution of the Fermi surface with doping (Salkola *et al.*, 1996; Ichioka and Machida, 1999; Zacher *et al.*, 2000, 2001; Eroles *et al.*, 2001; Granath *et al.*, 2001, 2002).

Finally, several probes have been used to search for the inhomogeneous distribution of bond lengths expected from the lattice response to local charge-stripe order. Pair-distribution-function analysis of scattering data and extended x-ray-absorption fine structure (EXAFS) spectroscopy can detect instantaneous distributions of nearest-neighbor bond lengths. Both techniques have the potential to provide indirect evidence of dynamic, as well as static, stripes; however, whether they have sufficient sensitivity to detect the very small bond-length variations associated with charge modulation in the cuprates remains a topic of some contention. Božin *et al.* (2000) reported a doping-dependent broadening of the in-plane Cu-O bond-length distribution in $La_{2-x}Sr_xCuO_4$ detected by pair-distribution-function analysis of neutron powder diffraction data. While the reported doping dependence is intriguing, the maximum enhancement of the bond-length spread is much too large to be compatible with the Debye-Waller factors measured in a single-crystal neutron-diffraction experiment on $La_{1.85}Sr_{0.15}CuO_4$ by Braden *et al.* (2001). A much more extreme discrepancy occurs with the EXAFS studies of $La_{2-x}Sr_xCuO_4$ (and other cuprates) by Bianconi's group (Bianconi *et al.*, 1996; Lanzara *et al.*, 1996; Saini *et al.*, 1997). They report a low-temperature splitting of the in-plane Cu-O bond lengths of 0.08 Å, which is not only incompatible with a large number of diffraction studies, but is also inconsistent with EXAFS analysis performed by other groups (Niemöller *et al.*,

[41]For a discussion of the electromagnetic signatures of charge-density-wave order, see Gruner (1994).

1998; Haskel *et al.*, 2000). Large atomic mean-square displacements detected in $YBa_2Cu_3O_{6+y}$ by ion channeling (Sharma *et al.*, 2000) have been attributed to transitions associated with dynamic stripes, but the magnitude of the displacements and the temperature dependence are difficult to reconcile with other experiments.

In short, these various local measures of the distribution of lattice displacements are, in principle, a very good way to look for local charge-ordering tendencies, but it is important to reconcile the results obtained with different techniques. Where apparent inconsistencies exist, they must be resolved before unambiguous inferences can be made.

VI. WEAK- AND STRONG-COUPLING PERSPECTIVES

Order in simple metals is typically thought of as arising from a Fermi-surface instability caused by the weak residual interactions between the lowest-energy quasiparticles. Specifically, density-wave order occurs when the band structure is such that there are nearly nested segments of the Fermi surface. Thus, even at temperatures above the ordering temperature, or if the interactions are slightly weaker than the critical strength needed for ordering, there will often be structure in the appropriate dynamical structure factors due to this near nesting which in some sense reflects the fact that the metal is close to an ordered state. In this section, we shall analyze the connection between this weak-coupling Fermi-liquid theory based perspective and the description in terms of the collective modes of the ordered or nearly ordered state which we have taken until now.

It is worth mentioning at the outset that one difficulty arises from the relative paucity of established theoretical results in the strong-coupling limit. More than half a century of concerted work has produced a rather complete understanding of the effects of weak residual interactions on the properties of a well-formed Fermi liquid in a simple metal. However, only in special circumstances is a comparably sound and complete understanding available in a strongly interacting system. For instance, in the weak-coupling limit, considerable useful information about the quasiparticle spectrum can be adduced directly from transport data, because Boltzmann transport theory relates the two properties in a precise manner. The theory of transport in a strongly interacting system is, in our opinion, not established. The upshot of this is that it is much easier to point to experiments that show that simple, weak-coupling ideas *cannot* be safely applied in many highly correlated materials, than to point to experiments that show that strong coupling notions can be applied.

A. Distinctions in principle

1. Thermodynamic distinctions

As mentioned in the Introduction, stripe-ordered states are ultimately defined by a specific set of broken symmetries. From this viewpoint, there is no distinction between the strong coupling-limit, in which spin stripes can be viewed as micro phase separation of charges into an array of rivers with strips of nearly insulating antiferromagnet between them, and the weak-coupling Hartree-Fock description of a spin-density wave that opens small gaps on various nearly nested segments of the Fermi surface. Indeed, in many circumstances, the two limits are adiabatically connected as a function of the interaction strength. However, this is not guaranteed. For instance, a stripe-ordered state can be either metallic or insulating. At $T=0$, metallic and insulating stripes are thermodynamically distinct states of matter.

There is a more subtle distinction possible between metallic spin-stripe states in the weak- and strong-coupling limits. Certainly, in the weak-coupling limit, the ungapped portions of the Fermi surface support well-defined quasiparticles, so the system remains a Fermi liquid unless, at still lower temperatures, it suffers an additional ordering transition, say to a superconducting state. On the other hand, in the strong-coupling limit, the metallic behavior in the stripe-ordered phase may or may not be well characterized by Fermi-liquid power laws. It is now established that non-Fermi-liquid states can, in principle, exist in more than one dimension.[42]

The character of charge-stripe order tends to more easily distinguish between strong- and weak-coupling limits. For repulsive interactions, weak-coupling Hartree-Fock theories always produce charge order which is parasitic on the fundamental spin order. In Landau theory, there is a cubic coupling between charge- and spin-density-wave order which, whenever the primary order parameter is the spin order, leads to charge-density-wave order, which onsets at the same T_c, but with a strength proportional to the square of the spin-density-wave order: $\langle \rho_{2\mathbf{Q}} \rangle \propto |\mathbf{S}_\mathbf{Q}|^2 \sim |T_c - T|^{2\beta}$. By contrast, in a strong-coupling picture of micro phase separation, if the spin ordering is only triggered when the holes agglomerate into stripes, one would typically expect the stripe-ordering transition to be first order, or for the charge ordering to precede spin ordering. Thus the measured sequence of transitions provides sharp criteria that can be used to discriminate between weak and strong coupling.

In the thermal or quantum disordered phase proximate to a stripe-ordered state, sharp thermodynamic distinctions between the strong- and weak-coupling limits are harder to draw. The only possible thermodynamic distinction is, again, that in the weak-coupling limit the disordered state is necessarily a Fermi liquid, while in strong coupling it may either be a Fermi liquid or a non-Fermi-liquid.

2. Quantitative distinctions

Even where no sharp thermodynamic distinctions exist, there are very many clear physical differences be-

[42] In particular, the existence of a non-Fermi-liquid "sliding" phase in a stripe-ordered system has been shown (Emery *et al.*, 2000; Vishwanath and Carpentier, 2001) for a class of interacting Luttinger liquids.

tween the weak- and strong-coupling limits. Of these, the most obvious is the relative importance of electron quasiparticles with a sharply defined Fermi surface. In the weak-coupling limit, the quasiparticle is the essential building block in terms of which all other properties are derived. In the strong-coupling limit, by contrast, even where it might be the case that well-defined quasiparticles (with very small weight Z) are recovered in the strict $T\to 0$ limit, such coherence may require such low temperatures as to be only of academic interest. Thus, on a practical level, "effective non-Fermi-liquids," in which the majority of the electronic excitations in the experimentally relevant ranges of temperature, energy, and wave number are not well-defined quasiparticles, cannot be sensibly treated in terms of a weak-coupling approach. Conversely, where well-defined quasiparticles are everywhere manifest, there is an *a priori* reason to prefer a weak-coupling viewpoint.

Another set of important quantitative distinctions concern the $\mathbf{k}$ and ω dependences of the magnetic dynamical structure factor $S(\mathbf{k},\omega)$. In a one band model of noninteracting electrons, the integral of S over all $\mathbf{k}$ and ω is $(1/8)[1-x^2]$, while in the large-interaction (local-moment) limit it is $(1/4)(1-x)$, which is not dramatically different. However, in weak coupling, the integrated intensity comes from a very broad range of energies, of order E_F, and momenta, of order $2k_F$, while for an antiferromagnet the integral is dominated by energies less than the exchange energy J and is highly peaked near the magnetic ordering vector, whether or not the system is actually ordered. Put another way, in weak coupling the structure factor is dominated by the particle-hole continuum, and there are signatures of well-defined collective modes (spin waves) only at energies $\omega \lesssim T_c$, while in the strong-coupling limit, deep in the ordered phase, spin waves dominate the structure factor even at energies of order J. Also, in the ordered state at weak coupling, the ordered moment m at $T=0$ is small, $m\sim\mu_B(T_c/E_F)$, while in the strong-coupling limit, not too close to a quantum critical point, $m\sim\mu_B$ is large.

As a concrete example, let us first consider the structure factor of a noninteracting electron gas in two dimensions. For momenta $q>2k_F$ it is

$$S(q,\omega)=\frac{k_F^2}{2\pi^2 v_F q}\sqrt{1-\left(\frac{q}{2k_F}-\frac{\omega}{v_F q}\right)^2} \tag{6.1}$$

when $v_F q(q/2k_F-1)<\omega<v_F q(q/2k_F+1)$ and zero otherwise. (The expression for $q<2k_F$ is somewhat more complicated.) Clearly, the spectral weight is distributed smoothly over the entire support of this particle-hole continuum, i.e., over a range of momenta of order $2k_F$ and of energies of order the bandwidth. From the weak-coupling perspective the chief qualitative effect of interactions is to produce (quasi)bound states that manifest themselves as peaks at or below the threshold of the continuum. In the broken-symmetry phase these bound states are Goldstone modes, which descend to zero energy and lose weight to the new Bragg peaks. What is important to note here is that even in the broken-symmetry phase, most of the spectral weight remains in the incoherent background, spread more or less uniformly over energies of the order of the bandwidth.

In contrast, consider the zero-temperature structure factor of an insulating antiferromagnet computed to first order in a $1/S$ expansion, where S is formally the magnitude of the spin, but more physically should be viewed as the "distance" of the system from the nearest quantum disordered phase. Here, on a square lattice,

$$\begin{aligned}S_{ij}(\mathbf{q},\omega)=&S(S-A)\hat{m}_i\hat{m}_j\delta(\omega)\,\delta(\mathbf{q}-\mathbf{Q}_{\mathrm{AF}})\\&+\frac{S}{8J}\sqrt{\frac{2-\cos q_x-\cos q_y}{2+\cos q_x+\cos q_y}}\,(\delta_{ij}-\hat{m}_i\hat{m}_j)\\&\times\delta(\omega-\omega_{\mathbf{q}}),\end{aligned} \tag{6.2}$$

where $\omega_{\mathbf{k}}=2SJ\sqrt{4-(\cos k_x+\cos k_y)^2}$ is the spin-wave dispersion (which depends on the lattice and the details of the exchange interactions), $\hat{m}$ is a unit vector parallel to the magnetization, and $A=0.3932+\cdots$. (Higher-order terms in $1/S$ typically produce finite lifetimes for all but the lowest-energy spin waves and also give rise to a multi-spin-wave continuum.) As promised, the basic energy scale is set by J, and a large portion of the total spectral weight is found in a small region of $\mathbf{k}$ space around $\mathbf{k}=\pi$.

Note that the energy scale J can be deduced from the value of the spin-wave energy near the zone boundary, $\omega_{\mathbf{k}_0}=4SJ=2J$, for $\mathbf{k}_0=(\pi,0)$. Even in the thermally disordered state, so long as $T\ll J$, the zone edge spin wave can be studied to get an idea of the relevant energy scales for magnetic excitations.

Finally, distinctions can be drawn based on the sensitivity of the signatures of order or proximate order to various weak perturbations: weak disorder, as we have discussed extensively above, can serve to pin fluctuating order and hence enhance the small ω portion of $S(\mathbf{q},\omega)$. However, in weak coupling, the principal effect of weak disorder is to scatter the quasiparticles and thus broaden any Fermi-surface features (i.e., nested segments) that might give rise to peaks at particular $\mathbf{q}$'s in $S(\mathbf{q},\omega)$. Thus, in weak coupling, we expect weak quenched disorder to suppress, rather than enhance low-frequency signatures of stripe order or incipient stripe order. Distinct responses to an applied magnetic field can also be expected to differentiate the weak- and strong-coupling limits. In particular, where the zero-field ground state is superconducting, induced order in vortex cores occurs under broad circumstances in the strong-coupling limit where there are competing orders; this sort of phenomena is generally much less prominent in the weak-coupling limit. These issues are discussed in a number of good recent reviews—see footnotes 23 and 24.

3. Intermediate coupling

It is worth remembering that in many materials the interaction strength is comparable to the Fermi energy, i.e., stability of matter (or some memory of the Virial theorem) conspires to place systems in the awkward re-

gime of intermediate coupling. Here, neither the weak-coupling nor the strong-coupling approaches is well justified, and one is typically forced to extrapolate results beyond their regime of validity. In this case, it is generally sensible to study the problem from both the strong- and weak-coupling perspectives. Some features (such as those that are most sensitive to the presence of a particle-hole continuum) may be best viewed from the weak-coupling perspective, while others (such as the role of collective modes) may be better viewed from strong coupling.

One traditional approach to understanding this regime is to include the effects of interactions in the context of the random-phase approximation (RPA). For the complex spin susceptibility χ, one writes

$$\chi(\mathbf{k},\omega)=\frac{\chi_0(\mathbf{k},\omega)}{1-U_{\mathbf{k}}\chi_0(\mathbf{k},\omega)}, \tag{6.3}$$

where χ_0 is the susceptibility for noninteracting electrons, and U characterizes the interaction. In the case of dominantly forward-scattering interactions (such as the long-range piece of the Coulomb interaction), the RPA summation of bubble diagrams is justified even when the interactions are relatively strong. For the case of short-range interactions, no such systematic justification exists to the best of our knowledge. However, the results obtained from RPA are explicit and often intuitively appealing. It is certainly reasonable, at least on a phenomenological level, to compare the results of an RPA treatment with experiment to determine whether the physics is simply connected to the weakly interacting limit or whether the interactions produce qualitatively new phenomena.

One of the first RPA calculations was performed by Bulut *et al.* (1990) to model the antiferromagnetic spin fluctuations detected by NMR; for the interaction, they selected $U_{\mathbf{k}}=U$, the on-site Coulomb repulsion. Littlewood *et al.* (1993) found significant structure in the bare $\chi_0''(\mathbf{k},\omega)$ from nearly nested features of the Fermi surface. By suitable choice of the chemical potential, and inclusion of band narrowing by a factor of 2–4 compared to band-structure calculations, they were able to find reasonable agreement with the early inelastic neutron scattering measurements of low-energy magnetic excitations in $La_{2-x}Sr_xCuO_4$ (Cheong *et al.*, 1991). Calculations for $YBa_2Cu_3O_{6+y}$ (Monthoux and Pines, 1993; Si *et al.*, 1993) have typically found it necessary to employ the RPA expression with $U_{\mathbf{k}}=-J[\cos(k_xa)+\cos(k_ya)]$ (or a similar form) in order to obtain reasonable consistency with experiment.[43] Several recent calculations (Brinckmann and Lee, 1999; Kao *et al.*, 2000; Norman, 2000; Onufrieva and Pfeuty, 2002) have addressed the resonance peak in $YBa_2Cu_3O_{6+y}$ and the downward-dispersing excitations that appear at slightly lower energies (Arai *et al.*, 1999; Bourges *et al.*, 2000; Ito *et al.*, 2002).

The lack of dispersion of the spin gap that develops below T_c in $La_{2-x}Sr_xCuO_4$ (Lake *et al.*, 1999), together with the enhancement of intensity above the gap (Mason *et al.*, 1996), have been interpreted in terms of the spin response of the electrons that participate in the superconducting state (Mason *et al.*, 1996; Lake *et al.*, 1999; Kao *et al.*, 2000; Morr and Pines, 2000).

B. Experimental evidence supporting a strong-coupling perspective in the cuprates

From a purely theoretical perspective, it may not be possible to determine *a priori* whether there is an advantage to either a weak- or strong-coupling approach; however, we believe that numerous experimental results point decisively towards the strong-coupling picture. Many of the relevant results involve measurements of magnetic correlations, and we have collected selected experimental quantities in Table I. (Some explanations of how the parameter values are taken from experiment are given in Appendix B.) Below we highlight some of the important observations, and explain their significance.

- Magnetism in undoped cuprates is quantitatively consistent with superexchange between local magnetic moments on copper ions.

The undoped parent compounds, such as La_2CuO_4 and $YBa_2Cu_3O_6$, are antiferromagnetic insulators with a charge-transfer gap of ~ 2 eV (Kastner *et al.*, 1998). The ordered magnetic moments are consistent with one unpaired spin per planar Cu ion, after zero-point spin fluctuations, given accurately by spin-wave theory (Igarashi, 1992), are taken into account. The effective superexchange energy, $J_{\mathrm{eff}}\sim 0.1$ eV, determined from measurements of the spin-wave dispersion, has been calculated from *ab initio* cluster models (Van Oosten *et al.*, 1996; Muñoz *et al.*, 2000), consistent with the local superexchange mechanism.

If the antiferromagnetic order corresponded to a spin-density wave due to Fermi-surface nesting, one would expect the magnetic correlations and the optical gap to disappear at the Néel temperature. Neither of these things happens; these materials remain correlated insulators in the disordered state, and the spin correlations are well described by a nonlinear sigma model (Chakravarty *et al.*, 1989) with parameters derived from the ordered state (Kastner *et al.*, 1998).[44]

- With light doping, local magnetic moments change little, even though long-range Néel order is destroyed.

In a μSR study of lightly doped $La_{2-x}Sr_xCuO_4$ and $Y_{1-x}Ca_xBa_2Cu_3O_6$, Niedermayer *et al.* (1998) showed

[43] Anderson (1997) has made a strong and compelling argument that antiferromagnetic exchange cannot be properly treated in RPA and that the approach is internally inconsistent.

[44] The recent observation by Coldea *et al.* (2001) that the spin-wave dispersion at large energies is better fit if a four-spin exchange interaction is included in the microscopic Heisenberg model is still consistent with a system of localized spins.

TABLE I. Various quantities characterizing the strength of antiferromagnetic correlations in doped and undoped cuprates and nickelates. All are determined at low temperature. The quantity p is the nominal hole concentration per planar Cu; for $YBa_2Cu_3O_{6+y}$ and $YBa_2Cu_4O_8$ this was estimated from the "universal" formula of Presland *et al.* (1991) relating $T_c/T_c^{\max}$ and p. The acronyms used under "phase" are AFI, antiferromagnetic insulator; CSO, charge-stripe order; SSO, spin-stripe order; SC, superconducting order. m is the magnetic moment per planar Cu, and m/m_0 is the moment relative to the AFI parent. $\int S(\mathbf{k},\omega)$ is the dynamical structure factor, integrated over a Brillouin zone and over energy up to 100 meV, and normalized to the AFI parent. J_{eff} is the effective superexchange energy characterizing the maximum energy of the magnetic excitations ($2J_{\text{eff}}$) measured by neutron scattering, or obtained from Raman scattering, assuming that the two-magnon peak is at $2.7J_{\text{eff}}$. Further discussion is given in Appendix B.

Material	p	Phase	m (μ_B)	m/m_0	$\int S(\mathbf{k},\omega)$	J_{eff} (meV)	T_{crit}
La_2CuO_4	0	AFI	0.60(5)[a]	1	1	152(6)[b]	$T_N \approx 300$ K
$La_2Cu_{0.8}(Zn,Mg)_{0.2}CuO_4$	0	AFI		0.72(5)[c]			$T_N \approx 100$ K
$La_{1.88}Ba_{0.12}CuO_4$	0.12	CSO, SSO		0.60(2)[d]			$T_{sso} \approx 35$ K
$La_{1.48}Nd_{0.4}Sr_{0.12}CuO_4$	0.12	CSO, SSO		0.60(2)[d]		120(25)[e]	$T_{sso} \approx 50$ K
$La_2CuO_{4.11}$	0.16	SSO, SC		0.62(2)[f]			$T_{sso} = T_c = 42$ K
$La_{1.86}Sr_{0.14}CuO_4$	0.14	SC	0	0	0.4[g]	140(10)[g]	$T_c = 35$ K
$YBa_2Cu_3O_{6.1}$	0	AFI	0.55(3)[h]	1	1	125(8)[i]	$T_N \approx 400$ K
$YBa_2Cu_3O_{6.5}$	0.09	SC	0	0	0.5[j]		$T_c \approx 52$ K
$YBa_2Cu_3O_{6.6}$	0.10	SC	0	0	0.6[k]	110(15)[k]	$T_c = 63$ K
$YBa_2Cu_3O_{6.7}$	0.11	SC	0	0	0.3[l]	125(5)[m]	$T_c \approx 70$ K
$YBa_2Cu_4O_8$	0.13	SC	0	0		125(5)[m]	$T_c = 80$ K
La_2NiO_4	0	AFI	1.0(1)[n]	1		31(1)[o]	$T_N \approx 330$ K
$La_2NiO_{4.133}$	0.27	CO	0.8(1)[p]	0.80(5)			$T_{sso} = 110$ K
$La_{2-x}Sr_xNiO_4$	~ 0.33	CO		1.11(5)[q]		20(1)[r]	$T_{sso} \approx 200$ K

[a] From neutron diffraction (Yamada *et al.*, 1987).
[b] From inelastic neutron scattering (Coldea *et al.*, 2001).
[c] From neutron diffraction (Vajk *et al.*, 2001).
[d] Local moment relative to La_2CuO_4 from μSR (Nachumi *et al.*, 1998).
[e] From two-magnon Raman scattering, assuming that the observed peak is at $2.7J$ (Nachumi *et al.*, 2002; Gozer *et al.*, 2003).
[f] Local moment relative to La_2CuO_4 from μSR (Savici *et al.*, 2002).
[g] From inelastic neutron scattering (Hayden *et al.*, 1996a).
[h] From neutron diffraction (Casalta *et al.*, 1994).
[i] From inelastic neutron scattering (Hayden *et al.*, 1996b) and two-magnon Raman scattering (Blumberg *et al.*, 1994, 1996).
[j] Based on inelastic neutron scattering results (Hayden *et al.*, 1996b; Fong *et al.*, 2000).
[k] Based on inelastic neutron scattering results (Hayden *et al.*, 1996b; Dai *et al.*, 1999).
[l] Based on inelastic neutron scattering results (Hayden *et al.*, 1996b; Fong *et al.*, 2000).
[m] From two-magnon Raman scattering (Blumberg *et al.*, 1994, 1996).
[n] From neutron diffraction (Wang *et al.*, 1992).
[o] From inelastic neutron scattering (Yamada *et al.*, 1991).
[p] From neutron diffraction (Tranquada, Lorenzo, *et al.*, 1995).
[q] Local moment relative to La_2NiO_4 from μSR (Jestädt *et al.*, 1999).
[r] From inelastic neutron scattering (Boothroyd *et al.*, 2003; Bourges *et al.*, 2003).

that there is essentially no change in the low-temperature ordered moment per planar Cu as the long-range antiferromagnet order is destroyed by increasing the hole concentration. This behavior has also been detected in NMR studies (Chou *et al.*, 1993). In the spin-glass regime that occurs in the doping range between the antiferromagnetic and superconducting phases, the ordered moments decrease gradually (Niedermayer *et al.*, 1998). We now know that for $La_{2-x}Sr_xCuO_4$ with $0.02 \lesssim x < 0.06$ the low-temperature phase involves ordering of magnetic moments in a diagonal spin-stripe structure (Wakimoto *et al.*, 1999; Fujita *et al.*, 2002). That identical behavior occurs in $Y_{1-x}Ca_xBa_2Cu_3O_6$ is supported by an NQR/NMR study (Singer and Imai, 2002).

• The energy scale of magnetic excitations and the strength of the dynamic structure factor at frequencies less than J change only modestly with doping.

One can see from Table I that J_{eff} decreases a relatively small amount with doping. There is also evidence in some underdoped $YBa_2Cu_3O_{6+y}$ samples of effects reminiscent of spin-wave-like dispersion at energies above 50 meV (Bourges, Fong, *et al.*, 1997; Fong *et al.*, 2000). The partially integrated dynamical structure factor decreases with doping, but remains substantial.

If the magnetic excitations corresponded to electron-hole excitations across the Fermi surface, one would expect that the magnetic energy scale should increase to a value comparable to the Fermi energy. For that scale to be the same as the J_{eff} of the undoped phase would seem to be an incredible coincidence. With a substantial increase in energy scale, one would expect a corresponding decrease in the integrated dynamical structure factor.

Similar trends in terms of a modest reduction of J_{eff} with doping and the survival of spin-wave-like excitations are found in stripe-ordered $La_{2-x}Sr_xNiO_4$ (Boothroyd *et al.*, 2003; Bourges *et al.*, 2003). This system is definitely in the strong-coupling limit, as it remains semiconducting above the charge-ordering temperature (Katsufuji *et al.*, 1996).

• The **k** dependence of the magnetic neutron scattering measured from superconducting samples of $YBa_2Cu_3O_{6+y}$ is consistent with spin density on planar Cu ions.

The magnetic scattering cross section is proportional to the square of the magnetic form factor (the Fourier transform of the magnetization density); this is true for both elastic and inelastic scattering. An early analysis of inelastic magnetic scattering at different **k** points in superconducting $YBa_2Cu_3O_{6+y}$ samples revealed an anisotropy (Rossat-Mignod *et al.*, 1992) that was later shown to be consistent with the anisotropy due to the magnetic form factor for a single spin in a $3d_{x^2-y^2}$ orbital (Shamoto *et al.*, 1993).

The coherence of spin excitations within the CuO_2 bilayers of $YBa_2Cu_3O_{6+y}$ also results in a bilayer structure factor. The structure factor is a sinusoidal function of momentum transfer perpendicular to the bilayers, with a period that is proportional to the spacing between the layers of the centers of spin density. The observed period is quantitatively consistent with the intrabilayer spacing of the Cu atoms, but is incompatible with the spacing of the oxygen atoms, which is significantly smaller (Tranquada *et al.*, 1992).

For electronic states at the Fermi level, there is a substantial amount of weight from planar O $2p$ states (Takahashi *et al.*, 1988). As a result, one would expect that magnetic scattering due to electron-hole excitations should, in real space, have significant weight associated with the oxygen sites. The measured modulations (Tranquada *et al.*, 1992; Bourges *et al.*, 1996; Fong *et al.*, 1996) are not compatible with a significant component corresponding to the oxygen spacing.

• When stripe order is observed in more heavily doped samples, the magnetic moments are large.

As indicated in the table, the local magnetic moments detected in stripe-ordered phases by μSR are comparable to the moment found in undoped La_2CuO_4. The large moments imply a strong modulation of hole density. The magnetic form factor determined by neutron diffraction is consistent with that expected for spin moments (Tranquada *et al.*, 1996).

• When stripe order is observed, charge orders before the spins, and the ordering wave vector grows with doping.

When charge and spin-stripe order are observed, as in $La_{1.6-x}Nd_{0.4}Sr_xCuO_4$, the charge order appears at a higher temperature than the stripe order (Tranquada *et al.*, 1996; Ichikawa *et al.*, 2000). (In $La_{1.875}(Ba,Sr)_{0.125}CuO_4$, the ordering temperatures for charge and spin are very close (Fujita *et al.*, 2002); nevertheless, the charge order parameter grows more rapidly than the spin order parameter.) It follows (Zachar *et al.*, 1998) that the charge order is not driven by the spin ordering.

This result is natural for a strong-coupling picture of stripe correlations, but it poses a considerable challenge for the weak-coupling approach. In the latter, if one attributes the spin-stripe order to a nesting instability of the Fermi surface, then one must find a distinct nesting feature, with a spanning wave vector corresponding to $\mathbf{Q}_{\text{ch}}$, to explain the charge-stripe order. Of course it is also necessary to explain the doping dependence of the ordering wave vectors. According to ARPES studies, the spanning wave vector near $\mathbf{k}=(2\pi/a)(\frac{1}{2},0)$ is close to $\mathbf{Q}_{\text{ch}}$. However, its variation with doping is opposite to that of $\mathbf{Q}_{\text{ch}}$ (Ding *et al.*, 1997; Ino *et al.*, 2002); with increasing x, the holelike Fermi surface approaches closer to the $(\pi,0)$ point, so the spanning wave vector decreases, while $\mathbf{Q}_{\text{ch}}$ increases. We are not aware of a plausible explanation for the combined charge and spin modulations from the weak-coupling perspective.

• Substituting Zn impurities into the CuO_2 planes pins stripe order in $La_{2-x}Sr_xCuO_4$.

The substitution of Zn into the CuO_2 planes causes a significant increase in normal-state resistivity without modifying the carrier density (Fukuzumi *et al.*, 1996). It also wipes out the dispersive feature near the nodal point observed by ARPES in the normal state (White *et al.*, 1999). We have already discussed the fact that Zn doping can induce static stripe order in $La_{2-x}Sr_xCuO_4$ (see Fig. 8). These results are incompatible with a mechanism for stripe order based on Fermi-surface nesting. The Zn impurities break translational symmetry and cause considerable scattering of the charge carriers. Any sharp features at the Fermi surface are smeared out in the presence of the Zn. Thus the Zn should destroy, not induce, a nesting instability.

• There is no evidence of well-defined quasiparticles in the normal state of underdoped and optimally doped cuprates.

There are many features of the doped system which suggest that, for the most part, there are no well-defined quasiparticles. ARPES spectra in $Bi_2Sr_2CaCu_2O_{8+\delta}$ and $La_{2-x}Sr_xCuO_4$ in some cases do exhibit features with a well-defined dispersion, and when one looks at the spectral intensity integrated over a small energy window about the Fermi energy, a Fermi surface of sorts is observed (Dessau *et al.*, 1993; Ding *et al.*, 1996; Ino *et al.*, 2002). However, in no case has a peak been observed with a width small compared to its mean, which we take to be the definition of a well-defined quasiparticle. In some ranges of temperature and **k**, there is no well-defined quasiparticle peak at all. Near the nodal points, there are marginally defined quasiparticles, in the sense that there is certainly a clear peak in the spectral function, but its width is approximately twice its mean energy (Valla *et al.*, 1999). There is corroborating evidence that any quasiparticles are at best marginal, which comes from the T linear dependence of the normal-state resis-

tivity and various other indirect (but bulk) measurements (Anderson 1987, 1992; Varma *et al.*, 1989; Lee, 1999).

In addition, there is considerable indirect evidence that the familiar Fermi-liquid power laws are strikingly absent. NMR experiments reveal significant temperature dependence to the nuclear $1/T_1T$ and dramatic violations of the Korringa relation, not only in the pseudogap regime, but even in the high-temperature regime at optimal doping (Takigawa *et al.*, 1991). The optical conductivity has a clearly non-Drude form (Collins *et al.*, 1989), above and beyond the peculiar temperature dependence of the dc conductivity. The Hall number, as well, is anomalously temperature dependent (Wang *et al.*, 1987).

All together, these results strongly imply that a picture of weakly interacting quasiparticles has limited validity in the cuprates. The one exception is the low-energy behavior ($E \ll \Delta_0$) of the cleanest superconducting materials, deep in the superconducting state. Here, considerable indirect evidence exists that there are remarkably long-lived nodal quasiparticles which dominate the physics (Sutherland *et al.*, 2003). However, direct evidence of these sharply defined excitations has yet to emerge in any single-particle experiment such as ARPES or STM.

VII. CONCLUSIONS

There are many reasons why identifying and studying fluctuations associated with the presence of nearby ordered states has become one of the main thrusts in the study of cuprate superconductors and related materials. To some extent, these states are interesting just because they occur somewhere in the (multidimensional) phase diagram of these intriguing materials. Quantum critical points associated with some of these orders have been proposed as an explanation for the notoriously peculiar high-temperature (normal-state) behavior observed in many experiments. The possibility that certain local orders are inextricably linked with the phenomenon of high-temperature superconductivity is the most enticing reason of all. However, before we can determine whether a particular form of local order, such as local stripe order, could possibly be central to the problem of high-temperature superconductivity, we need to determine whether or not it is ubiquitous in the families of materials that exhibit high-temperature superconductivity. Regardless of one's motivation, it is clear that the ability to identify proximity to an ordered phase by the signatures of fluctuating order is very useful. This paper has focused on practical considerations pertinent to this task.

A combination of rather general scaling considerations concerning quantum critical phenomena, and specific insights gleaned from the solvable models studied, has led us to articulate a number of "lessons" concerning the optimal way of obtaining information about nearby ordered states from experiment:

(1) The information is best obtained from the low-frequency part of the dynamic structure factor, preferably integrated over a small, but nonzero range of frequencies, with the scale of frequencies set by the characteristic frequency of quantum fluctuations, $E_G/\hbar$.
(2) Weak disorder can make it easier, especially for static probes, to image the local order, as it can pin the fluctuations without greatly disrupting the intrinsic correlations.
(3) Experiments that reveal strongly dispersing features generally give information about the elementary excitations of the system; however, distinguishing dispersing features that arise from well-defined quasiparticles from the multiparticle continua characteristic of quantum critical points can be exceedingly subtle. Specifically, even where one set of experiments can be sensibly interpreted in terms of band-structure effects, care must be taken in interpreting this as evidence of well-defined electronlike quasiparticles.
(4) Several aspects of the E and $\mathbf{k}$ dependence of the local density of states (measurable by STM) in the presence of weak disorder allow one, in principle, to distinguish interference effects due to scattering of elementary excitations from impurities, from the effects of pinned incipient order. Interference effects in two dimensions produce peaks along *curves* in $\mathbf{k}$ space, which disperse as a function of energy in a manner is directly related to the quasiparticle dispersion relations, such as could be measured in ARPES, and they may or may not have a strongly energy-dependent phase. Pinning of incipient order produces peaks at well-defined points in $\mathbf{k}$ space which depend only weakly on energy, and generally have an energy-independent phase.
(5) It will often be true that interference effects and collective pinning will jointly produce complicated $\mathbf{k}$- and E-dependent properties in the local density of states that arise from a combination of both effects, especially in energy ranges in which the interference and pinning features lie at nearby values of $\mathbf{k}$.

In Sec. IV of this paper, we applied these ideas to an analysis of the evidence of local stripe order in a number of neutron scattering and STM measurements on various cuprate superconductors. The evidence of both spin- and charge-stripe order is unambiguous in the La_2CuO_4 family of high-temperature superconductors. However, there is increasingly strong evidence of substantial local charge-stripe order, and probably nematic order as well, in $Bi_2Sr_2CaCu_2O_{8+\delta}$ and $YBa_2Cu_3O_{6+y}$. Conversely, no evidence of incipient stripe order has been reported to date in the electron-doped cuprates $Ne_{2-x}Ce_xCuO_{4\pm\delta}$ and $Pr_{2-x}Ce_xCuO_{4\pm\delta}$.

Note added: After this work was completed, we received an advance copy of a colloquium article by Sachdev (2003) that has overlapping material with the

present paper and that reaches similar conclusions concerning the effects of incipient stripe order on the STM spectra.

ACKNOWLEDGMENTS

We would like to dedicate this paper to our friend and collaborator, Victor J. Emery, whose untimely death we mourn. Many of the ideas discussed in this paper have been strongly influenced by his seminal contributions to this field. We thank K. B. Cooper, S. L. Cooper, J. C. Davis, J. P. Eisenstein, J. Hoffman, P. Johnson, D.-H. Lee, P. B. Littlewood, A. Polkovnikov, S. Sachdev, D. J. Scalapino, Z.-X. Shen, A. Yazdani, and X. Zhou for useful and stimulating discussions. This work was supported in part by the National Science Foundation through Grant Nos. DMR 01-10329 (S.A.K. at UCLA), DMR 01-32990 (E.F. at the University of Illinois), DMR 99-78074 (V.O. at Princeton University), by the David and Lucille Packard Foundation (V.O. at Princeton University and A.K. and C.H. at Stanford), and by the Department of Energy's Office of Science, under Contract Nos. DE-AC02-98CH10886 (J.M.T. at Brookhaven National Laboratory), DE-FG03-01ER45929-A000 (A.K. and C.H. at Stanford University), and DE-FG03-00ER45798 (I.P.B. at UCLA).

APPENDIX A: LUTTINGER LIQUIDS AS ONE-DIMENSIONAL QUANTUM CRITICAL CHARGE-ORDERED STATES

In Sec. III we discussed how a single impurity induces charge order in the simplest and best understood quantum critical system, the Tomonaga-Luttinger model of a one-dimensional electron gas. In this appendix we give a summary of the physics and of essential technical aspects of the discussion of Sec. III, presenting only the aspects of the theory relevant to the derivation of the expressions used in Sec. III. There are a number of excellent reviews that cover the theory of the 1DEG in great depth, and we refer the interested reader to that literature (Emery, 1979; Fradkin, 1991; Stone, 1994; Gogolin *et al.*, 1998).

Consider a one-dimensional system of interacting spin-one-half fermions (electrons). We shall denote by $\Psi_\sigma(x)$ the Fermi field for an electron with spin $\sigma=\uparrow,\downarrow$, and by $\psi_{\pm,\sigma}(x)$ its right- and left-moving components, respectively:

$$\Psi_\sigma(x)=e^{ik_F x}\psi_{+,\sigma}(x)+e^{-ik_F x}\psi_{-,\sigma}(x), \tag{A1}$$

where k_F is the Fermi wave vector. In what follows we shall assume that the electron density is incommensurate and ignore umklapp scattering effects. Thus we shall be working in a regime in which the dynamics of the right- and left-moving components of the electron are slowly varying and hence are well described by an effective continuum Hamiltonian density $\mathcal{H}=\mathcal{H}_0+\mathcal{H}_{\rm int}$, where

$$\mathcal{H}_0=-iv_F\sum_{\sigma=\uparrow,\downarrow}(\psi^\dagger_{+,\sigma}\partial_x\psi_{+,\sigma}-\psi^\dagger_{-,\sigma}\partial_x\psi_{-,\sigma}) \tag{A2}$$

is the Hamiltonian density for noninteracting electrons in the low-energy regime where the dispersion is linearized; here v_F is the Fermi velocity. As usual, irrelevant operators which account for corrections to the linear dispersion are not included (however, see below for caveats). The effects of interactions are included in $\mathcal{H}_{\rm int}$.

The best way to describe the physics of the 1DEG is by means of bosonization methods. Bosonization of an interacting system of fermions is possible because the low-energy spectrum of the 1DEG is exhausted by a long-lived bosonic excitation described by a field $\phi_\sigma(x)$ which represents particle-hole fluctuations of spin σ near the Fermi points $\pm k_F$. It turns out that the field ϕ_σ also describes the phase fluctuations of a $2k_F$ charge-density-wave. Consequently the electron-density operator $\rho_\sigma(x)$ is decomposed into a long-wavelength piece j_0^σ and a $2k_F$ piece related to the density-wave order parameter. The long-wavelength electron density for spin projection σ, $j_0^\sigma(x)$, is

$$j_0^\sigma(x)=\psi^\dagger_{+,\sigma}\psi_{+,\sigma}+\psi^\dagger_{-,\sigma}\psi_{-,\sigma} \tag{A3}$$

and the long-wavelength current density with spin projection σ, $j_1^\sigma(x)$, is

$$j_1^\sigma(x)=\psi^\dagger_{+,\sigma}\psi_{+,\sigma}-\psi^\dagger_{-,\sigma}\psi_{-,\sigma}. \tag{A4}$$

Here j_0^σ and j_1^ν are operators normal ordered with respect to the filled Fermi sea.

The density and current-density operators obey the equal-time bosonic commutation relations

$$[j_0^\sigma(x),j_1^\nu(y)]=\frac{i}{\pi}\partial_x\delta(x-y)\,\delta_{\sigma,\nu}, \tag{A5}$$

where $\sigma,\nu=\uparrow,\downarrow$. One can identify $j_0^\sigma(x)$ and $j_1^\sigma(x)$ with

$$j_0^\sigma(x)=\frac{1}{\sqrt{\pi}}\partial_x\phi_\sigma(x),$$

$$j_1^\sigma(x)=\frac{1}{\sqrt{\pi}}\Pi_\sigma(x), \tag{A6}$$

where $\phi_\sigma(x)$ is a Bose field and $\Pi_\sigma(x)$ is its canonically conjugate momentum; they obey the canonical equal-time commutation relations,

$$[\phi_\sigma(x),\Pi_\nu(y)]=i\,\delta_{\sigma,\nu}\delta(x-y). \tag{A7}$$

The (slowly varying) Fermi fields $\psi_{\pm,\sigma}(x)$ can themselves be reconstructed from the Bose field $\phi_\sigma(x)$:

$$\psi_{\pm,\sigma}(x)=\frac{1}{\sqrt{2\pi\alpha}}\mathcal{N}_\sigma e^{i\sqrt{\pi}[\pm\phi_\sigma(x)-\theta_\sigma(x)]} \tag{A8}$$

(here $\alpha\sim v_F/D$ is a short-distance cutoff and D is the fermion bandwidth), where we have introduced the dual field $\theta_\sigma(x)$ defined by the identity

$$\partial_x\theta_\sigma(x)=\Pi_\sigma(x), \tag{A9}$$

and where $\mathcal{N}_\sigma$, the Klein factor, is an operator that guarantees that Fermi fields with different spin labels anticommute with each other.

It is convenient to introduce the charge and spin Bose fields ϕ_c and ϕ_s,

$$\phi_c=\frac{1}{\sqrt{2}}(\phi_\uparrow+\phi_\downarrow),$$

$$\phi_s=\frac{1}{\sqrt{2}}(\phi_\uparrow-\phi_\downarrow). \tag{A10}$$

The Hamiltonian density of the interacting system can be written as a sum of operators, which are marginal (with scaling dimension equal to 2), relevant (with scaling dimension smaller than 2), and irrelevant (with scaling dimension larger than 2). For an incommensurate 1DEG, the effective low-energy Hamiltonian, which contains only marginal operators, has the spin-charge separated form

$$\mathcal{H}=\mathcal{H}_c+\mathcal{H}_s, \tag{A11}$$

where the charge Hamiltonian density $\mathcal{H}_c$ in bosonized form has the universal (Tomonaga-Luttinger) form

$$\mathcal{H}_c=\frac{v_c}{2}K_c\Pi_c^2+\frac{v_c}{2K_c}(\partial_x\phi_c)^2, \tag{A12}$$

where v_c is the charge velocity and K_c is the charge Luttinger parameter. For repulsive interactions, the spin Hamiltonian density $\mathcal{H}_s$ has the same form,

$$\mathcal{H}_s=\frac{v_s}{2}K_s\Pi_s^2+\frac{v_s}{2K_s}(\partial_x\phi_s)^2. \tag{A13}$$

The nonuniversal charge and spin velocities and the Luttinger parameters encode the dependence of this low-energy theory on the microscopic parameters of the system. Quite generally, for a system with repulsive interactions, the charge Luttinger parameter obeys the inequality $K_c<1$, and for spin rotationally invariant interactions the spin Luttinger parameter satisfies the equality $K_s=1$. Typically the charge and spin velocities satisfy the inequality $v_c>v_s$. In the weak-coupling limit, and neglecting all irrelevant operators, simple expressions for K_c, v_c, and v_s in terms of the backscattering and forward-scattering amplitudes can be written down.[45]

Physical observables of the 1DEG have simple expressions in the bosonized theory. Since the Tomonaga-Luttinger model is strictly quadratic in Bose fields, it allows for a straightforward computation of the correlation functions of all observables of interest, at both zero and finite temperature, as well as for different types of boundary conditions. For the purposes of this review it will be sufficient to note that the electron density has the decomposition

$$\begin{aligned}\rho(x)=&\frac{2k_F}{\pi}+j_0(x)+e^{i2k_Fx}\mathcal{O}_{\mathrm{CDW}}(x)\\&+e^{-i2k_Fx}\mathcal{O}_{\mathrm{CDW}}^\dagger(x)+e^{i4k_Fx}\mathcal{O}_{4k_F}(x)\\&+e^{-i4k_Fx}\mathcal{O}_{4k_F}^\dagger(x),\end{aligned} \tag{A14}$$

where

$$j_0=j_0^\uparrow+j_0^\downarrow=\sqrt{\frac{2}{\pi}}\partial_x\phi_c \tag{A15}$$

is the long-wavelength charge density, and

$$\mathcal{O}_{\mathrm{CDW}}=\sum_\sigma\psi_{+,\sigma}^\dagger\psi_{-,\sigma}=\frac{1}{\pi\alpha}\cos(\sqrt{2\pi}\phi_s)e^{-i\sqrt{2\pi}\phi_c} \tag{A16}$$

is the charge-density-wave order parameter (i.e., the $2k_F$ amplitude of the charge density), and $\mathcal{O}_{4k_F}$ is the $4k_F$ charge-density-wave order parameter (which we shall not discuss here).

In particular this implies that the charge dynamical structure factor for wave vectors close to $2k_F$, discussed in Sec. III, is the (retarded) correlation function of the charge-density-wave order parameter:

$$S_{\mathrm{CDW}}(x,t)=\langle\mathcal{O}_{\mathrm{CDW}}^\dagger(x,t)\mathcal{O}_{\mathrm{CDW}}(0,0)\rangle, \tag{A17}$$

whereas for small wave vectors it is given instead by the (retarded) density correlator

$$S_0(x,t)=\langle j_0(x,t)j_0(0,0)\rangle. \tag{A18}$$

In particular, the spectral function for $S_{\mathrm{CDW}}(x,t)$, which we shall denote by $\tilde{S}_{\mathrm{CDW}}(k,\omega)$, has the scaling form

$$\tilde{S}_{\mathrm{CDW}}(k,\omega)=\frac{v_c}{16\pi^4}\left(\frac{\pi T\alpha}{v_c}\right)^{K_c-1}\Phi_{\mathrm{CDW}}\left(\frac{v_sk}{\pi T},\frac{\omega}{\pi T}\right), \tag{A19}$$

where $\Phi_{\mathrm{CDW}}(x,y)$ is the (dimensionless) scaling function (Orgad *et al.*, 2001)

$$\begin{aligned}\Phi_{\mathrm{CDW}}(x,y)\equiv&\int_{-\infty}^{\infty}du\int_{-\infty}^{\infty}dv\,h_{K_c/2}\left(\frac{u+v}{2}\right)\\&\times h_{K_c/2}^*\left(\frac{u-v}{2}\right)h_{1/2}\left(-\frac{ru+v}{2}\right)\\&\times h_{1/2}^*\left(\frac{ru-v}{2}\right).\end{aligned} \tag{A20}$$

Here $r=v_s/v_c<1$ and $h_\nu(z)$ is given by (Orgad *et al.*, 2001)

$$h_\nu(z)=\mathrm{Re}\left[(2i)^\nu B\left(\frac{\nu-iz}{2},1-\nu\right)\right], \tag{A21}$$

where $B(x,y)$ is the Euler beta function,

$$B(x,y)=\frac{\Gamma(x)\Gamma(y)}{\Gamma(x+y)}, \tag{A22}$$

and $\Gamma(z)$ is the gamma function.

We now turn to the calculation of the tunneling density of states discussed in Sec. III. There we presented the behavior of the $2k_F$ component of the tunneling density of states $N(2k_F+q,E)$, the Fourier transform in x and t of the $2k_F$ component of the electron spectral function. At zero temperature and for a semi-infinite system with $0\leqslant x<L$ (with $L\to\infty$), the $2k_F$ component

[45] At intermediate and strong coupling the effective low-energy theory still has the same form but with significant renormalization of these parameters.

of the fermion Green's function, $g_{2k_F}(x,t)$, is given by (Eggert *et al.*, 1996; Mattsson *et al.*, 1997; Eggert, 2000)

$$g_{2k_F}(x,t) \equiv \langle \psi^\dagger_{+,\sigma}(x,t)\psi_{-,\sigma}(x,0)\rangle \sim \frac{1}{2\pi}\frac{\alpha^{a+b-1/2}(2x/v_c\tau)^c}{(v_s\tau-2x)^{1/2}(v_c\tau-2x)^a(v_c\tau+2x)^b}, \tag{A23}$$

where $\tau=t+i0^+$. Notice that in Eq. (A23) we have kept the dependence on the short-distance cutoff α; consequently, $g_{2k_F}(x,t)$ naively has units of α^{-1}. However, in a Luttinger liquid the fermion operator has an anomalous scaling dimension. For this semi-infinite geometry the scaling dimension is governed by the exponents a, b, and c, which are given by

$$a=\frac{(K_c+1)^2}{8K_c}, \quad b=\frac{(K_c-1)^2}{8K_c}, \quad c=\frac{1}{4}\left(\frac{1}{K_c}-K_c\right). \tag{A24}$$

At finite temperature $T>0$, $g_{2k_F}(x,t;T)$ becomes

$$g_{2k_F}(x,t;T)\sim \frac{1}{2\pi\alpha}\left(\frac{\pi T\alpha}{v_s}\right)^{1/2}\left(\frac{\pi T\alpha}{v_c}\right)^{(1/4)(K_c+K_c^{-1})} \times\left(\frac{-i}{\sinh\left[\frac{\pi T}{v_s}(v_s\tau-2x)\right]}\right)^{1/2} \times\left(\frac{-i}{\sinh\left[\frac{\pi T}{v_c}(v_c\tau-2x)\right]}\right)^{a} \times\left(\frac{-i}{\sinh\left[\frac{\pi T}{v_c}(v_c\tau+2x)\right]}\right)^{b} \times\left(\frac{\sinh\left(\frac{2\pi Tx}{v_c}\right)}{\sinh\left(\frac{\pi T\tau}{v_c}\right)}\right)^{c}. \tag{A25}$$

As with the structure factor, $N(q+2k_F,E)$ can also be expressed in terms of a scaling function Φ as

$$N(q+2k_F,E)\equiv\int_0^\infty dx\int_{-\infty}^\infty dt\, e^{-i(qx-Et)}g_{2k_F}(x,t) =\frac{B}{2E}\left(\frac{\alpha E}{v_c}\right)^{2b}\Phi\left(\frac{2E}{v_cq},\frac{E}{k_BT}\right), \tag{A26}$$

which also depends on the charge Luttinger parameter K_c and on the ratio of the charge and spin velocities v_c/v_s. B is the dimensionless quantity

$$B=\frac{e^{-i\pi(c+1)/2}}{\Gamma\left(a+b+c-\frac{1}{2}\right)}. \tag{A27}$$

The behavior of $N(2k_F+q,E;T)$ for $T>0$ is shown in Figs. 3 and 4 in Sec. III. At $T=0$ the scaling function $\Phi(2E/v_cq)$ is given by

$$\Phi(u)=\sqrt{\frac{v_c}{v_s}}u^{c+1}\int_0^1 dt\, t^c(1-t)^{a+b-3/2}(1-ut)^{-a} \times(1+u^*t)^{-b}\left(1-\frac{v_c}{v_s}ut\right)^{-1/2}. \tag{A28}$$

Here $u=2|E|/qv_c+i0^+$. We have obtained analytic expressions for the singular pieces of $N(k,E)$ at $T=0$, for a general value of the charge Luttinger parameter in the range of interest $0<K_c<1$, and general v_c/v_s. $N(k,E)$ has power-law singularities as $2E/v_cq\to\pm1$, $2E/v_cq\to0$, and $2E/v_cq\to\infty$ and $2E/v_cq\to v_s/v_c$.

Physically the nonanalyticities at $2E/v_cq=\pm1$ and $2E/v_sq=1$ represent the threshold of the continuum of propagating excitations of appropriate type, moving to the right and to the left, respectively. The singularity at $2E/v_cq\to\infty$ corresponds to the $2k_F$ charge-density-wave stabilized (pinned) by the boundary.

Close to the right-dispersing charge-related singularity at $q\to2E/v_c$ we find

$$N(2k_F+q,E)\sim\frac{1}{2E}\left(\frac{\alpha E}{v_c}\right)^{2b}A_+\left[1-\frac{2E}{v_cq}\right]^{b-1/2}, \tag{A29}$$

where A_+ is a finite complex coefficient determined by the strength of the singularity. An important feature of this result is that, as E goes through this singularity at fixed q, the phase of $N(2k_F+q,E)$ jumps by $\pi(b-1/2)$ (see Fig. 4). Close to the right-dispersing spin-related singularity at $q\to2E/v_s$ we find

$$N(2k_F+q,E)\sim\frac{1}{2E}\left(\frac{\alpha E}{v_s}\right)^{2b}\left(\frac{v_s}{v_c}\right)^{a+b+c-1} \times A'_+\left[1-\frac{2E}{v_sq}\right]^{2b-1/2}, \tag{A30}$$

where A' is another complex coefficient. In the noninteracting limit $K_c=1$ and $v_s=v_c$, these two singularities coalesce into a simple pole for a particle moving to the right. However, for $K_c<1$, the Tomonaga-Luttinger liquid does not have quasiparticles but massless soliton states instead. As usual, the power laws reflect the multisoliton continuum. [More generally, the limit $v_s/v_c\to1$ is somewhat subtle (Bindloss *et al.*, 2003).] Similarly, for $q\to-2E/v_c$,

$$N(2k_F+q,E)\sim\frac{1}{2E}\left(\frac{\alpha E}{v_c}\right)^{2b}A_-\left[1+\frac{2E}{v_cq}\right]^{b}, \tag{A31}$$

where, once again, A_- is a finite complex coefficient specific to this singularity. However, unlike the singularity at $E=+v_cq$, the behavior near $E=-v_cq$ although nonanalytic is not divergent, since $b>0$ for repulsive interactions.

In addition to propagating excitations, we also find that $N(2k_F+q,E)$ has a singularity associated with the nonpropagating charge-density-wave as $q\to0$:

$$N(2k_F+q,E)\propto\frac{1}{2E}\left(\frac{\alpha E}{v_c}\right)^{2b}\left(\frac{v_s}{v_c}\right)^{1/2}\left[\frac{2E}{v_c q}\right]^{(1-K_c)/2}, \tag{A32}$$

which diverges as $q\to 0$. This singularity also exhibits a phase jump as $q\to 0^{\pm}$, equal to $\pi(1-K_c)/2$.

At low voltages $E\to 0$ and at fixed q, we find

$$N(2k_F+q,E)\propto\frac{1}{2E}\left(\frac{\alpha E}{v_c}\right)^{2b}\left(\frac{v_s}{v_c}\right)^{1/2}\left[\frac{2E}{v_c q}\right]^{c+1}. \tag{A33}$$

Finally, we summarize here the calculation of the induced density of states in the weak-impurity limit, $E>T_K$. In Sec. II.C we showed that the density of states at wave vector k and voltage E induced by an impurity potential with amplitude $V(k)$ at wave vector k defines the susceptibility $\chi_{\rm DOS}(k,E)$ given in Eq. (2.8). Here we shall sketch the calculation of $\chi_{\rm DOS}(2k_F+q,E)$ to leading order in $V(k)$ for a Luttinger liquid. We must first find the Green's function,

$$G(z_1,z_2,z_3)=\langle\psi^{\dagger}_{+,\uparrow}(z_1)\psi_{-,\uparrow}(z_2)\times[\psi^{\dagger}_{-,\uparrow}(z_3)\psi_{+,\uparrow}(z_3)+\uparrow\leftrightarrow\downarrow]\rangle, \tag{A34}$$

which can be computed readily using bosonization methods. At $T=0$ and for an infinite system the time-ordered Green's function $G(z_1,z_2,z_3)$, in imaginary time, is given by

$$\begin{aligned}G(z_1,z_2,z_3)=&\frac{1}{2\pi^2\alpha^2}|z_1-z_2|^{-(1-K_c^2)/4K_c}\\&\times(z_1-z_3)^{-(K_c-1)/4}(z_2-z_3)^{-(K_c+1)/4}\\&\times(w_1-w_3)^{-1/4}(\overline{z_1}-\overline{z_3})^{-(K_c+1)/4}\\&\times(\overline{z_2}-\overline{z_3})^{-(K_c-1)/4}(\overline{w_2}-\overline{w_3})^{-1/4},\end{aligned} \tag{A35}$$

where we have used the charge and spin complex coordinates $z=x+iv_c\tau$ and $w=x+iv_s\tau$. The susceptibility $\chi_{\rm DOS}(2k_F+q,E)$ is obtained, upon analytic continuation to real frequencies, from

$$\chi_{\rm DOS}(2k_F+q,E)=\mathrm{Im}\int_{-\infty}^{\infty}dx\int_{-\infty}^{\infty}d\tau\, e^{-i(kx-E\tau)}\times\int d\tau' G(x,\tau;x,0;0,\tau'). \tag{A36}$$

The result for the integrated density of states $\tilde{N}(2k_F+q,D)$ presented in Sec. III, Eq. (3.13) follows from integrating Eq. (A36) over energies large compared with the low-energy cutoff T_K.

APPENDIX B: EXPERIMENTALLY DETERMINED SCALES OF MAGNETISM IN VARIOUS MATERIALS

Here we explain some of the assumptions behind the parameter values specified in Table I. For antiferromagnetic phases, the meaning of the parameters is relatively straightforward, but extracting parameters from measurements on doped systems can require extrapolations from simple models. Note that we have not addressed important issues related to possible novel forms of orbital magnetism that have been proposed (Varma, 1997; Chakravarty, Kee, and Nayak, 2001).

1. Magnitude of the ordered moments

a. Absolute moments from neutron scattering

In the case of long-range antiferromagnetic order, the absolute magnitude m of the average ordered moment per planar Cu is obtained from an elastic neutron-diffraction measurement by comparing the intensities of the magnetic Bragg superlattice peaks with those of Bragg peaks from the chemical lattice. It has been observed that m is correlated with the Néel temperature T_N in both La_2CuO_4 (Yamada *et al.*, 1987) and $YBa_2Cu_3O_{6+y}$ (Tranquada *et al.*, 1988). In the earliest measurements of La_2CuO_4, samples typically contained excess oxygen, resulting in values of m and T_N significantly lower than those of the stoichiometric material. Another complication is that determination of m requires knowledge of the magnetic form factor, which turns out to be considerably more anisotropic (Shamoto *et al.*, 1993) than was appreciated initially.

For comparison, it is worth noting that for a spin-$\frac{1}{2}$ Heisenberg model on a square lattice with only nearest-neighbor interactions, the magnitude of the average ordered spin per Cu, to second order in a $1/S$ expansion (Igarashi, 1992) is $\langle S\rangle=0.307$. For a moment due to spin only, $g=2$ and $m=g\langle S\rangle\mu_B=0.61\mu_B$. Although it has not been possible to measure the g factor for Cu in the layered cuprates,[46] a typical value for a Cu^{2+} ion in a distorted octahedral environment is 2.2 (Abragam and Bleaney, 1970), which implies a typical moment of $0.67\mu_B$. The fact that the observed maximum moments in La_2CuO_4 and $YBa_2Cu_3O_{6+y}$ are 10–20 % smaller than this could be a result of hybridization of the Cu $3d_{x^2-y^2}$ orbital with O $2p_\sigma$ orbitals. (By symmetry, the net spin density on oxygen sites is zero in the Néel structure.)

b. Relative moments from μSR

In μSR, one measures a precession frequency, which is directly proportional to the local hyperfine field at the μ^+ site. Determination of the absolute moment requires knowledge of the μ^+ location (obtained by calculation rather than experiment) and a calculation of the magnetic field at that site due to the ordered Cu moments. Alternatively, under the assumption that the μ^+ site is unchanged by doping, one can determine the local moment in a doped sample relative to that in the parent insulator. An advantage of the μSR technique is that its sensitivity does not depend on the existence of long-range order. A beautiful example of this is the study of Niedermayer *et al.* (1998) in which it was shown that the local ordered moment (at very low temperature) changes little as long-range antiferromagnetic order is

[46] Despite numerous attempts, it has not been possible to detect an electron-spin resonance signal from Cu^{2+} in planar cuprates (Simon *et al.*, 1993).

destroyed by doping in $La_{2-x}Sr_xCuO_4$ and $Y_{1-x}Ca_xBa_2Cu_3O_6$. In a complementary study, Klauss *et al.* (2000) showed that substantial moments associated with local antiferromagnetic order (presumably stripe order pinned by the tetragonal structure) are present in $La_{1.8-x}Eu_{0.2}Sr_xCuO_4$ for $0.08 \lesssim x \lesssim 0.18$.

In a stripe-ordered sample, the muons sample a distribution of local hyperfine fields, resulting in a fairly rapid damping of the precession signal (Nachumi *et al.*, 1998; Klauss *et al.*, 2000; Savici *et al.*, 2002). The relative moment quoted in the table corresponds to the maximum of that distribution.

2. Integrated low-energy spectral weight

Neutron scattering measures the dynamical magnetic structure factor $S(\mathbf{Q},\omega) \equiv S_{zz}(\mathbf{Q},\omega)$. Actually, the spin structure factor is the tensorial quantity $S_{\alpha\beta}(\mathbf{Q},\omega)$, which obeys the sum rule

$$\int_0^\infty d\omega \int_{BZ} d\mathbf{Q} \sum_\alpha S_{\alpha\alpha}(\mathbf{Q},\omega) = S(S+1), \tag{B1}$$

where S is the spin per magnetic ion. For cuprates in general, and superconducting samples in particular, it is challenging to measure the magnetic scattering to sufficiently high energies (with sufficient signal-to-noise ratio) that the sum rule can be evaluated; however, there do exist a few studies that allow one to evaluate the energy integral up to 100 meV. While there are significant uncertainties in evaluating the integral from published data, these should be smaller than the uncertainty in the calibration of the sample volume contributing to the signal, which for superconducting samples can be on the order of 30% (Fong *et al.*, 2000).

Since we are interested in the change of this integrated quantity with doping, we have normalized it to the value measured for the relevant parent antiferromagnet. Note that, for the latter case, the integral includes the signal in the magnetic Bragg peaks as well as that from the spin waves.

Another quantity that one can evaluate is the relative weight under the resonance peak, which appears below T_c in the superconducting state. Values, normalized to the full sum-rule weight, have been tabulated by Kee *et al.* (2002). For $YBa_2Cu_3O_{6+y}$ samples with T_c varying from 52 to 93 K, they found the normalized weight to be about 1.5%; for a sample of $Bi_2Sr_2CaCu_2O_{8+\delta}$ with $T_c = 91$ K, the value is $\sim 6\%$. It should be noted that integrating $S(\mathbf{Q},\omega)$ up to 100 meV for the experimental measurements on antiferromagnetic $YBa_2Cu_3O_{6.15}$ (Hayden *et al.*, 1996b) gives just 20% of the full sum-rule weight; hence, using the same normalization as for $\int S(\mathbf{Q},\omega)$ in Table I, the weight of the resonance peak in $YBa_2Cu_3O_{6+y}$ is about 0.08.

3. Energy scale of spin fluctuations

a. From neutron scattering

In the spin-wave theory of a Heisenberg model on a square lattice with only nearest-neighbor coupling, the zone-edge magnon with $\mathbf{q}_0 = (\pi,0)$ has energy $\epsilon_{\mathbf{q}_0} = 4SJ_{\text{eff}} = 2J_{\text{eff}}$, where the final equality applies for $S = \frac{1}{2}$. Longer-range couplings have observable effects in the spin-wave dispersion curves measured for La_2CuO_4 (Coldea *et al.*, 2001); nevertheless, it is useful to characterize $\epsilon_{\mathbf{q}_0}$, which is essentially the local energy to flip a spin, in terms of J_{eff}. Assuming that a local superexchange coupling is still active between local moments in doped samples, we have used the same formula to define J_{eff} in terms of the maximum spin-excitation energy observed in superconducting cuprates.

b. From two-magnon Raman scattering

While Raman scattering is not sensitive to individual spin waves, it does provide a valuable probe of two-magnon correlations in 2D square-lattice antiferromagnets (Lyons *et al.*, 1988). The dominant part of the response has B_{1g} symmetry and appears at low temperature as a strong peak occurring at an energy of $2.8J_{\text{eff}}$ for $S = \frac{1}{2}$ and $6.8J_{\text{eff}}$ for $S = 1$ (Canali and Girvin, 1992). The scattering mechanism is believed to involve relatively short-range excitations, so that the response is not very sensitive to the existence of long-range order. Although there is no formal justification for it, we have used the formula for peak energy in the antiferromagnetic state in order to extract a characteristic value for J_{eff} from the two-magnon signal measured from superconducting samples. Note that there are also results available on $Bi_2Sr_2CaCu_2O_{8+\delta}$ (Blumberg *et al.*, 1997; Sugai and Hosokawa, 2000), which we have not included in Table I.

REFERENCES

Abragam, A., and B. Bleaney, 1970, *Electron Paramagnetic Resonance of Transition Ions* (Clarendon, Oxford).

Aeppli, G., T. E. Mason, S. M. Hayden, H. A. Mook, and J. Kulda, 1997, Science **278**, 1432.

Akoshima, M., and Y. Koike, 1998, J. Phys. Soc. Jpn. **67**, 3653.

Akoshima, M., Y. Koike, I. Watanabe, and K. Nagamine, 2000, Phys. Rev. B **62**, 6761.

Anderson, P. W., 1987, Science **235**, 1169.

Anderson, P. W., 1992, Science **256**, 1526.

Anderson, P. W., 1997, Adv. Phys. **46**, 3.

Ando, Y., 2002, Proceedings of the ICTP Workshop on Intrinsic Multi-Scale Structure and Dynamics in Complex Oxides, Triese (Italy) (World Scientific, in press).

Ando, Y., G. S. Boebinger, A. Passner, N. L. Wang, C. Geibel, F. Steglich, I. E. Trofimov, and F. F. Balakirev, 1997, Phys. Rev. B **56**, 8530.

Ando, Y., A. N. Lavrov, and K. Segawa, 1999, Phys. Rev. Lett. **83**, 2813.

Ando, Y., and K. Segawa, 2002, Phys. Rev. Lett. **88**, 167005.

Ando, Y., K. Segawa, S. Komiya, and A. N. Lavrov, 2002, Phys. Rev. Lett. **88**, 137005.

Arai, M., T. Nishijima, Y. Endoh, T. Egami, S. Tajima, K. Tomimoto, Y. Shiohara, M. Takahashi, A. Garrett, and S. M. Bennington, 1999, Phys. Rev. Lett. **83**, 608.

Arovas, D. P., A. J. Berlinsky, C. Kallin, and S.-C. Zhang, 1997, Phys. Rev. Lett. **79**, 2871.

Axe, J. D., and M. K. Crawford, 1994, J. Low Temp. Phys. **95**, 271.
Baberski, O., A. Lang, O. Maldonado, M. Hücker, B. Büchner, and A. Freimuth, 1998, Europhys. Lett. **44**, 335.
Balakirev, F. F., J. B. Betts, G. S. Boebinger, S. Ono, Y. Ando, and T. Murayama, 2002, *Proceedings of Physical Phenomena at High Magnetic Fields—IV* (World Scientific, Singapore), pp. 275–278.
Basov, D. N., 2002, private communication.
Basov, D. N., R. Liang, D. A. Bonn, W. N. Hardy, B. Dabrowski, M. Quijada, D. B. Tanner, J. P. Rice, D. M. Ginsberg, and T. Timusk, 1995, Phys. Rev. Lett. **74**, 598.
Bednorz, J. G., and K. A. Müller, 1986, Z. Phys. B: Condens. Matter **64**, 189.
Bernhard, C., T. Holden, J. Humlíček, D. Munzar, A. Golnik, M. Kläser, T. Wolf, L. Carr, C. Homes, B. Keimer, and M. Cardona, 2001, Solid State Commun. **121**, 93.
Bianconi, A., N. L. Saini, A. Lanzara, M. Missori, T. R. H. Oyanagi, H. Yamaguchi, K. Oka, and T. Ito, 1996, Phys. Rev. Lett. **76**, 3412.
Bindloss, I. P., S. A. Kivelson, E. Fradkin, and V. Oganesyan, 2003, unpublished.
Blumberg, G., P. Abbamonte, M. V. Klein, W. C. Lee, D. M. Ginsberg, L. L. Miller, and A. Zibold, 1996, Phys. Rev. B **53**, R11 930.
Blumberg, G., M. Kang, M. V. Klein, K. Kadowaki, and C. Kendziora, 1997, Science **278**, 1427.
Blumberg, G., P. Littlewood, A. Gozar, B. S. Dennis, N. Motoyama, H. Eisaki, and S. Uchida, 2002, Science **297**, 584.
Blumberg, G., R. Liu, M. V. Klein, W. C. Lee, D. M. Ginsberg, C. Gu, B. W. Veal, and B. Dabrowski, 1994, Phys. Rev. B **49**, 13 295.
Boothroyd, A. T., D. Prabhakaran, P. G. Freeman, S. J. S. Lister, M. Enderle, A. Hiess, and J. Kulda, 2003, Phys. Rev. B **67**, 100407.
Bourges, P., H. Casalta, L. P. Regnault, J. Bossy, P. Burlet, C. Vettier, E. Beaugnon, P. Gautier-Picard, and R. Tournier, 1997, Physica B **234-236**, 830.
Bourges, P., H. F. Fong, L. P. Regnault, J. Bossy, C. Vettier, D. L. Milius, I. A. Aksay, and B. Keimer, 1997, Phys. Rev. B **56**, R11 439.
Bourges, P., L. P. Regnault, Y. Sidis, and C. Vettier, 1996, Phys. Rev. B **53**, 876.
Bourges, P., Y. Sidis, M. Braden, K. Nakajima, and J. M. Tranquada, 2003, Phys. Rev. Lett. **90**, 147202.
Bourges, P., Y. Sidis, H. F. Fong, L. P. Regnault, J. Bossy, A. Ivanov, and B. Keimer, 2000, Science **288**, 1234.
Božin, E. S., G. H. Kwei, H. Takagi, and S. J. L. Billinge, 2000, Phys. Rev. Lett. **84**, 5856.
Braden, M., M. Meven, W. Reichardt, L. Pintschovius, M. T. Fernandez-Diaz, G. Heger, F. Nakamura, and T. Fujita, 2001, Phys. Rev. B **63**, 140510.
Brinckmann, J., and P. A. Lee, 1999, Phys. Rev. Lett. **82**, 2915.
Briner, B. G., P. Hofmann, M. Doering, H.-P. Rust, E. W. Plummer, and A. M. Bradshaw, 1998, Phys. Rev. B **58**, 13 931.
Brown, S. E., W. Yu, F. Zamborszky, and B. Alavi, 2003, Synth. Met. **137**, 1299.
Büchner, B., M. Breuer, A. Freimuth, and A. P. Kampf, 1994, Phys. Rev. Lett. **73**, 1841.
Bulut, N., D. Hone, D. J. Scalapino, and N. E. Bickers, 1990, Phys. Rev. Lett. **64**, 2723.
Byers, J. M., M. E. Flatté, and D. J. Scalapino, 1993, Phys. Rev. Lett. **71**, 3363.
Campuzano, J. C., M. R. Norman, and M. Randeria, 2003, in *Physics of Conventional and Unconventional Superconductors*, edited by K. H. Bennemann and J. B. Ketterson (Springer, Berlin).
Canali, C. M., and S. M. Girvin, 1992, Phys. Rev. B **45**, 7127.
Capriotti, L., D. J. Scalapino, and R. D. Sedgewick, 2003, Phys. Rev. B **68**, 014508.
Cardy, J., 1999, Physica A **263**, 215.
Carlson, E. W., V. J. Emery, S. A. Kivelson, and D. Orgad, 2003, in *The Physics of Conventional and Unconventional Superconductors*, edited by K. H. Bennemann, and J. B. Ketterson (Springer, Berlin).
Carlson, E. W., S. A. Kivelson, V. J. Emery, and E. Manousakis, 2000, Phys. Rev. Lett. **83**, 612.
Carlson, E. W., D. Orgad, S. A. Kivelson, and V. J. Emery, 2001, Phys. Rev. B **62**, 3422.
Casalta, H., P. Schleger, E. Brecht, W. Montfrooij, N. H. Andersen, B. Lebech, W. W. Schmahl, H. Fuess, R. Liang, W. N. Hardy, and T. Wolf, 1994, Phys. Rev. B **50**, 9688.
Castellani, C., C. Di Castro, and M. Grilli, 1995, Phys. Rev. Lett. **75**, 4650.
Castro Neto, A. H., 2001, Phys. Rev. B **64**, 104509.
Castro Neto, A. H., and C. Morais Smith, 2003, "Charge inhomogeneities in strongly-correlated systems," e-print cond-mat/0304094.
Chaikin, P. M., and T. C. Lubensky, 1995, *Principles of Condensed Matter Physics* (Cambridge University, Cambridge, UK).
Chakravarty, S., B. I. Halperin, and D. R. Nelson, 1989, Phys. Rev. B **39**, 2344.
Chakravarty, S., H.-Y. Kee, and C. Nayak, 2001, Int. J. Mod. Phys. B **15**, 2901.
Chakravarty, S., R. B. Laughlin, D. K. Morr, and C. Nayak, 2001, Phys. Rev. B **64**, 094503.
Chen, C. H., S.-W. Cheong, and A. S. Cooper, 1993, Phys. Rev. Lett. **71**, 2461.
Chen, H.-D., J.-P. Hu, S. Capponi, E. Arrigoni, and S.-C. Zhang, 2002, Phys. Rev. Lett. **89**, 137004.
Cheong, S.-W., G. Aeppli, T. E. Mason, H. Mook, S. M. Hayden, P. C. Canfield, Z. Fisk, K. N. Clausen, and J. L. Martinez, 1991, Phys. Rev. Lett. **67**, 1791.
Chernyshev, A. L., A. H. Castro Neto, and A. R. Bishop, 2000, Phys. Rev. Lett. **84**, 4922.
Cho, J. H., F. Borsa, D. C. Johnston, and D. R. Torgeson, 1992, Phys. Rev. B **46**, 3179.
Chou, F. C., F. Borsa, J. H. Cho, D. C. Johnston, A. Lascialfari, D. R. Torgeson, and J. Ziolo, 1993, Phys. Rev. Lett. **71**, 2323.
Chubukov, A. V., S. Sachdev, and J. Ye, 1994, Phys. Rev. B **49**, 11 919.
Cohn, J. L., C. P. Popoviciu, Q. M. Lin, and C. W. Chu, 1999, Phys. Rev. B **59**, 3823.
Coldea, R., S. M. Hayden, G. Aeppli, T. G. Perring, C. D. Frost, T. E. Mason, S.-W. Cheong, and Z. Fisk, 2001, Phys. Rev. Lett. **86**, 5377.
Collins, R. T., Z. Schlesinger, F. Holtzberg, P. Chaudhari, and C. Feild, 1989, Phys. Rev. B **39**, 6571.
Cooper, K. B., M. P. Lilly, J. P. Eisenstein, T. Jungwirth, L. N. Pfeiffer, and K. W. West, 2001, Solid State Commun. **119**, 89.
Cooper, K. B., M. P. Lilly, J. P. Eisenstein, L. N. Pfeiffer, and K. W. West, 2002, Phys. Rev. B **65**, 241313(R).
Crawford, M. K., W. E. Farneth, E. M. McCarron III, R. L. Harlow, and A. H. Moudden, 1990, Science **250**, 1390.

Crawford, M. K., R. L. Harlow, E. M. McCarron, W. E. Farneth, J. D. Axe, H. Chou, and Q. Huang, 1991, Phys. Rev. B **44**, 7749.
Crommie, M. E., C. P. Lutz, and D. M. Eigler, 1993, Nature (London) **363**, 524.
Curro, N. J., P. C. Hammel, B. J. Suh, M. Hücker, B. Büchner, U. Ammerahl, and A. Revcolevschi, 2000, Phys. Rev. Lett. **85**, 642.
Curro, N. J., C. Milling, J. Haase, and C. P. Slichter, 2000, Phys. Rev. B **62**, 3473.
Dai, H., H. Chen, and C. M. Lieber, 1991, Phys. Rev. Lett. **66**, 3183.
Dai, P., H. A. Mook, G. Aeppli, S. M. Hayden, and F. Doğan, 2000, Nature (London) **406**, 965.
Dai, P., H. A. Mook, S. M. Hayden, G. Aeppli, T. G. Perring, R. D. Hunt, and F. Doğan, 1999, Science **284**, 1344.
Damascelli, A., Z. Hussain, and Z.-X. Shen, 2003, Rev. Mod. Phys. **75**, 473.
de Gennes, P. G., 1974, *The Physics of Liquid Crystals* (Clarendon, Oxford).
Demler, E., S. Sachdev, and Y. Zhang, 2001, Phys. Rev. Lett. **87**, 067202.
Derro, D. J., E. W. Hudson, K. M. Lang, S. H. Pan, J. C. Davis, J. T. Markert, and A. L. de Lozanne, 2002, Phys. Rev. Lett. **88**, 097002.
Dessau, D. S., Z.-X. Shen, D. M. King, D. S. Marshall, L. W. Lombardo, P. H. Dickinson, A. G. Loeser, J. D. C.-H. Park, A. Kapitlnik, and W. E. Spicer, 1993, Phys. Rev. Lett. **71**, 2781.
Ding, H., A. F. Bellman, J. C. Campuzano, M. Randeria, T. Yokoya, T. Takahashi, H. Katayama-Yoshida, T. Mochiku, K. Kadowaki, G. Jennings, and G. P. Brivio, 1996, Phys. Rev. Lett. **76**, 1533.
Ding, H., J. C. Campuzano, A. F. Bellman, T. Yokoya, M. R. Norman, M. Randeria, T. Takahashi, H. Katayama-Yoshida, T. Mochiku, K. Kadowaki, and G. Jennings, 1995, Phys. Rev. Lett. **74**, 2784.
Ding, H., M. R. Norman, T. Yokoya, T. Takeuchi, M. Randeria, J. C. Campuzano, T. Takahashi, T. Mochiku, and K. Kadowaki, 1997, Phys. Rev. Lett. **78**, 2628.
Du, R. R., D. C. Tsui, H. L. Stormer, L. N. Pfeiffer, K. W. Baldwin, and K. W. West, 1999, Solid State Commun. **109**, 389.
Eggert, S., 2000, Phys. Rev. Lett. **84**, 4413.
Eggert, S., H. Johannesson, and A. Mattsson, 1996, Phys. Rev. Lett. **76**, 1505.
Emery, V. J., 1979, in *Highly Conducting One-Dimensional Solids*, edited by J. T. Devreese, R. P. Evrard, and V. E. van Doren (Perseus, New York), p. 327.
Emery, V. J., E. Fradkin, S. A. Kivelson, and T. C. Lubensky, 2000, Phys. Rev. Lett. **85**, 2160.
Emery, V. J., and S. A. Kivelson, 1993, Physica C **209**, 597.
Emery, V. J., S. A. Kivelson, and J. M. Tranquada, 1999, Proc. Natl. Acad. Sci. U.S.A. **96**, 8814.
Eroles, J., G. Ortiz, A. V. Balatsky, and A. R. Bishop, 2001, Phys. Rev. B **64**, 174510.
Fedorov, A. V., T. Valla, P. D. Johnson, Q. Li, G. D. Gu, and N. Koshizuka, 1999, Phys. Rev. Lett. **82**, 2179.
Fisher, D. C., 1992, Phys. Rev. Lett. **69**, 534.
Fogler, M. M., A. A. Koulakov, and B. I. Shklovskii, 1996, Phys. Rev. B **54**, 1853.
Fong, H. F., P. Bourges, Y. Sidis, L. P. Regnault, J. Bossy, A. Ivanov, D. L. Millius, I. A. Aksay, and B. Keimer, 2000, Phys. Rev. B **61**, 14 773.
Fong, H. F., B. Keimer, D. Reznik, D. L. Milius, and I. A. Aksay, 1996, Phys. Rev. B **54**, 6708.
Fradkin, E., 1991, *Field Theories of Condensed Matter Systems* (Addison-Wesley, Reading, MA).
Fradkin, E., and S. A. Kivelson, 1999, Phys. Rev. B **59**, 8065.
Fradkin, E., S. A. Kivelson, E. Manousakis, and K. Nho, 2000, Phys. Rev. Lett. **84**, 1982.
Friedel, J., 1958, Nuovo Cimento, Suppl. **7**, 287.
Fujita, M., H. Goka, K. Yamada, and M. Matsuda, 2002, Phys. Rev. Lett. **88**, 167008.
Fukuyama, H., P. Platzman, and P. W. Anderson, 1979, Phys. Rev. B **19**, 5211.
Fukuzumi, Y., K. Mizuhashi, K. Takenaka, and S. Uchida, 1996, Phys. Rev. Lett. **76**, 684.
Gogolin, A. O., A. A. Nersesyan, and A. M. Tsvelik, 1998, *Bosonization and Strongly Correlated Systems* (Cambridge University, Cambridge, England).
Goto, T., K. Chiba, M. Mori, T. Suzuki, K. Seki, and T. Fukase, 1997, J. Phys. Soc. Jpn. **66**, 2870.
Goto, T., S. Kazama, K. Miyagawa, and T. Fukase, 1994, J. Phys. Soc. Jpn. **63**, 3494.
Gozar, A., B. S. Dennis, T. Siegrist, Y. Horibe, G. Blumberg, S. Komiya, and Y. Ando, 2003, Phys. Rev. B **68**, 052511.
Granath, M., V. Oganesyan, S. A. Kivelson, E. Fradkin, and V. J. Emery, 2001, Phys. Rev. Lett. **87**, 167011.
Granath, M., V. Oganesyan, D. Orgad, and S. A. Kivelson, 2002, Phys. Rev. B **65**, 184501.
Griffiths, R. B., 1969, Phys. Rev. Lett. **23**, 17.
Gruner, G., 1994, *Density Waves in Solids* (Addison-Wesley, Reading, MA).
Gweon, G.-H., J. D. Denlinger, J. W. Allen, R. Claesson, C. G. Olson, H. Hoechst, J. Marcus, C. Schlenker, and L. F. Schneemeyer, 2001, J. Electron Spectrosc. Relat. Phenom. **117-118**, 481.
Haase, J., and C. P. Slichter, 2003, J. Supercond. **16**, 473.
Haase, J., C. P. Slichter, R. Stern, C. T. Milling, and D. G. Hinks, 2000, Physica C **341-348**, 1727.
Han, J. H., Q.-H. Wang, and D.-H. Lee, 2001, Int. J. Mod. Phys. B **15**, 1117.
Haskel, D., E. A. Stern, F. Dogan, and A. R. Moodenbaugh, 2000, Phys. Rev. B **61**, 7055.
Hasselmann, N., A. H. Castro Neto, and C. Morais Smith, 2002, Phys. Rev. B **65**, 220511.
Hasselmann, N., A. H. Castro Neto, C. Morais Smith, and Y. Dimashko, 1999, Phys. Rev. Lett. **82**, 2135.
Hawthorn, D. G., *et al.*, 2003, Phys. Rev. Lett. **90**, 197004.
Hayden, S. M., G. Aeppli, H. A. Mook, T. G. Perring, T. E. Mason, S.-W. Cheong, and Z. Fisk, 1996a, Phys. Rev. Lett. **76**, 1344.
Hayden, S. M., G. Aeppli, T. G. Perring, H. A. Mook, and F. Doğan, 1996b, Phys. Rev. B **54**, R6905.
Hayden, S. M., G. H. Lander, J. Zaretsky, P. J. Brown, C. Stassis, P. Metcalf, and J. M. Honig, 1992, Phys. Rev. Lett. **68**, 1061.
Hellberg, C. S., and E. Manousakis, 1997, Phys. Rev. Lett. **78**, 4609.
Hellberg, C. S., and E. Manousakis, 2000, Phys. Rev. B **61**, 11 787.
Hess, C., B. Büchner, M. Hücker, R. Gross, and S.-W. Cheong, 1999, Phys. Rev. B **59**, 10 397.

Hirota, K., 2001, Physica C **357-360**, 61.
Hirota, K., K. Yamada, I. Tanaka, and H. Kojima, 1998, Physica B **241-243**, 817.
Hoffman, J. E., E. W. Hudson, K. M. Lang, V. Madhavan, H. Eisaki, S. Uchida, and J. C. Davis, 2002, Science **295**, 466.
Hoffman, J. E., K. McElroy, D. H. Lee, K. M. Lang, H. Eisaki, S. Uchida, and J. C. Davis, 2002, Science **297**, 1148.
Homes, C. C., A. W. McConnell, B. P. Clayman, D. A. Bonn, R. Liang, W. N. Hardy, M. Inoue, H. Negishi, P. Fournier, and R. L. Greene, 2000, Phys. Rev. Lett. **84**, 5391.
Hornbaker, D. J., S.-J. Kahng, S. Misra, B. W. Smith, A. T. Johnson, E. J. Miele, D. E. Luzzi, and A. Yazdani, 2002, Science **295**, 828.
Howald, C., H. Eisaki, N. Kaneko, M. Greven, and A. Kapitulnik, 2003a, Phys. Rev. B **67**, 014533.
Howald, C., H. Eisaki, N. Kaneko, and A. Kapitulnik, 2003b, Proc. Natl. Acad. Sci. U.S.A. **100**, 9705.
Hudson, E. W., S. H. Pan, A. K. Gupta, K. W. Ng, and J. C. Davis, 1999, Science **285**, 88.
Hunt, A. W., P. M. Singer, A. F. Cederström, and T. Imai, 2001, Phys. Rev. B **64**, 134525.
Hunt, A. W., P. M. Singer, K. R. Thurber, and T. Imai, 1999, Phys. Rev. Lett. **82**, 4300.
Ichikawa, N., S. Uchida, J. M. Tranquada, T. Niemöller, P. M. Gehring, S.-H. Lee, and J. R. Schneider, 2000, Phys. Rev. Lett. **85**, 1738.
Ichioka, M., and K. Machida, 1999, J. Phys. Soc. Jpn. **68**, 4020.
Igarashi, J., 1992, Phys. Rev. B **46**, 10 763.
Iguchi, I., T. Yamaguchi, and A. Sugimoto, 2001, Nature (London) **412**, 420.
Ino, A., C. Kim, T. Mizokawa, Z. X. Shen, A. Fujimori, M. Takaba, K. Tamasaku, H. Eisaki, and S. Uchida, 1999, J. Phys. Soc. Jpn. **68**, 1496.
Ino, A., C. Kim, M. Nakamura, T. Yoshida, T. Mizokawa, Z.-X. Shen, A. Fujimori, T. Kakeshita, H. Eisaki, and S. Uchida, 2002, Phys. Rev. B **65**, 094504.
Ito, M., H. Harashina, Y. Yasui, M. Kanada, S. Iikubo, M. Sato, A. Kobayashi, and K. Kakurai, 2002, J. Phys. Soc. Jpn. **71**, 265.
Ivanov, D. A., P. A. Lee, and X.-G. Wen, 2000, Phys. Rev. Lett. **84**, 3958.
Jankó, B., I. Kosztin, K. Levin, M. R. Norman, and D. J. Scalapino, 1999, Phys. Rev. Lett. **82**, 4304.
Janossy, A., F. Simon, and T. Fehér, 2000, Phys. Rev. Lett. **85**, 474.
Jestädt, T., K. H. Chow, S. J. Blundell, W. Hayes, F. L. Pratt, B. W. Lovett, M. A. Green, J. E. Millburn, and M. J. Rosseinsky, 1999, Phys. Rev. B **59**, 3775.
Julien, M.-H., F. Borsa, P. Carretta, M. Horvatić, C. Berthier, and C. T. Lin, 1999, Phys. Rev. Lett. **83**, 604.
Julien, M.-H., A. Campana, A. Rigamonti, P. Carretta, F. Borsa, P. Kuhns, A. P. Reyes, W. G. Moulton, M. Horvatić, C. Berthier, A. Vietkin, and A. Revcolevschi, 2001, Phys. Rev. B **63**, 144508.
Kajimoto, R., K. Ishizaka, H. Yoshizawa, and Y. Tokura, 2003, Phys. Rev. B **67**, 014511.
Kakuyanagi, K., K. Kumagai, and Y. Matsuda, 2002, Phys. Rev. B **65**, 060503.
Kakuyanagi, K., K. Kumagai, Y. Matsuda, and M. Hasegawa, 2003, Phys. Rev. Lett. **90**, 197003.
Kane, C., and M. P. A. Fisher, 1992, Phys. Rev. Lett. **68**, 1220.
Kane, C., and M. P. A. Fisher, 1994, Phys. Rev. B **72**, 724.
Kao, Y. J., Q. Si, and K. Levin, 2000, Phys. Rev. B **61**, 11 898.
Kapitulnik, A., N. Mason, S. A. Kivelson, and S. Chakravarty, 2001, Phys. Rev. B **63**, 125322.
Kastner, M. A., R. J. Birgeneau, G. Shirane, and Y. Endoh, 1998, Rev. Mod. Phys. **70**, 897.
Kataev, V., B. Rameev, B. Büchner, M. Hücker, and R. Borowski, 1997, Phys. Rev. B **55**, R3394.
Kataev, V., B. Rameev, A. Validov, B. Büchner, M. Hücker, and R. Borowski, 1998, Phys. Rev. B **58**, R11 876.
Katano, S., M. Sato, K. Yamada, T. Suzuki, and T. Fukase, 2000, Phys. Rev. B **62**, R14 677.
Katsufuji, T., T. Tanabe, T. Ishikawa, Y. Fukuda, T. Arima, and Y. Tokura, 1996, Phys. Rev. B **54**, R14230.
Kee, H.-Y., S. A. Kivelson, and G. Aeppli, 2002, Phys. Rev. Lett. **88**, 257002.
Khaykovich, B., Y. S. Lee, R. W. Erwin, S.-H. Lee, S. Wakimoto, K. J. Thomas, M. A. Kastner, and R. J. Birgeneau, 2002, Phys. Rev. B **66**, 014528.
Kimura, H., *et al.*, 1999, Phys. Rev. B **59**, 6517.
Kivelson, S. A., G. Aeppli, and V. J. Emery, 2001, Proc. Natl. Acad. Sci. U.S.A. **98**, 11903.
Kivelson, S. A., E. Fradkin, and V. J. Emery, 1998, Nature (London) **393**, 550.
Kivelson, S. A., D.-H. Lee, E. Fradkin, and V. Oganesyan, 2002, Phys. Rev. B **67**, 144516.
Klauss, H.-H., W. Wagener, M. Hillberg, W. Kopmann, H. Walf, F. J. Litterst, M. Hücker, and B. Büchner, 2000, Phys. Rev. Lett. **85**, 4590.
Koike, Y., A. Kobayashi, T. Kawaguchi, M. Kato, T. Noji, Y. Ono, T. Hikita, and Y. Saito, 1992, Solid State Commun. **82**, 889.
Koulakov, A. A., M. M. Fogler, and B. I. Shklovskii, 1996, Phys. Rev. Lett. **76**, 499.
Lake, B., G. Aeppli, K. N. Clausen, D. F. McMorrow, K. Lefmann, N. E. Hussey, N. Mangkorntong, M. Mohara, H. Takagi, T. E. Mason, and A. Schroder, 2001, Science **291**, 1759.
Lake, B., G. Aeppli, T. E. Mason, A. Schröder, D. F. McMorrow, K. Lefmann, M. Isshiki, M. Nohara, H. Takagi, and S. M. Hayden, 1999, Nature (London) **400**, 43.
Lake, B., *et al.*, 2002, Nature (London) **415**, 299.
Lang, K. M., V. Madhavan, J. E. Hoffman, E. W. Hudson, H. Eisaki, S. Uchida, and J. C. Davis, 2000, Phys. Rev. Lett. **85**, 1536.
Lanzara, A., N. L. Saini, T. Rossetti, A. Bianconi, H. Oyanagi, H. Yamaguchi, and Y. Maeno, 1996, Solid State Commun. **97**, 93.
Lee, P. A., 1999, Physica C **317-318**, 194.
Lee, S.-H. and S.-W. Cheong, 1997, Phys. Rev. Lett. **79**, 2514.
Lee, Y. S., R. J. Birgeneau, M. A. Kastner, Y. Endoh, S. Wakimoto, K. Yamada, R. W. Erwin, S.-H. Lee, and G. Shirane, 1999, Phys. Rev. B **60**, 3643.
Lefebvre, S., P. Wzietek, S. Brown, C. Bourbonnais, D. Jerome, C. Mezière, M. Fourmigue, and P. Batail, 2000, Phys. Rev. Lett. **85**, 5420.
Li, J., Y. Zhu, J. M. Tranquada, K. Yamada, and D. J. Buttrey, 2003, Phys. Rev. B **67**, 012404.
Lilly, M. P., K. B. Cooper, J. P. Eisenstein, L. N. Pfeiffer, and K. W. West, 1999a, Phys. Rev. Lett. **82**, 394.
Lilly, M. P., K. B. Cooper, J. P. Eisenstein, L. N. Pfeiffer, and K. W. West, 1999b, Phys. Rev. Lett. **83**, 824.
Littlewood, P. B., J. Zaanen, G. Aeppli, and H. Monien, 1993, Phys. Rev. B **48**, 487.

Liu, Z. Y., H. H. Wen, T. Xiang, S. Komiya, X. F. Sun, and Y. Ando, 2003, "Core size effect on the vortex quasiparticle excitations in overdoped $La_{2-x}Sr_xCuO_4$ single crystals," e-print cond-mat/0301366.
Loeser, A. G., Z. X. Shen, M. C. Schabel, C. Kim, M. Zhang, A. Kapitulnik, and P. Fournier, 1997, Phys. Rev. B **56**, 14 185.
Lorenzana, J., C. Castellani, and C. Di Castro, 2001a, Phys. Rev. B **64**, 235127.
Lorenzana, J., C. Castellani, and C. Di Castro, 2001b, Phys. Rev. B **64**, 235128.
Lorenzana, J., and G. Seibold, 2002, Phys. Rev. Lett. **89**, 136401.
Löw, U., V. J. Emery, K. Fabricius, and S. A. Kivelson, 1994, Phys. Rev. Lett. **72**, 1918.
Lyons, K. B., P. A. Fleury, J. P. Remeika, A. S. Cooper, and T. J. Negran, 1988, Phys. Rev. B **37**, 2353.
Machida, K., 1989, Physica C **158**, 192.
Mason, T. E., A. Schröder, G. Aeppli, H. A. Mook, and S. M. Hayden, 1996, Phys. Rev. Lett. **77**, 1604.
Matsuda, M., R. J. Birgeneau, H. Chou, Y. Endoh, M. A. Kastner, H. Kojima, K. Kuroda, G. Shirane, I. Tanaka, and K. Yamada, 1993, J. Phys. Soc. Jpn. **62**, 443.
Matsuda, M., Y. S. Lee, M. Greven, M. A. Kastner, R. J. Birgeneau, K. Yamada, Y. Endoh, P. Böni, S.-H. Lee, S. Wakimoto, and G. Shirane, 2000, Phys. Rev. B **61**, 4326.
Mattsson, A., S. Eggert, and H. Johannesson, 1997, Phys. Rev. B **56**, 15 615.
May, C., R. W. Hill, C. Lupien, L. Taillefer, P. Lambert, R. Gagnon, and P. Fournier, 2000, Phys. Rev. B **62**, 3554.
McCoy, B., and T. T. Wu, 1968, Phys. Rev. **176**, 631.
McElroy, K., R. W. Simmonds, J. E. Hoffman, D.-H. Lee, J. Orenstein, H. Eisaki, S. Uchida, and J. C. Davis, 2003, Nature (London) **422**, 592.
Mesot, J., *et al.*, 1999, Phys. Rev. Lett. **83**, 840.
Miller, R. I., R. F. Kiefl, J. H. Brewer, J. E. Sonier, J. Chakhalian, S. Dunsiger, G. D. Morris, A. N. Price, D. A. Bonn, W. H. Hardy, and R. Liang, 2002, Phys. Rev. Lett. **88**, 137002.
Millis, A. J., 1993, Phys. Rev. B **48**, 7183.
Mitrović, V. F., E. E. Sigmund, M. Eschrig, H. N. Bachman, W. P. Halperin, A. P. Reyes, P. Kuhns, and W. G. Moulton, 2001, Nature (London) **413**, 501.
Mitrović, V. F., E. E. Sigmund, W. P. Halperin, A. P. Reyes, P. Kuhns, and W. G. Moulton, 2003, Phys. Rev. B **67**, 220503.
Moessner, R., and J. T. Chalker, 1996, Phys. Rev. B **54**, 5006.
Monthoux, P., and D. Pines, 1993, Phys. Rev. B **47**, 6069.
Moodenbaugh, A. R., Y. Xu, M. Suenaga, T. J. Folkerts, and R. N. Shelton, 1988, Phys. Rev. B **38**, 4596.
Mook, H. A., 2002, private communication.
Mook, H. A., P. Dai, and F. Doğan, 2002, Phys. Rev. Lett. **88**, 097004.
Mook, H. A., P. Dai, F. Doğan, and R. D. Hunt, 2000, Nature (London) **404**, 729.
Mori, S., C. H. Chen, and S.-W. Cheong, 1998a, Nature (London) **392**, 473.
Mori, S., C. H. Chen, and S.-W. Cheong, 1998b, Phys. Rev. Lett. **81**, 3972.
Morr, D. K., and D. Pines, 2000, Phys. Rev. B **61**, R6483.
Moskvin, A. S., and Y. D. Panov, 2002, Solid State Commun. **122**, 253.
Muñoz, D., F. Illas, and I. P. R. Moreira, 2000, Phys. Rev. Lett. **84**, 1579.
Nachumi, B., C. Kendziora, N. Ichikawa, Y. Nakamura, and S. Uchida, 2002, Phys. Rev. B **65**, 092504.
Nachumi, B., *et al.*, 1998, Phys. Rev. B **58**, 8760.
Niedermayer, C., C. Bernhard, T. Blasius, A. Golnik, A. Moodenbaugh, and J. I. Budnick, 1998, Phys. Rev. Lett. **80**, 3843.
Niemöller, T., B. Büchner, M. Cramm, C. Huhnt, L. Tröger, and M. Tischer, 1998, Physica C **299**, 191.
Noda, T., H. Eisaki, and S. Uchida, 1999, Science **286**, 265.
Norman, M., M. Randeria, H. Ding, and J. C. Campuzano, 1994, Phys. Rev. B **52**, 615.
Norman, M. R., 2000, Phys. Rev. B **61**, 14 751.
Odom, T. W., J.-L. Huang, and C. M. Lieber, 2002, J. Phys.: Condens. Matter **14**, 18.
Ohsugi, S., Y. Kitaoka, H. Yamanaka, K. Ishida, and K. Asayama, 1994, J. Phys. Soc. Jpn. **63**, 2057.
Ono, S., Y. Ando, T. Murayama, F. E. Balakirev, J. B. Betts, and G. S. Boebinger, 2000, Phys. Rev. Lett. **85**, 638.
Onufrieva, F., and P. Pfeuty, 2002, Phys. Rev. B **65**, 054515.
Orenstein, J., and A. J. Millis, 2000, Science **288**, 468.
Orgad, D., S. A. Kivelson, E. W. Carlson, V. J. Emery, X. J. Zhou, and Z. X. Shen, 2001, Phys. Rev. Lett. **86**, 4362.
Pan, S. H., E. W. Hudson, A. K. Gupta, K.-W. Ng, H. Eisaki, S. Uchida, and J. C. Davis, 2000a, Phys. Rev. Lett. **85**, 1536.
Pan, S. H., E. W. Hudson, K. M. Lang, H. Eisaki, S. Uchida, and J. C. Davis, 2000b, Nature (London) **403**, 746.
Pan, S. H., *et al.*, 2001, Nature (London) **413**, 282.
Pan, W., T. Jungwirth, H. L. Stormer, D. C. Tsui, A. H. MacDonald, S. M. Girvin, L. Smrcka, L. N. Pfeiffer, K. W. Baldwin, and K. W. West, 2000, Phys. Rev. Lett. **85**, 3257.
Panagopoulos, C., J. L. Tallon, B. D. Rainford, T. Xiang, J. R. Cooper, and C. A. Scott, 2002, Phys. Rev. B **66**, 064501.
Pintschovius, L., W. Reichardt, M. Kläser, T. Wolf, and H. v. Löhneysen, 2002, Phys. Rev. Lett. **89**, 037001.
Podolsky, D., E. Demler, K. Damle, and B. I. Halperin, 2002, Phys. Rev. B **67**, 094514.
Poilblanc, D., and T. M. Rice, 1989, Phys. Rev. B **39**, 9749.
Polkovnikov, A., S. Sachdev, and M. Vojta, 2003, Physica C **388-389**, 19.
Polkovnikov, A., M. Vojta, and S. Sachdev, 2002, Phys. Rev. B **65**, 220509.
Prelovšek, P., T. Tohyama, and S. Maekawa, 2001, Phys. Rev. B **64**, 052512.
Presland, M. R., J. L. Tallon, R. G. Buckley, R. S. Liu, and N. E. Flower, 1991, Physica C **176**, 95.
Radaelli, P. G., D. E. Cox, L. Capogna, S.-W. Cheong, and M. Marezio, 1999, Phys. Rev. B **59**, 14 440.
Renner, C., B. Revaz, K. Kadowaki, I. Maggio-Aprile, and O. Fischer, 1998, Phys. Rev. Lett. **80**, 3606.
Rossat-Mignod, J., L. P. Regnault, C. Vettier, P. Bourges, P. Burlet, J. Bossy, J. Y. Henry, and G. Lapertot, 1992, Physica B **180&181**, 383.
Rübhausen, M., S. Yoon, S. L. Cooper, K. H. Kim, and S.-W. Cheong, 2000, Phys. Rev. B **62**, R4782.
Sachdev, S., 1999a, Phys. World **12** (4), 33.
Sachdev, S., 1999b, *Quantum Phase Transitions* (Cambridge University, Cambridge, UK).
Sachdev, S., 2000, Science **288**, 475.
Sachdev, S., 2002, in *Developments in Mathematical and Experimental Physics, Volume B: Statistical Physics and Beyond*, edited by A. Macias, F. Uribe, and E. Diaz (Kluwer Academic, New York).
Sachdev, S., 2003, Rev. Mod. Phys. **75**, 913.

Sachdev, S., C. Buragohain, and M. Vojta, 1999, Science **286**, 2479.
Saini, N. L., A. Lanzara, H. Oyanagi, H. Yamaguchi, K. Oka, T. Ito, and A. Bianconi, 1997, Phys. Rev. B **55**, 12 759.
Salkola, M., V. J. Emery, and S. A. Kivelson, 1996, Phys. Rev. Lett. **77**, 155.
Savici, A. T., Y. Fudamoto, I. M. Gat, T. Ito, M. I. Larkin, Y. J. Uemura, G. M. Luke, K. M. Kojima, Y. S. Lee, M. A. Kastner, R. J. Birgeneau, and K. Yamada, 2002, Phys. Rev. B **66**, 014524.
Schollwoeck, U., S. Chakravarty, J. O. Fjaerestad, J. B. Marston, and M. Troyer, 2003, Phys. Rev. Lett. **90**, 186401.
Schulz, H. J., 1989, J. Phys. (Paris) **50**, 2833.
Seibold, G., E. Sigmund, and V. Hizhnyakov, 1998, Phys. Rev. B **57**, 6937.
Sera, M., S. Shamoto, M. Sato, I. Watanabe, S. Nakashima, and K. Kumagai, 1990, Solid State Commun. **74**, 951.
Seul, M., and D. Andelman, 1995, Science **267**, 476.
Shamoto, S., M. Sato, J. M. Tranquada, B. J. Sternlieb, and G. Shirane, 1993, Phys. Rev. B **48**, 13 817.
Sharma, R. P., S. B. Ogale, Z. H. Zhang, J. R. Liu, W. K. Chu, B. Veal, A. Paulikas, H. Zheng, and T. Venkatesan, 2000, Nature (London) **404**, 736.
Si, Q., Y. Zha, K. Levin, and J. P. Lu, 1993, Phys. Rev. B **47**, 9055.
Simon, P., J. M. Bassat, S. B. Oseroff, Z. Fisk, S. W. Cheong, A. Wattiaux, and S. Schultz, 1993, Phys. Rev. B **48**, 4216.
Simovič, B., P. C. Hammel, M. Hücker, B. Büchner, and A. Revcoleschi, 2003, Phys. Rev. B **68**, 012415.
Singer, P. M., A. W. Hunt, A. F. Cederström, and T. Imai, 1999, Phys. Rev. B **60**, 15 345.
Singer, P. M., A. W. Hunt, and T. Imai, 2002, Phys. Rev. Lett. **88**, 047602.
Singer, P. M., and T. Imai, 2002, Phys. Rev. Lett. **88**, 187601.
Sondhi, S. L., S. M. Girvin, J. P. Carini, and D. Shahar, 1997, Rev. Mod. Phys. **69**, 315.
Sprunger, P. T., L. Petersen, E. W. Plummer, E. Laegsgaard, and F. Besenbacher, 1997, Science **275**, 1764.
Sternlieb, B. J., J. M. Tranquada, G. Shirane, M. Sato, and S. Shamoto, 1994, Phys. Rev. B **50**, 12 915.
Stock, C., W. J. L. Buyers, R. Liang, D. Peets, Z. Tun, D. Bonn, W. N. Hardy, and R. J. Birgeneau, 2003, "Superconducting gap and a long-lived resonance in $YBa_2Cu_3O_{6.5}$ ortho-II superconductor," cond-mat/0308168.
Stock, C., W. J. L. Buyers, Z. Tun, R. Liang, D. Peets, D. Bonn, W. N. Hardy, and L. Taillefer, 2002, Phys. Rev. B **66**, 024505.
Stone, M., 1994, *Bosonization* (World Scientific, Singapore).
Sugai, S., and T. Hosokawa, 2000, Phys. Rev. Lett. **85**, 1112.
Suh, B. J., P. C. Hammel, M. Hücker, and B. Büchner, 1999, Phys. Rev. B **59**, R3952.
Suh, B. J., P. C. Hammel, M. Hücker, B. Büchner, U. Ammerahl, and A. Revcolevschi, 2000, Phys. Rev. B **61**, R9265.
Sun, X. F., S. Komiya, and Y. Ando, 2003, Phys. Rev. B **67**, 184512.
Sutherland, M., *et al.*, 2003, Phys. Rev. B **67**, 174520.
Suzuki, T., T. Goto, K. Chiba, T. Shinoda, T. Fukase, H. Kimura, K. Yamada, M. Ohashi, and Y. Yamaguchi, 1998, Phys. Rev. B **57**, R3229.
Takahashi, T., H. Matsuyama, H. Katayama-Yoshida, Y. Okabe, S. Hosoya, K. Seki, H. Fujimoto, M. Sato, and H. Inokuchi, 1988, Nature (London) **334**, 691.
Takeya, J., Y. Ando, S. Komiya, and X. F. Sun, 2002, Phys. Rev. Lett. **88**, 077001.
Takigawa, M., A. P. Reyes, P. C. Hammel, J. D. Thompson, R. H. Heffner, Z. Fisk, and K. C. Ott, 1991, Phys. Rev. B **43**, 247.
Tallon, J. L., C. Bernhard, H. Shaked, R. L. Hitterman, and J. D. Jorgensen, 1995, Phys. Rev. B **51**, 12 911.
Teitel'baum, G. B., I. M. Abu-Shiekah, O. Bakharev, H. B. Brom, and J. Zaanen, 2001, Phys. Rev. B **63**, 020507.
Teitel'baum, G. B., B. Büchner, and H. de Gronckel, 2000, Phys. Rev. Lett. **84**, 2949.
Thurston, T. R., R. J. Birgeneau, M. A. Kastner, N. W. Preyer, G. Shirane, Y. Fujii, K. Yamada, Y. Endoh, K. Kakurai, M. Matsuda, Y. Hidaka, and T. Murakami, 1989, Phys. Rev. B **40**, 4585.
Thurston, T. R., P. M. Gehring, G. Shirane, R. J. Birgeneau, M. A. Kastner, Y. Endoh, M. Matsuda, K. Yamada, H. Kojima, and I. Tanaka, 1992, Phys. Rev. B **46**, 9128.
Tou, H., M. Matsumura, and H. Yamagata, 1993, J. Phys. Soc. Jpn. **62**, 1474.
Tranquada, J. M., 1998a, in *Neutron Scattering in Layered Copper-Oxide Superconductors*, edited by A. Furrer (Kluwer, Dordrecht, The Netherlands), p. 225.
Tranquada, J. M., 1998b, Physica B **241-243**, 745.
Tranquada, J. M., J. D. Axe, N. Ichikawa, A. R. Moodenbaugh, Y. Nakamura, and S. Uchida, 1997, Phys. Rev. Lett. **78**, 338.
Tranquada, J. M., J. D. Axe, N. Ichikawa, Y. Nakamura, S. Uchida, and B. Nachumi, 1996, Phys. Rev. B **54**, 7489.
Tranquada, J. M., D. J. Buttrey, V. Sachan, and J. E. Lorenzo, 1994, Phys. Rev. Lett. **73**, 1003.
Tranquada, J. M., P. M. Gehring, G. Shirane, S. Shamoto, and M. Sato, 1992, Phys. Rev. B **46**, 5561.
Tranquada, J. M., N. Ichikawa, K. Kakurai, and S. Uchida, 1999a, J. Phys. Chem. Solids **60**, 1019.
Tranquada, J. M., N. Ichikawa, and S. Uchida, 1999b, Phys. Rev. B **59**, 14 712.
Tranquada, J. M., J. E. Lorenzo, D. J. Buttrey, and V. Sachan, 1995, Phys. Rev. B **52**, 3581.
Tranquada, J. M., K. Nakajima, M. Braden, L. Pintschovius, and R. J. McQueeney, 2002, Phys. Rev. Lett. **88**, 075505.
Tranquada, J. M., B. J. Sternlieb, J. D. Axe, Y. Nakamura, and S. Uchida, 1995, Nature (London) **375**, 561.
Tranquada, J. M., *et al.*, 1988, Phys. Rev. B **38**, 2477.
Tyler, A. W., Y. Ando, F. E. Balakirev, A. Passner, G. S. Boebinger, A. J. Schofield, A. P. Mackenzie, and O. Laborde, 1998, Phys. Rev. B **57**, 728.
Ussishkin, I., S. L. Sondhi, and D. A. Huse, 2002, Phys. Rev. Lett. **89**, 287001.
Vajk, O. P., P. K. Mang, M. Greven, P. M. Gehring, and J. W. Lynn, 2002, Science **295**, 1691.
Vaknin, D., J. L. Zarestky, and L. L. Miller, 2000, Physica C **329**, 109.
Valla, T., A. V. Fedorov, P. D. Johnson, B. O. Wells, S. L. Hulbert, Q. Li, G. D. Gu, and N. Koshizuka, 1999, Science **285**, 2110.
Van Oosten, A. B., R. Broer, and W. C. Nieupoort, 1996, Chem. Phys. Lett. **257**, 207.
Varma, C. M., 1997, Phys. Rev. B **55**, 14 554.
Varma, C. M., P. B. Littlewood, S. Schmitt-Rink, E. Abrahams, and A. E. Ruckenstein, 1989, Phys. Rev. Lett. **63**, 1996.
Vershinin, M., S. Misra, Y. Abe, Y. Ando, and A. Yazdani, 2003, Bull. Am. Phys. Soc. **48** (1), 372.
Vishwanath, A., and D. Carpentier, 2001, Phys. Rev. Lett. **86**, 676.
Vojta, M., and S. Sachdev, 1999, Phys. Rev. Lett. **83**, 3916.

Wakimoto, S., G. Shirane, Y. Endoh, K. Hirota, S. Ueki, K. Yamada, R. J. Birgeneau, M. A. Kastner, Y. S. Lee, P. M. Gehring, and S. H. Lee, 1999, Phys. Rev. B **60**, R769.
Wakimoto, S., J. M. Tranquada, T. Ono, K. M. Kojima, S. Uchida, S.-H. Lee, P. M. Gehring, and R. J. Birgeneau, 2001, Phys. Rev. B **64**, 174505.
Wang, Q.-H., and D.-H. Lee, 2003, Phys. Rev. B **67**, 020511.
Wang, R., J. Gui, Y. Zhu, and A. R. Moodenbaugh, 2000, Phys. Rev. B **61**, 11 946.
Wang, X.-L., C. Stassis, D. C. Johnston, T. C. Leung, J. Ye, B. N. Harmon, G. H. Lander, A. J. Schultz, C.-K. Loong, and J. M. Honig, 1992, Phys. Rev. B **45**, 5645.
Wang, Y., Z. A. Xu, T. Kakeshita, S. Uchida, S. Ono, Y. Ando, and N. P. Ong, 2001, Phys. Rev. B **64**, 224519.
Wang, Z. Z., J. Clayhold, N. P. Ong, J. M. Tarascon, L. H. Greene, W. R. McKinnon, and G. W. Hull, 1987, Phys. Rev. B **36**, 7222.
Watanabe, I., T. Adachi, K. Takahashi, S. Yairi, Y. Koike, and K. Nagamine, 2002, Phys. Rev. B **65**, 180516.
Watanabe, I., M. Akoshima, Y. Koike, S. Ohira, and K. Nagamine, 2000, Phys. Rev. B **62**, 14 524.
White, P. J., Z. X. Shen, D. L. Feng, C. Kim, M. Z. Hasan, J. M. Harris, A. G. Loeser, H. Ikeda, R. Yoshikazi, G. D. Gu, and N. Koshizuka, 1999, e-print cond-mat/9901349.
White, S. R., I. Affleck, and D. J. Scalapino, 2002, Phys. Rev. B **65**, 165122.
White, S. R., and D. J. Scalapino, 1998, Phys. Rev. Lett. **80**, 1272.
White, S. R., and D. J. Scalapino, 2000, Phys. Rev. B **61**, 6320.
Xu, Z. A., N. P. Ong, Y. Wang, T. Kakeshita, and S. Uchida, 2000, Nature (London) **406**, 486.
Yamada, K., M. Arai, Y. Endoh, S. Hosoya, K. Nakajima, T. Perring, and A. Taylor, 1991, J. Phys. Soc. Jpn. **60**, 1197.
Yamada, K., E. Kudo, Y. Endoh, Y. Hidaka, M. Oda, M. Suzuki, and T. Murakami, 1987, Solid State Commun. **64**, 753.
Yamada, K., K. Kurahashi, T. Uefuji, M. Fujita, S. Park, S.-H. Lee, and Y. Endoh, 2003, Phys. Rev. Lett. **90**, 137004.
Yamada, K., S. Wakimoto, G. Shirane, C. H. Lee, M. A. Kastner, S. Hosoya, M. Greven, Y. Endoh, and R. J. Birgeneau, 1995, Phys. Rev. Lett. **75**, 1626.
Yamada, K., *et al.*, 1998, Phys. Rev. B **57**, 6165.
Yang, W. L., H. H. Wen, and Z. X. Zhao, 2000, Phys. Rev. B **62**, 1361.
Yazdani, A., C. M. Howald, C. P. Lutz, A. Kapitulnik, and D. M. Eigler, 1999, Phys. Rev. Lett. **83**, 176.
Yoon, S., M. Rübhausen, S. L. Cooper, K. H. Kim, and S.-W. Cheong, 2000, Phys. Rev. Lett. **85**, 3297.
Yoshizawa, H., T. Kakeshita, R. Kajimoto, T. Tanabe, T. Katsufuji, and Y. Tokura, 2000, Phys. Rev. B **61**, R854.
Zaanen, J., 1998, J. Phys. Chem. Solids **59**, 1769.
Zaanen, J., 2000, Nature (London) **404**, 714.
Zaanen, J., and O. Gunnarsson, 1989, Phys. Rev. B **40**, 7391.
Zaanen, J., and P. B. Littlewood, 1994, Phys. Rev. B **50**, 7222.
Zaanen, J., O. Y. Osman, H. V. Kruis, Z. Nussinov, and J. Tworzydło, 2001, Philos. Mag. B **81**, 1485.
Zachar, O., 2000, Phys. Rev. B **62**, 13 836.
Zachar, O., S. A. Kivelson, and V. J. Emery, 1998, Phys. Rev. B **57**, 1422.
Zacher, M. G., R. Eder, E. Arrigoni, and W. Hanke, 2000, Phys. Rev. Lett. **85**, 2585.
Zacher, M. G., R. Eder, E. Arrigoni, and W. Hanke, 2001, Phys. Rev. B **65**, 045109.
Zhang, S.-C., 1997, Science **275**, 1089.
Zhang, Y., E. Demler, and S. Sachdev, 2002, Phys. Rev. B **66**, 094501.
Zhao, G.-M., M. B. Hunt, H. Keller, and K. A. Müller, 1997, Nature (London) **385**, 236.
Zhou, X. J., P. Bogdanov, S. A. Kellar, T. Noda, H. Eisaki, S. Uchida, Z. Hussain, and Z.-X. Shen, 1999, Science **286**, 268.
Zhou, X. J., *et al.*, 2001, Phys. Rev. Lett. **86**, 5578.
Zhu, J., W. Pan, H. L. Stormer, L. N. Pfeiffer, and K. W. West, 2002, Phys. Rev. Lett. **88**, 116803.